Contract No:

This document was prepared in conjunction with work accomplished under Contract No. DE-AC09-08SR22470 with the U.S. Department of Energy (DOE) Office of Environmental Management (EM).

Disclaimer:

Evaluation of Alternate Impurity Removal Getters - Year 2

David W. James

Gregg A. Morgan Jr

November 2016

SRNL-STI-2016-00542, Revision 0

DISCLAIMER

Printed in the United States of America

Prepared for
U.S. Department of Energy

SRNL-STI-2016-00542
Revision 0

Keywords:
ST909,
Getters,
TPS,

Retention: *Permanent*

Evaluation of Alternate Impurity Removal Getters - Year 2

David W. James
Gregg A. Morgan Jr

November 2016

Prepared for the U.S. Department of Energy under contract number DE-AC09-08SR22470.

REVIEWS AND APPROVALS

AUTHORS:

David W. James, Hydrogen Processing Group Date

Gregg A. Morgan Jr, Hydrogen Processing Group Date

TECHNICAL REVIEW:

Katie J. Heroux, Hydrogen Processing Group Date

APPROVAL:

David W. Babineau, Manager Date
Hydrogen Processing Group

ACKNOWLEDGEMENTS

The authors thank the Savannah River Tritium Enterprises (SRTE) Engineering and Operations, Savannah River Field Office, and National Nuclear Security Administration (NNSA) Technology Maturation Division (NA-123.2) for the Plant Directed Research and Development (PDRD) program funding of this project.

The authors acknowledge Anita Poore's contributions and insights. Brittany Hodge also helped contribute to this work by compiling the μ-GC data sets. Both of their efforts are greatly appreciated.

EXECUTIVE SUMMARY

The Savannah River Site Tritium Facilities use various getter materials (SAES® ST909 and ST198) as part of the tritium process stripper (TPS) for the removal of impurity species. Benefits of ST909 are found in both environmental stewardship and gas processing improvements. The tritium capturing performance of ST198 is affected by impurities such as ammonia and carbon monoxide. SAES ST198 is used as a final polisher to remove trace amounts of tritium in the process stream before discharge through the stack. ST909 decomposes impurities such as tritiated water, methane, and ammonia. Therefore the upstream material, ST909, is important to environmental safety. ST909 also provides the benefit of capturing oxygen and carbon oxides.

ST909 is a trade name for a zirconium (Zr) – manganese (Mn) – iron (Fe) alloy manufactured by SAES Getters. Although ST909 provides many benefits it also has challenges that should be considered. SAES ST909 is a consumable product that cannot be regenerated without the potential of reintroducing impurities back into the process. In addition, SAES ST909 is supplied from a foreign sole-source provider, and the cost of the material is ~$4200-$5300/kg (depending on the quantity ordered). Implementing alternative materials or utilizing other competitive manufacturers could provide cost benefits over the life of the facility if cheaper or more cost effective alternatives can be found and utilized. If ST909 is no longer available from SAES, this represents a risk to mission viability and sustainability and therefore the evaluation of alternative impurity removal getters is vital for the continued success of the tritium mission.

The scope of the Evaluation of Alternate Impurity Removal Getters, which has been funded by the Plant Directed Research and Development (PDRD) program, has been revised through several iterations as facility needs have changed. The original PDRD project was to evaluate replacement materials for the ST198 getter material. The scope was then amended very early in the project to identify a potential replacement material for the ST909 getter material. Based on a literature survey conducted in FY15 no known single material that can replace ST909 for use with three carrier gas streams (including: hydrogen, helium, and nitrogen) has been identified.

The goal of FY16 activities was to identify a combination of materials (or a material) that can crack methane and ammonia under the high nitrogen conditions found specifically in the TPS with at least the same efficiency as the ST909. In addition to the evaluation of potential replacement materials for ST909 for this PDRD project, the effects of various impurities on the hydrogen gettering of the ST198 were evaluated in FY15 and results provided in a separate report issued in FY16 [1]. The separate report shows that based on operating temperature of the ST198 getter bed the various impurities that could be present in the process stream if the ST909 bed was not operating at optimal efficiency could impact the tritium getter performance of ST198.

The following materials were tested during FY16 for ST909 replacement considerations: ST909 – for establishing baseline –, nickel on kieselguhr (Ni/k), SAES ST707 which is a ZrVFe getter, American Elements (AME) TiMoZr, AME AlNiFe, AME ZrMnFeAl and AME ZrNi. Each test was operated with gas streams representative of the nominal impurities related to the feed sources from N_2 flush gas, zeolite-bed (Z-bed) recovery, and tritium extraction facility (TEF) flush gas. The cracking/decomposition efficiency of methane and/or ammonia was determined for each of the materials.

Although SAES ST909 and AME ZrMnFeAl have similar compositions, the preparation method of the materials seems to affect performance levels. ST909 is prepared from powdered metallurgy, whereas AME ZrMnFeAl is prepared from melted ingots. Methane cracking efficiencies observed during testing suggests that the different sample preparation method will affect methane cracking efficiencies. A methane cracking efficiency of ~10% for AME ZrMnFeAl when exposed to an argon rich gas stream was observed. ST909 had a methane cracking efficiency of ~20% when exposed to a gas of similar composition.

It was observed that Ni/k has excellent cracking efficiency in a nitrogen rich gas mixture. The efficiency of ammonia cracking was reduced to roughly 60% for Ni/k over the course of testing. Other materials tested showed decomposition efficiencies greater than 90% where decomposition efficiency is equal to one minus the ratios of the ammonia signal to an inert carrier gas of the test and feed streams.

Combination testing shows that the AME alumina nickel iron alloy has an improved methane cracking efficiency even though ammonia was initially present. An improvement of 8% at the end of the test is noted compared to other materials subjected to gas mixture without ammonia. Combination testing showed increased CH_4 cracking capability as well as the need for optimization.

For an argon rich gas with both ammonia and methane impurities present, combination testing of AME ZrMnFeAl with AME AlNiFe showed methane cracking efficiencies greater than 35%. AME ZrNi had a better methane cracking efficiency at ~48%. AME AlNiFe had 80% an ammonia cracking efficiency and AME ZrNi had a cracking efficiency of ~97% when exposed to the same gas. Combination test of the AME ZrMnFeAl with AME AlNiFe made little difference compared to tests with just the AME AlNiFe.

It is recommended that an evaluation of the various gas streams and the order in which they are processed by the ST909 be completed. The tests reported in this document show that changing gas compositions have the potential for ammonia formation under certain circumstances depending on the history of the sample. It may be appropriate to evacuate TPS before changing the gas composition to minimize impurity formation.

Several holes still exist in the data before an alternate material can be recommended as a replacement for the ST909. The data provided show that a combination of materials may be able to perform the same workload as ST909. However, the optimization of the process at the research and development level is needed. Additional combination testing and the optimization is recommended before any one specific material or set of materials can be recommended.

Based on the results presented in this report there are potentials that have showed to perform better than ST909 under the conditions tested Additional funding is recommended to continue the combination testing of the potential replacement materials for the ST909. In addition, it is necessary to test various combinations of materials under a broader range of operating conditions relevant to the TPS operating conditions. The additional work should be adequate to identify a potential replacement material or combination of materials for the ST909.

TABLE OF CONTENTS

LIST OF TABLES

LIST OF FIGURES

LIST OF ABBREVIATIONS

Units of Measurement

°C	Degrees Celsius
gm	gram
K	Kelvin
kg	kilogram
L	Liter
mL	Milliliter
mm	Millimeter
sccm	Standard cubic centimeters per minute

Abbreviations

AME	American Elements
ΔH_f	Standard enthalpy of formation
EDXRF	Energy Dispersive X-ray Fluorescence
FY	Fiscal Year
ICP-MS	Inductively Coupled Plasma Mass Spectrometry
IDL	Instrument Detection Limit
μ-GC	Gas Chromatograph, Gas Chromatography
MDL	Method of Detection Limit
Ni/k	nickel on kieselguhr
NNSA	National Nuclear Security Administration
PDRD	Plant Directed Research and Development
RGA	Residual Gas Analyzer
RGD	Residual Gas Dryer

RMS	Root mean square
RSD	Relative standard deviation
SAES	Società Apparecchi Electrici e Scientifici
SRNL	Savannah River National Laboratory
SRTE	Savannah River Tritium Enterprise
TEF	Tritium Extraction Facility
TGA	Thermogravimetric analysis
TPS	Tritium Process Stripper
XRD	x-Ray powder diffraction
Z-Bed	Zeolite bed

Chemicals/Elements

Al	Aluminum
Ar	Argon
C	Elemental carbon
Co	Cobalt
CO	Carbon monoxide
CO_2	Carbon dioxide
CH_4 or CQ_4	Methane with various hydrogen isotopes
Cr	Chromium
Cu	Copper
Fe	Iron
H_2	Protium hydrogen isotope
He-3	Helium 3 or ^3He
Hf	Hafnium
Mn	Manganese
N_2	Nitrogen
Ni	Nickel
NH_3 or NQ_3	Ammonia with various hydrogen isotopes
NO_x	Nitrous oxide
O	Elemental Oxygen

O_2	Oxygen
Q_2	Hydrogen isotopes (Protium (H), Deuterium (D), or Tritium (T))
Q_2O	Water with various hydrogen isotopes
Si	Silicon
Sn	Tin
Ti	Titanium
V	Vanadium
Zr	Zirconium

1.0 Introduction

The Savannah River Site Tritium Facilities use various getter materials (SAES® ST909 and ST198) as part of the tritium process stripper (TPS) for the removal of select gas species. ST909 is a consumable getter material placed in the process within the diffuser train prior to the ST198 bed. ST909 cracks various impurities (methane, carbon oxides, ammonia and others), and releases tritium bound in the compounds for further processing while gettering impurities in the process stream. Palladium-silver diffusers are used to separate the released hydrogen from the gas stream. The ST198 bed removes any residual hydrogen isotopes from the gas stream before eventual discharge through the stack. During FY15, impacts of an upset of ST909 in the process to the downstream ST198 bed were explored. The results from testing were presented in the document SRNL-STI-2015-00466 [1]. Results of FY15 testing indicate that ST198's susceptibility to poisoning is highly related to bed operating temperature.

The relative expense of ST909 (up to ~$5300/kg depending on quantity ordered) as well as the difficulty in obtaining it (foreign sole source provider) make the exploration of alternative materials and/or getter suppliers a pressing need before issues arise. If the supply chain is disrupted, it would leave the Tritium Facilities without an in-kind replacement material for the ST909 getter beds and would in turn hamper operational capabilities; possibly putting the overall mission at risk.

In the event that ST909 is no longer available from SAES Getters, an alternative material or materials need to be identified well in advance. This report summarizes test work performed during FY16 as part of the Plant Directed Research and Development (PDRD) project for the evaluation of alternative getter materials. The goal of this project is to provide recommendations for an alternative material or material combination that can provide the same efficiency currently seen for methane cracking and ammonia decomposition when using SAES ST909. The expense of ST909 as well as availability from a sole-source-foreign supplier (and thus a greater potential that the material may become unavailable) are the primary reasons that replacement materials need to be identified.

2.0 Background Information

Getter materials are designed to preferentially react with select gas species present. The gettering process depends on the adsorption of gas molecules on the surface and the absorption of the gas molecules and elements into the solid. Chemical binding or reaction of the gases with the surface atoms allows chemical bonds to be broken.

Although ST909 is effective under a variety of carrier gases and operating conditions, ST909 is a consumable product that cannot be regenerated. It is a sacrificial material which releases bound tritium from molecular compounds (thus prevents inventory loss) and protects the diffuser series from impurities that could lower performance. The ST909 material also removes impurities that could potentially have deleterious effects on the downstream ST198's hydrogen gettering effectiveness.

2.1 Operating Condition Considerations

The ability of getter materials to function properly is highly dependent on operating temperature, the concentration of species present in a gas stream undergoing treatment, and the

carrier gas used. This means that the movement of a getter material from one point in a process to another may inadvertently alter performance. For instance ST198 functions well in the gettering of residual hydrogen in a nitrogen carrier gas stream at temperatures around 350°C when ST909 is placed upstream of it. The ST909 removes gas constituents such as carbon monoxide (CO) and ammonia (NQ_3) that can diminish the performance of the ST198 [1]. If the ST198 was operated at lower temperatures it is more likely to be deactivated and performance would decrease if CO or NQ_3 are present. If ST198 were operated at temperatures above 425°C in a nitrogen rich environment, ST198 could undergo exothermic nitriding reactions.

Zirconium based materials can be used as hydride materials which is seen in the use of ST198 as a tritium polisher. For the case of ST198 the temperature must be kept high enough that the active sites for impurity processing remain open, yet low enough for continued hydrogen absorption. Researchers have found that lower operating temperatures (250°C) increases ST198 hydrogen gettering performance [2]. However, it is known that the plateau pressure of hydrogen, which relates to the absorption and desorption capability of the isotopes on a hydride material, will change based on the operating temperature of the getter. Though some hydrogen isotopes will be lost to the getter, by keeping the temperatures elevated high enough, most of the hydrogen should pass through to additional downstream processing.

A nitrogen carrier gas will interfere with the gettering ability of ST909 towards other compounds at higher bed operating temperatures. The literature suggests that ST909 may absorb up to eight to nine percent of its initial weight in nitrogen [3]. This has been confirmed in the laboratory during the testing in FY16.

Any material identified as a replacement of the ST909 bed in the TPS must account for the variable operating conditions of the process stream. Process design must also be able to account for changes that the getter imposes on the gas constituents. For example, carbon dioxide may be reduced in the presence of ammonia; yet, carbon monoxide becomes more abundantly present [4]. The presence of either carbon monoxide or oxygen will decrease the methane cracking efficiency of ST909 [4].

ST909 and ST198 are used in the tritium process stripper within the diffuser train. A simplified illustration of the tritium-purification-system-diffuser train is found in Figure 2-1.

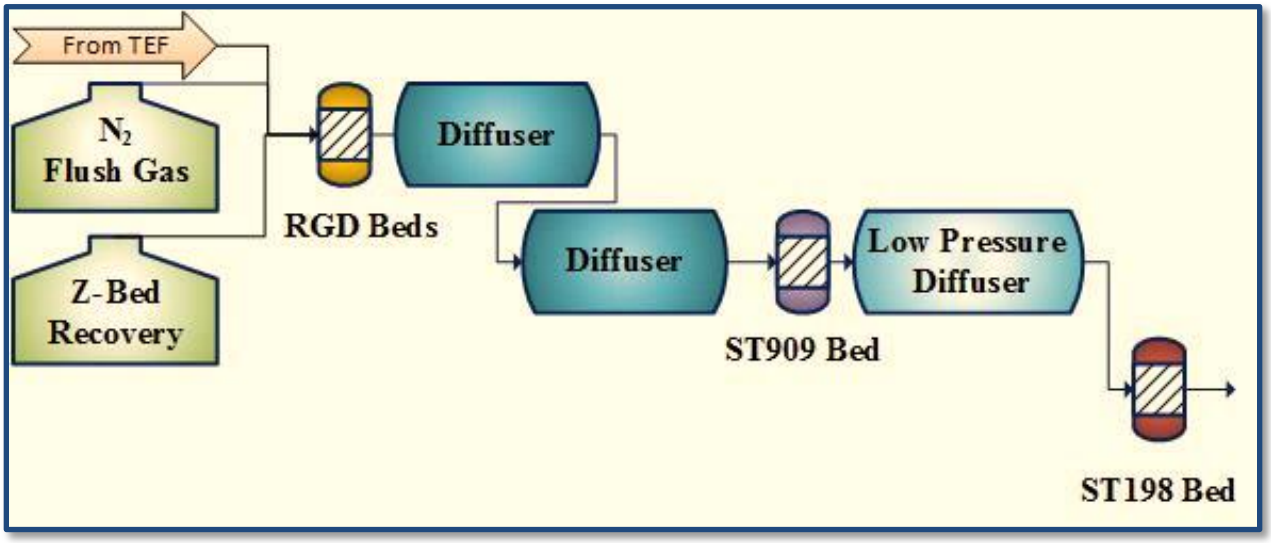

Figure 2-1: Simplified flow diagram of the tritium process stripper

Several source gases feed the tritium process stripper. These sources include gases from the Tritium Extraction Facility (TEF), N_2 flush gas, Z-bed recovery system, and others. The variety of sources causes great variability in the process conditions in which anywhere from zero to (theoretically) one hundred percent nitrogen could be passed processed. Average operating conditions indicate that the N_2 will be present in significant quantities and should be regarded as the typical carrier gas.

The identified major components of the gas stream prior to the residual gas dryer (RGD) include: N_2, argon (Ar), hydrogen (Q_2 where Q represents any hydrogen isotope – protium (H), deuterium (D), or tritium (T)), helium (He-3), methane (CQ_4), NQ_3, CO, carbon dioxide (CO_2), oxygen (O_2), and water (Q_2O). Relative quantities of these gases are dependent on operations.

Though ammonia is also considered, the main impurity of interest for ST909 interaction is methane for PDRD FY16 testing. The other gas components will be treated prior to the ST909. The diffusers will remove the bulk of the hydrogen; whereas the RGD will remove the bulk of the water. Due to the fact that separating water and ammonia is more complicated, it is likely that much of the ammonia present will also be removed at the RGD stage. The positioning of the RGD, as shown in Figure 2-1, indicates that water may not be a major constituent of the gas stream.

If water can be neglected, only O_2, N_2, CO, CO_2, NQ_3 and CQ_4 remain to be cracked and their non-hydrogen isotopes to be gettered as appropriate. Because the concentration of the gas is quite low and because CO_2 interaction with ST909 was previously studied, it was therefore considered less pertinent for FY16 testing [4, 5].

2.2 SAES ST909

SAES ST909 is the trade name for a zirconium-manganese-iron alloy getter produced by SAES Getters. ST909 is useful for the removal of carbon oxides and oxygen. This getter material

can also decompose compounds of tritiated water, methane, and ammonia that are contained in process gas streams. ZrMnFeAl is an intermetallic ternary compound [6]. The composition of SAES ST909 provides a basis as to why it is effective for use in decomposing tritiated water, methane, and/or ammonia in various conditions. ST909 has a nominal alloy atomic composition of $Zr(Mn0.5Fe0.5)_2$ or Zr-Mn-Fe (40.5% Zr, 24.5% Mn, 25.0% Fe, 10% Al) [7]. Manganese and iron provide catalytic active sites for the decomposition of the various impurity gases – CQ_4, NQ_3, CO, and CO_2- and zirconium provides the active sites for the gettering of elements. Zirconium is a hydride material however the hydrogen plateau pressure lowers as operating temperature increases.

2.3 Theory of how ST909 Works

In order for ST909 to crack and remove impurities from the gas stream, the getter material must first be activated. Although zirconium can form hydrides at room temperature, zirconium can also quickly oxidize at room temperature. The safety data sheet for ST909 indicates that it is potentially pyrophoric [8] yet it is loaded and stored in an oxygen rich environment. This is possible due to the fact that a passivated layer exists on the surface at ambient conditions. A type of passivation layer is illustrated in Figure 2-2.

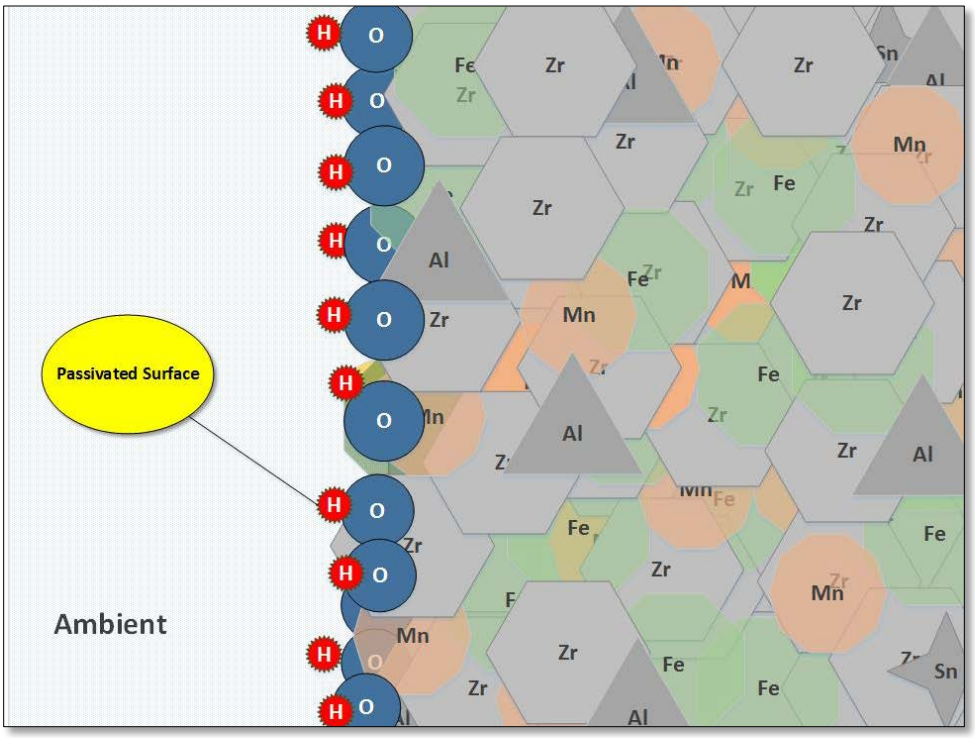

Figure 2-2: Illustration showing passivated surface on ST909

Activation of the materials is performed at high temperature under a flowing inert gas. At elevated temperatures the oxide layer initially on the surface of the ST909 diffuses into the bulk metal of the non-evaporable getter. This movement provides a 'clean' surface that is ready to adsorb more gas. Volatile species are also swept away with the flowing inert gas. The proper

outgassing temperature for many zirconium getter alloys lies somewhere between 1000°C and 1700°C. However, where it is deemed inadvisable to heat the getter material to that temperature range (because of alloy material characteristics, process conditions, or other reasons), a minimum outgassing temperature of 700°C is necessary for activating the surface of several zirconium getters. During activation, some loosely bound surface elements may be released into the gas phase and swept away with the flowing argon. Other released components may re-attach to the surface of the material and interact with the active sites. Components may be dissociated and the elemental constituents will diffuse into the bulk mass as zirconium bonds are transferred. A simplified illustration of the activation process is shown in Figure 2-3.

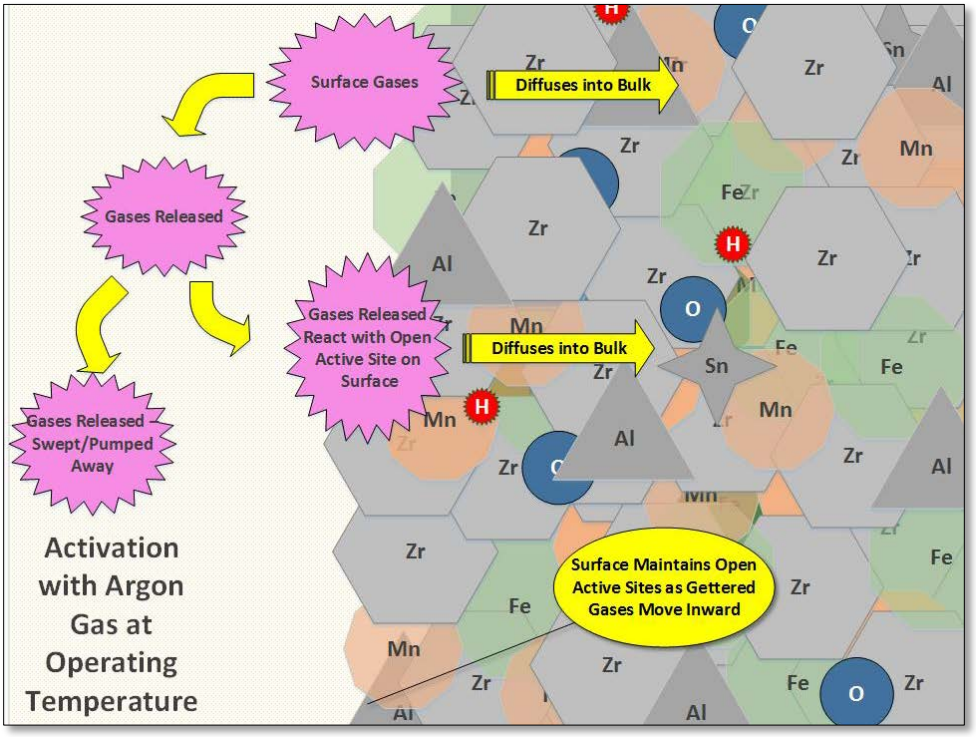

Figure 2-3: Illustration showing ST909 activation with argon

As long as enough energy (or in this case a great enough temperature) is present, the active sites on the surface will remain clean as elements are transferred inward. At 670°C, diffusion of oxygen and other impurities into the ST909 occurs at an acceptable rate such that the getter can operate in the presence of low concentrations of impurities while still retaining reasonably high adsorption and absorption rates of gettered elements. Otherwise, the thin layer of oxide (or other zirconium compounds, such as carbides and nitrides) further hinders the diffusion of oxygen, nitrogen and carbon into the bulk mass of the ST909 material. The various components gettered will initially bind with active sites on the surface of the material. An oxide layer on the surface of the alloy prevents reaction with the material.

The strength of chemical bonds varies with the elements involved. The standard state enthalpy changes for several bonds of interest are shown in Table 2-1. The presented data relate

to bond dissociation enthalpy or bond dissociation energy (enthalpy change) for a bond A-B, which is broken through the reaction:

$$AB \leftrightarrow A + B$$

Table 2-1: Various bond dissociation energies of gas phase compounds ΔH_f at 298K [9]

Bond Type	ΔH_f (kJ/mol)	Bond Type	ΔH_f (kJ/mol)	Bond Type	ΔH_f (kJ/mol)
D-D	444.34	**H-CH_3**	431.8	**H-NH_2**	435 ± 8
H-H	436.0	**H-CH_2**	473 ± 4	**H-NH**	377 ± 8.4
H-OH	498.7 ± 8	**H-CH**	421.7	**H-N**	356 ± 8
C≡O	1076.5 ± 0.4	**H-C**	339 ± 2.1	**N≡N**	945.42 ± 0.04

The various bond dissociation energies, which include Zr, Fe, and Mn for metal ligand (ion or molecule attached to a metal atom by coordinate bonding) and other types of bonds, are found in Table 2-2: The greater the value of the dissociation energy, the more energy required to cleave the bonds.

Table 2-2: Metal ligand bond dissociation energies ΔH_f at 298K [9-11]

Bond Type	ΔH_f (kJ/mol)	Bond Type	ΔH_f (kJ/mol)	Bond Type	ΔH_f (kJ/mol)
Zr-O	760	**Fe-O**	409	**Mn-O**	406
Zr-N	565	**Fe-CH_3**	242 ± 10	**Mn-CH_3**	213 ± 8
		Fe-CH_2	347 ± 17	**Mn-CH_2**	297 ± 13
		Fe-CH	426 ± 30		
Zr-C	561	**Fe-C**	397 ± 30		

Getters act as a catalyst and allow the reaction to follow a different pathway:

$$AB + metal \leftrightarrow AB^* + metal$$

$$AB^*/metal \leftrightarrow (A \cdots B)/metal$$

This means that the ligand bonds to the iron or manganese are much easier to form, rearrange, and cleave. Bond strengths are illustrated in Figure 2-4. Individually, the element zirconium forms rather stable bonds and the movement of gettered atoms would be too slow for practical purposes. By alloying the zirconium together with the iron and manganese the bonds between the elements in the getter with the oxygen, nitrogen, and carbon can be more easily transferred.

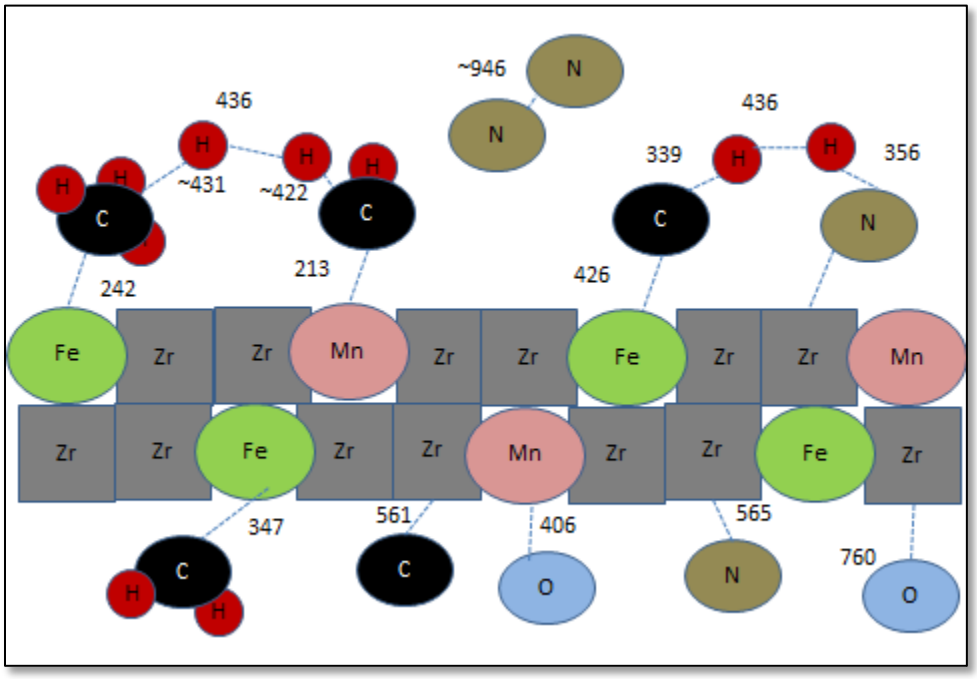

Figure 2-4: Illustration showing various relationships of bond dissociation energies (kJ/mol at 298K)

Aspects of the nature of gettering in ST909 are shown in Figure 2-5. Based on the bond dissociation energies it can be theorized that at elevated temperatures zirconium reacts preferentially with oxygen; next with nitrogen found in nitrogen containing compounds (e.g., ammonia, nitrogen gas); then carbon from carbon based impurities, such as methane; and finally hydrogen. This has been observed in the literature [12, 13]. This means that bound active sites on the surface of a pellet by more preferential elements will inhibit further gettering abilities of less preferential elemental species.

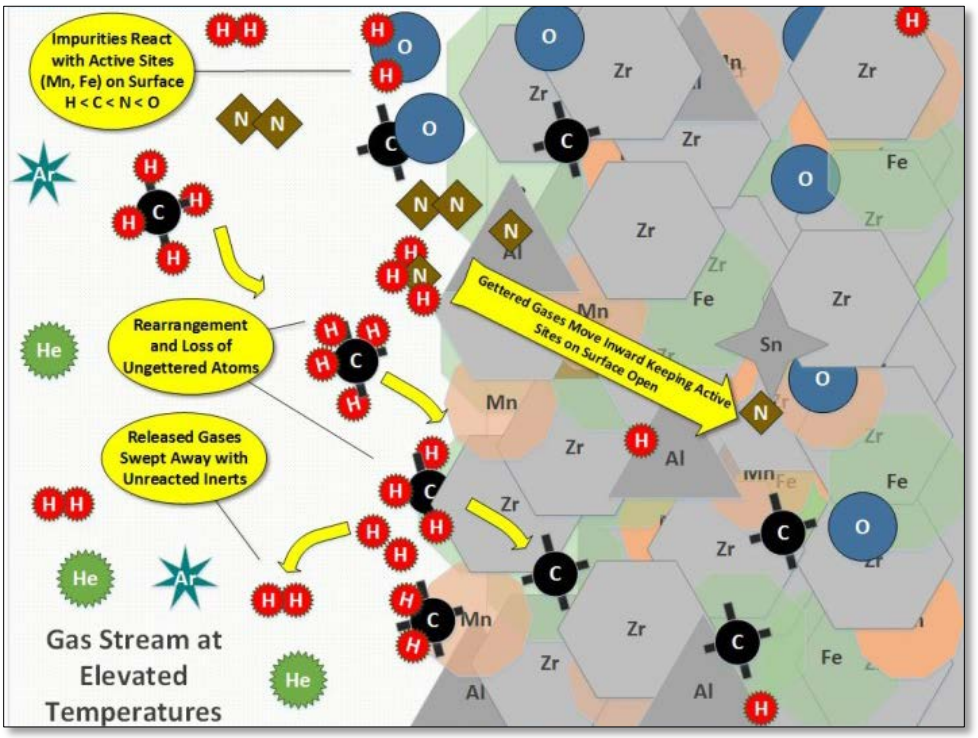

Figure 2-5: Illustration of ST909 cracking and decomposing of various compounds

It may be possible to semi-reactivate a getter if the gettering capacity is compromised following the addition of a poisoning compound, such as sulfur based compounds. This is possible if the elements are only chemisorbed on the surface of the getter [14]. Reactivation could be accomplished by heating the material to a higher temperature, which may allow the reversible hydriding material to be freed from the material. However, heating may also release some of the elements that were previously gettered, (oxygen, nitrogen, carbon, and sulfur) which would need to be processed. Metal carbides are the least reversible upon heating [14]. Decrepitation should also be considered if reactivation of a gettered material is attempted. During the gettering process the bonds that hold the alloy together are rearranged. Removal of newly formed bonds could allow the material to cleave along boundary lines and thus induce the formation/introduction of small particulate matter in the process.

Water has been shown to decompose on ST909 particles at temperatures greater than 350°C into hydrogen and oxides. Methane has been shown to decompose at temperatures greater than 650°C into hydrogen and zirconium carbides [15]. Some researchers have indicated that methane removal generally requires temperatures greater than 400°C [16]. Carbon monoxide was not present within these tests but the temperature would likely need to be elevated to prevent deactivation.

From the literature, a diagram depicting equilibrium decomposition for methane at 760 torr as a function of composition and temperature is shown in Figure 2-6 [17]. Compositions to the left of an isotherm favor methane decomposition, whereas compositions to the right of an isotherm favor methane reformation.

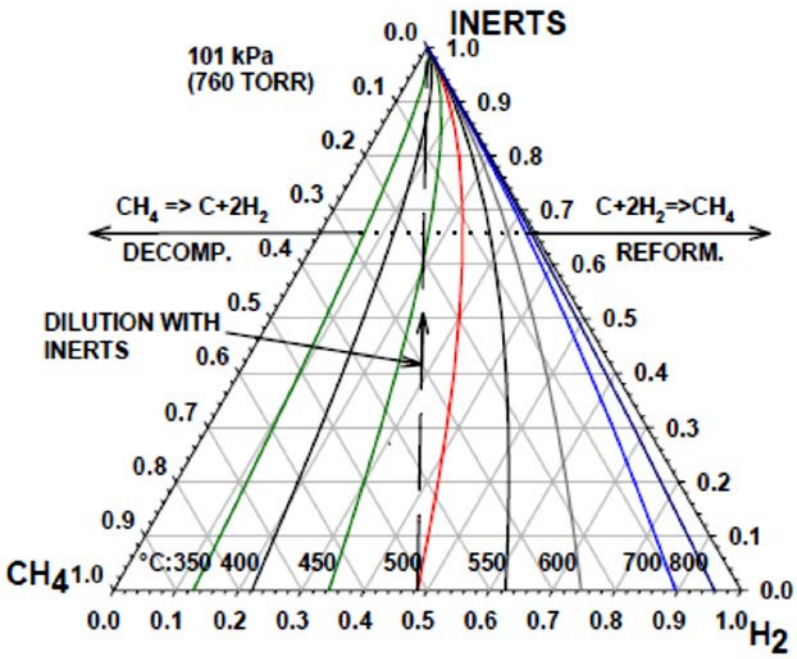

Figure 2-6: Methane decomposition equilibrium plot [17]

Although protium was used in the calculations, based on the diagram the optimal operating conditions for methane cracking can be construed based on a particular placement on the chart. The diagram can be used to explain why recombination effects can cyclically occur at a given temperature if the methane is simply cracked rather than having the carbon 'irreversibly' gettered.

In industry, ammonia is formed at high pressures generally using catalysts such as iron treated with potassium hydroxide. The formation of NQ_3 is described by the reversible reaction:

$$N_2 + 3Q_2 \leftrightarrow 2NQ_3$$

In the forward direction the reaction is exothermic (ΔH_f = -46.1 kJ/mol). Based on Le Chatelier's principle, as temperature increases, the equilibrium should shift to the left. This implies that at higher temperatures (greater than 400 – 450 °C) ammonia will decompose and more moles of Q_2 and N_2 will be in the gas phase. Below 400 – 450°C the reaction kinetics favoring ammonia decomposition is far slower. Above 1100°C the reaction is most favorable towards decomposition. However, this temperature represents an added challenge for glovebox operation. The presence of a catalyst changes the reaction kinetics as it provides a surface whereon the reversible reactions can occur at less extreme temperatures.

Figure 2-7 shows the equilibrium based calculation of the quantity of moles that could be formed based on equilibrium considerations (see Appendix A for calculation details). A gas mixture consisting of 1 mole total at an initial pressure of 760 torr of a combination of protium (H_2) and nitrogen (N_2) are allowed to react to complete conversion. The moles of NH_3 formed for each initial mole fraction of H_2 are graphed.

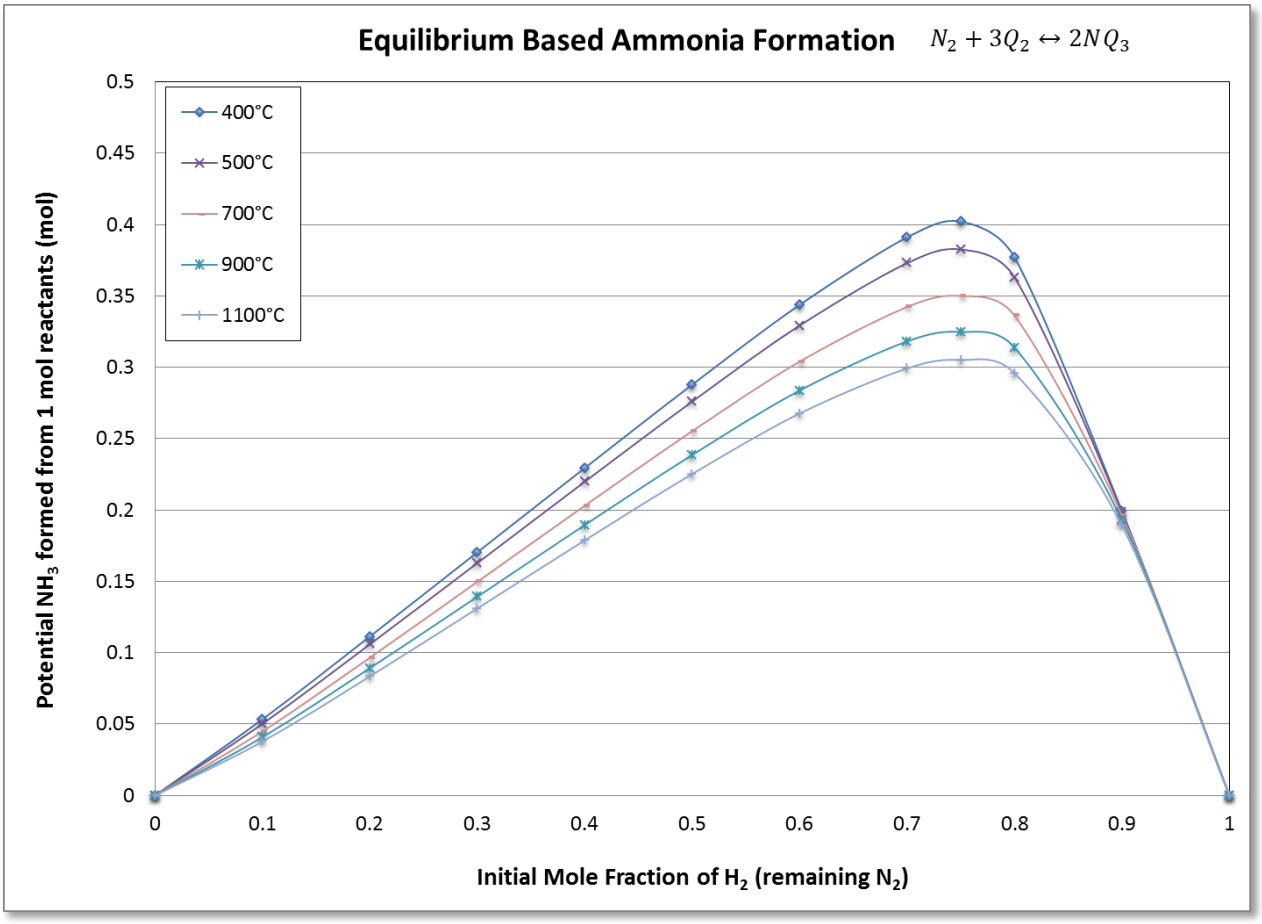

Figure 2-7: Ammonia formation equilibrium plot

Switching gas compositions during operations could cause ammonia formation if conditions are ideal. The transition time from a high hydrogen gas to a high nitrogen gas in the same vessel could inadvertently induce ammonia formation based on Le Chatelier's principle wherein an iron surface, such as a heated wall of a tank, could act as a catalyst. Minimizing high pressure, high temperatures, and gas mixtures favorable to ammonia formation within the process should help minimize ammonia formation. However, it is recommended that the equilibrium based reaction shown in Figure 2-7 be considered especially when identifying getters for the decomposition of ammonia. Figure 2-7 shows a transition around 0.75 moles of H_2 present where the number of moles of NH_3 formed decreases. In practice, higher pressure favors ammonia formation.

Even though equilibrium calculations favor ammonia formation, it could take up to several years for the reactions to reach complete conversion at lower temperatures. For this reason, the gas temperature and pressure should be such that the formation of ammonia is minimized when hydrogen isotopes are expected to come in contact with nitrogen rich streams. The localized radiolytic effects induced from tritium decay could make such a suggestion inconsequential as ammonia formation could occur even if a vessel is maintained at lower operating temperatures.

2.4 The Periodic Table of Elements Generally Considered [18]

Review of the periodic table of elements provides a useful means of getter material down selection. A quick evaluation of the 115 known elements considered whether the elements are product gases, the intended gettered elements, halides, toxic, nonreactive noble gases, known product-gas getters, artificially prepared, not appropriate for the application, expensive, or could generate undesirable compounds. Based on a quick evaluation of these criteria only 33 elements remained for selection. Figure 2-8 shows the down selection criteria performed on the periodic table of elements and the elements remaining for use within alloys for cracking methane and ammonia.

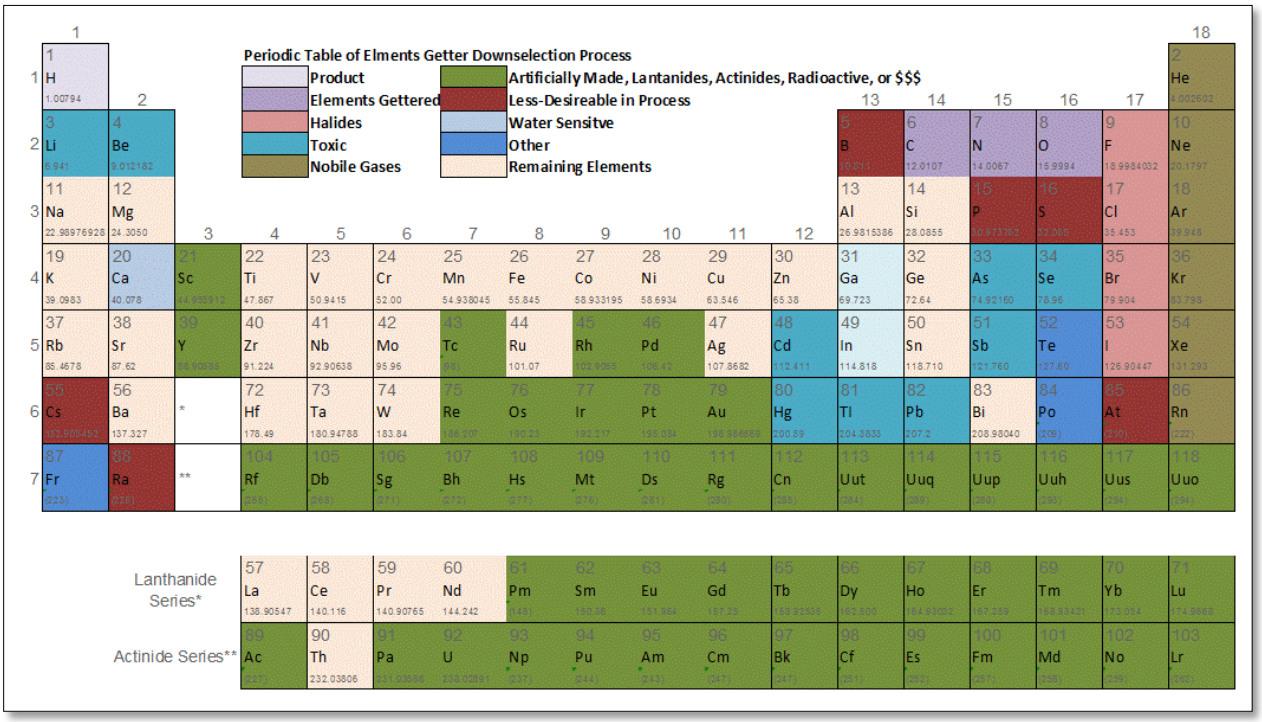

Figure 2-8: Periodic table of elements reviewed as potential getter material component

Group IV metals (shown in Figure 2-8 which includes zirconium) are generally well suited as getter materials. Getter alloys are generally comprised of zirconium and/or titanium with other transition metals or aluminum. Therefore, commercially available alloys containing zirconium and titanium were reviewed for their potential at gettering oxygen, nitrogen, and carbon. Although tantalum could potentially work as well, it has historically been more expensive than zirconium and requires somewhat lower operating temperatures. Both zirconium and titanium have the potential of gettering hydrogen, however, operating conditions and competing rates for gettering of the gas species should be taken into account as was discussed in sections 2.1 and 2.3. The cracking efficiency of a getter material is generally related to the other metals (in the case of ST909 manganese and iron) which are part of the alloy as well as the operating temperature conditions.

The original patent relating to ST909 covered compounds with the formula ZrM_1M_2, where M is any transition metal selected from the group consisting of Cr, Mn, Fe, Co, Ni and mixtures thereof [6]. Each constituent of the ST909 alloy is needed for ST909 to function well for methane cracking.

Before carbon gettering can occur, the methane must first be cracked. The cracking of methane by ST909 requires both iron and manganese [19]. This can also be inferred in that at 350°C, ST198 (a Zr-Fe getter material) shows only slight cracking efficiency for methane.

Literature suggests that alumina supported manganese oxides are effective in the reduction of NO_x and ammonia [20]. The aluminum content of ST909 is initially found in many phases within the ZrMnFeAl alloy. Alloys containing aluminum, carbon, as well as the other available elements have been found to decompose ammonia during methane cracking tests at temperatures above 650°C [21]. This may imply that the aluminum also plays an active role in methane cracking.

2.5 Temperature

Once activated, zirconium getters can generally serve as a getter at temperatures greater than 400°C [22]. On the low end of the temperature range, SAES ST198 (a zirconium iron material) can be activated at 450°C in an argon atmosphere and operated at between 250°C and 350°C for hydrogen gettering activities in a nitrogen atmosphere. Above 425°C, the risk of a runaway nitriding reaction is present and is unadvisable if a nitrogen carrier gas is used. For ST198, lower temperatures cause the getter material to become more susceptible to deactivation [1]. This is likely true for other getter materials as well. Literature indicates that zirconium-based materials have shown a reduction in methane cracking performance by nitride formation when tested with a nitrogen carrier gas [23].

A zirconium, vanadium, iron alloy, ST172, can be operated at various temperatures to achieve varying results [16]. If two beds of the material are operated at 650°C and 110°C, respectively, the first bed will crack methane and the second could be used to getter hydrogen. This hydrogen gettering ability is a function of the impurities previously being removed by the first bed and the fact that the gas stream tested was a mixture of helium, methane and hydrogen as opposed to a nitrogen rich stream.

2.6 Catalyst Materials in General

Getters are composed of catalyst materials in that the addition of certain elemental species within a metal matrix lowers the activation energy needed for the decomposition of undesirable species within a gas stream. What makes a getter useful is the ability to selectively remove undesired constituents. Although many catalysts can decompose CO, CO_2, NQ_3 or CQ_4, their application is not advisable if unwanted byproducts are formed. For instance, ruthenium on alumina is a relatively expensive material ($7700/kg, 5% Ru loading) that is useful for the decomposition of ammonia. However, carbon dioxide is known to decompose over a ruthenium catalyst and in a hydrogen environment the freed carbon and oxygen elements can form methane and water, respectively.

2.7 Non-Evaporable Getters

Unlike a catalyst that can simply crack compounds, getters provide the added benefit of forming stable bonds with selected elements, which undergo adsorption and absorption processes in the material. Chemical bonds of the gases are broken on the surface of the getter material. The rates at which bonds are broken and absorption occurs within the getter material are based on temperature. If lower temperatures are used then the adsorbed elements may form a passivation layer, which prevents the absorption of elements to the inner portions of the material. Gases will interact with a non-evaporable getter in several ways. Hydrogen isotopes are adsorbed reversibly whereas CO, CO_2, O_2, and N_2 are adsorbed irreversibly. Hydrocarbons, Q_2O, and NQ_3 are adsorbed in a combination of reversible and irreversible processes. Hydrocarbons are adsorbed more slowly than water and efficiency is low below 450°C. Noble gases are not adsorbed.

Based on a preliminary review conducted in FY15, a single, commercially available off the shelf material that can replace the ST909 and perform all of the same functions was not identified at that time. Other materials can effectively decompose the various impurities on an individual basis; however, the use of multiple compounds could require significant changes to the process to effectively remove all of the same impurities as the ST909. A series of screening experiments was completed in 2007 in an attempt to find a potential replacement material for ST909. A report was subsequently issued (WSRC-STI-2007-0141) that described results related to the screening tests for improved methane cracking materials [24, 25].

Literature suggests that although many materials, including other SAES getter materials, may have better methane cracking performance than ST909, no other single material was ideal for use in all three carrier gas streams (helium, hydrogen, and nitrogen) tested in previous experiments [23]. However, the main carrier gas in TPS is nitrogen. Therefore, the ability of the getter to function in three carrier gas streams may be irrelevant.

3.0 Vendors

There are a limited number of vendors for getter materials. The Italian based Società Apparecchi Electrici e Scientifici, or ***SAES,*** group is considered the primary supplier of non-evaporable getter materials world-wide. SAES labels alloys according to the nomenclate ST, which means stabil, followed by a number.

Other international companies who deal in general getter materials include:

- ***Nanjing TPY Getter Material Co***. (China), the ***Zhenjiang Star Group*** (China) and ***GTI*** (Hong Kong China).
- ***KBM Affilips Master Alloys*** (The Netherlands) – produces an 80% Zr balance Fe alloy, ZrNi, and 30% Mn balance Te alloy.
- The Canadian company, ***Tyne Engineering***, produces getter beds. The types of getter beds they produce range in size of 1 gram to 5 kg of material. The materials employed include depleted uranium, zirconium iron, nickel, titanium, molecular sieves, and zirconium cobalt. However, trade restrictions may interfere with obtaining any materials from Tyne Engineering for use in the tritium facility.

U.S. based companies who produce non-evaporable getters supply various products. Identified producers include:

- ***Gamma Vacuum***, based in Minnesota, produces non-evaporable getter cartridges which contain zirconium vanadium and iron alloys.
- ***Johnson Matthey*** produces several zeolite materials that can absorb CO_2 and Q_2O and Q_2. However, zeolite materials do not appear to be capable of decomposing the materials for eventual hydrogen isotope recovery which means they would not serve as a good replacement for ST909.

Some companies do not identify the zirconium alloys they produce as a getter material. However, this does not imply that the materials will not work if the material can be activated.

- ***All Metal Sales*** of Westlake, Ohio, can produce zirconium vanadium alloys.
- ***American Elements***, (AME) has been identified as a supplier of zirconium alloys that may be potentially used as getter materials. They produce a variety of materials which include: Ti:Mo:Zr:Fe, and Zr:Fe. They are willing to produce Zr:Mn:Fe:Al pellets but this is a special order item. During FY16 it was found that AME did not produce their materials by powdered metallurgy which is employed by SAES. AME produced materials using a melted ingot approach.
- ***ATI Metals*** of Pittsburgh, Pennsylvania produces several zirconium, titanium, niobium, nickel and cobalt products. They produce alloys of nickel titanium and iron.
- ***Belmont Metals*** in Brooklyn, New York, indicates that they can produce zirconium alloys. However, they do not indicate which alloys they produce. This implies these are likely not off the shelf materials that require special order and thus added expense. Even with the added expense their costs may be lower than importing a product from a foreign provider.
- ***California Metal & Supply Inc***. located in Santa Fe Springs, California, can produce alloys of titanium with iron, aluminum, vanadium, and molybdenum.
- ***Eagle Alloys*** corporation of Talbott, Tennessee, produces zirconium niobium alloys
- ***Mil-Spec industries*** of Glen Cove, New York, list zirconium silicate, zirconium nickel alloy, and NiAlZr powder.
- ***Colonial Metals Inc.***, located in Elkton, Maryland specializes in precious metals but they may have the ability to produce other materials.

Identified getter materials, vendors, and differing applications of the materials are found in Appendix D.

4.0 Alternative Materials Individually Considered

Several materials were obtained for testing purposes. A generalized description of each material is found in subsections 4.1 to 4.6.

4.1 AME ZrMnFeAl

The composition of the zirconium-manganese-iron-aluminum pieces obtained from American Elements is approximately 40.5/24.5/25/10 wt%, respectively. For safety information

see the related safety data sheet [26]. The American Elements reported trace element composition is:

Table 4-1: Reported trace element composition of AME AlNiFe

Analysis	%
Ni	0.0032
Si	0.0028
Cr	0.0026
Ti	0.0008
Cu	0.0045
O	0.0680

4.2 ST707

For ZrVFe based alloys a measureable depletion of methane requires temperatures in excess of 500°C while an appreciable depletion occurs at temperatures greater than 600°C [27]. At lower temperatures (between 200°C and 300°C) researchers have shown that SAES ZrVFe getters will encourage the reaction of hydrogen and carbon monoxide to produce methane and oxygen [27, 28]. The ZrVFe getter will act more like a hydride material at temperatures lower than 150°C to 300°C if the impurity carbon monoxide is not present. For safety information see the related safety data sheet [29].

4.3 Ni/k

Johnson Matthey supplied Pricat Ni60/15 T 6 mm pellets. The average weight per pellet is ~0.241 grams. For safety information see the related safety data sheet [30].

Nickel on kieslesghur is relatively inexpensive ($770/kg 66% Ni loading) and is also known for its ability to crack methane by the formation of long carbon nano-strand filaments. However, at temperatures below 200°C in the presence of carbon monoxide the highly unstable-explosive compound, nickel carbonyl, $Ni(CO)_4$, can be formed. This material may still be useable if adequate safeguards are in place for temperature control and gas composition. Previous reports indicated that Ni/k did not perform well for methane cracking in a hydrogen carrier environment [23]. The cracking efficiency of methane over Ni/k is directly related to the dispersion of nickel within the support material, smaller nickel particles show better cracking performance.

Nickel in itself is not necessarily inappropriate for use within the tritium containing process stream. If proper temperatures are maintained, nickel containing materials have the ability to perform quite well. If the nickel material is present and decomposition of carbon monoxide to carbon and oxygen occurs and those elements are gettered then undue harm is less likely to ensue. In the event of an upset, it is likely that the surface of many getter materials could become passivated if the temperature of a vessel decreased. Passivation by impurity species is more likely to occur at lower temperatures.

Kieselghur has some inherent characteristics that must also be considered before implementation in a tritium facility. Kieselghur is diatomaceous earth and as such is a naturally occurring rock that is friable and brittle that may have varying composition based on when and

where it is mined. As a naturally occurring soft siliceous sedimentary rock, Kieselghur has waters of hydration that can vary from source location and time of mining. These waters of hydration may be removed during activation but could also remove some of the nickel thus forming small particulate matter that can clog filters. Supplier manufacturing techniques would need to be considered during procurement due to the variable quantity of the waters of hydration. The variable nature of the material could cause performance changes if activation is not performed well. The oxygen content of the amorphous silica is also something that should be considered.

4.4 AME TiMoZr

The composition of the titanium-molybdenum-zirconium-iron pellets obtained from American Elements (listed as AME TiMoZr within this document) is approximately 83.4/11.5/0.6/4.5 wt%, respectively. For safety information see the related safety data sheet [31]. The American Elements reported trace element composition is:

Table 4-2: Reported trace element composition of AME TiMoZr

Analysis	%
Si	0.0063
Mg	0.0026
Ca	0.0015
Cu	0.0055
Al	0.0018
O	0.0630

4.5 AME AlNiFe

The composition of the alumina-nickel-iron (Al_2O_3:Ni:Fe) pieces obtained from American Elements is approximately 50/25/25 wt%, respectively. For safety information see the related safety data sheet [32]. The American Elements reported trace element composition is:

Table 4-3: Reported trace element composition of AME AlNiFe

Analysis	%
Si	0.0072
Sn	0.0003
Mn	0.0043
Cr	0.0004
Cu	0.0017
Mg	0.0002

4.6 AME ZrNi

Zirconium nickel does not perform well in a nitrogen carrier gas stream [23]. However, at temperatures greater than 400°C, Zr_2Ni was shown to effectively crack methane [33]. The

composition of the zirconium nickel pieces obtained from American Elements is approximately 76.5/23.5 wt%, respectively. For safety information see the related safety data sheet [34]. The American Elements reported trace element composition is:

Table 4-4: Trace element composition of AME ZrNi

Analysis	%
Fe	0.0165
Cu	0.0032
Al	0.0115
Cr	0.0036
Si	0.0038
Mg	0.0005

5.0 Comparison of SAES ST909 Versus AME ZrMnFeAl

The US Patent relating to the invention of ST909 was originally issued in 1993 [6]. This means that, as far as can be ascertained, the patent has recently expired. American Elements has indicated a willingness to produce a ZrMnFeAl alloy pellet. If a US supplier can manufacture a material that performs nearly identical to ST909, this would lower the risk to the Tritium Facilities mission.

The cost of the ZrMnFeAl alloy pellet produced by American Elements is roughly 60% less than the cost of ST909 from SAES for the same quantity ordered. If 20 kg of material is ordered the cost for the material would be $1530/kg compared to ~$4200/kg for the SAES ST909 material.

It is unclear if the production methods employed by American Elements are compatible with the requirements given in WSRC-RP-98-00009 for use within a tritium environment. Analysis of both ST909 and AME ZrMnFeAl samples has been performed to compare the materials. This analysis includes a review of sample preparation as well as chemical characterization performed at SRNL. Characterization testing performed at SRNL includes X-ray fluorescence, X-ray diffraction, and inductively coupled plasma-mass spectrometry (ICP-MS).

5.1 Analytical Dissolution

The samples were dissolved in a mixture of HF-HCl-boric acid and the resulting solution is analyzed for elemental composition. Dissolution is the sample preparation step required before elemental analysis by ICP-MS. Both samples required 100 mL dissolution volume of HF-HCl-boric acid for digestion. The digestion factor for ST909 was 166.39 mL/gram with an initial sample weight of 0.6010 grams. The American Element ‘equivalent’ sample had a digestion factor of 489.96 mL/g with an initial sample weight of 0.2041 grams. The digestion factor is used to establish a comparison point of intensities in peaks. In this case, the differences in digestion factor are a matter of initial sample weights rather than difficulty in digesting the materials.

5.2 Analytical ICP

A Perkin Elmer Nexion 300D ICP-MS is used for the quantitative analysis of aqueous solutions at low concentrations (mg/L). The liquid samples generated via dissolution in aqua regia described in section 5.1 of this document were analyzed so that a comparison between the elements present in the ST909 and the AME ZrMnFeAl samples could be made. According to procedure L16.1-ADS-1577 rev1 [35]:

> The ICP-MS provides multi-element analysis of aqueous solutions based on the measurement of atomic species from their ions created in the plasma. Liquid samples are nebulized and the aerosol transported to an argon plasma. In the high temperature plasma (up to 10,000 K) metallic species are ionized. The ions generated by the plasma enter the mass spectrometer through a sampling cone set near the end of the plasma. The ions are separated by quadrupole mass filter and focused on a detector. The detector in this instrument is a dual-mode detector.

The Method of Detection Limit (MDL) is the Instrument Detection Limit (IDL) times the Dilution/digestion factor given in section 5.1 for the respective alloys. Uncertainty in results is the root mean square (RMS) of the method uncertainty and the sample uncertainty. Results showing major elements are found in Table 5-1. The major elements, Zr, Mn, Fe, and Al are bolded for table ease of use. The Relative Standard Deviation (RSD) of each weight percent is also reported. The RSD indicates that standard deviation of the mean value shown. Elements shown with the less than symbol (<) were scanned for but did not have a signal great enough to distinguish it from the background signal.

Table 5-1: Perkin Elmer ICP-MS results for ST909 and AME ZrMnFeAl

Element	SAES ST909 (wt%)		AME ZrMnFeAl (wt%)	
Al	10.5	(10.1 %RSD)	10.5	(10 %RSD)
Ba	0.00599	(18.4 %RSD)	< 0.008	
Co	0.0499	(11.8 %RSD)	< 0.065	
Cr	0.0424	(10.7 %RSD)	< 0.038	
Cu	0.0549	(15.4 %RSD)	< 0.122	
Fe	24.1	(10.1 %RSD)	23.2	(10 %RSD)
Mn	25.4	(10 %RSD)	19.8	(10 %RSD)
Si	0.915	(19.8 %RSD)	1.55	(22.5 %RSD)
Sn	0.634	(10.8 %RSD)	< 0.32	
V	0.0596	(12.5 %RSD)	< 0.085	
Zr	39.5	(10 %RSD)	34.6	(10 %RSD)

The major differences shown in the two samples are the weight percentages of Mn, (25.4 wt% and 19.8 wt%) and Zr, (39.5 wt% and 34.6 wt%) for ST909 and AME ZrMnFeAl, respectively. Additionally, ST909 contains Ba, CO, Cr, Cu, Sn, and V, which appear to be absent from AME ZrMnFeAl.

Elements that were scanned for using the ICP-MS instrument but were not found in great enough concentration to have a signal greater than the background signal are shown in Table 5-2.

Table 5-2: Results of additional elements scanned for using Perkin Elmer results ICP-MS for ST909 and AME ZrMnFeAl

Element	SAES ST909 (wt%)	AME ZrMnFeAl (wt%)
Ag	< 0.084	< 0.247
Ca	< 0.095	< 0.279
Cd	< 0.009	< 0.026
Ce	< 0.207	< 0.61
K	< 0.995	< 2.93
La	< 0.033	< 0.097
Li	< 0.017	< 0.049
Mg	< 0.001	< 0.004
Mo	< 0.049	< 0.144
Na	< 0.183	< 0.539
Nb	< 0.029	< 0.084
Nd	< 0.09	< 0.264
Ni	< 0.024	< 0.072
P	< 0.061	< 0.18
Pb	< 0.143	< 0.421
Re	< 0.036	< 0.105
S	< 0.407	< 0.238
Sr	< 8E-04	< 0.002
Ti	< 0.014	< 0.042
Zn	< 0.011	< 0.032

The sulfur content shown in Table 5-2 for SAES ST909 is reported from the 180.7 nm emission line. The 190.0 nm line yielded 0.623 wt % with a 10.1% RSD. The 190.0 nm emission appeared to be from positive spectral interference from another element in the sample. The revised observation was substantiated by replication at a greater dilution.

5.3 Analytical XRD

A Bruker D8 Advance X-ray diffraction system was also used to compare the ST909 and 'equivalent' American Elements ZrMnFeAl sample. According to procedure L16.1-ADS-1117 rev3 [36]:

> 'Samples are ground in an agate mortar and pestle one at a time with 1 to 2 ml of isopropanol, ethanol, or acetone on the benchtop. The samples are dried and typically will be mounted onto a glass slide one at a time with an amyl acetate/colloidal solution on the benchtop. The slide is allowed to dry prior to performing the analysis.'

The phenomenon of diffraction involves the scattering of x-rays by atoms of a crystal and the reinforcement of scatter rays in definite directions away from the crystal. When a collimated beam of monochromatic x-rays strikes a crystal, the rays penetrate and are partially scattered from many successive planes within the crystal. Diffraction from a succession of equally spaced lattice places results in a diffraction maximum which has sufficient intensity to be recorded. Since the majority of compounds have different interatomic distances in three dimensions. The angles at which diffraction occurs will be distinct for a particular compound. The interatomic distances within a compound result in a unique array of diffraction maxima, which serves to identify that compound. The intensity of these maxima can also be used to quantify the amount of this compound in a mixture.

The scintillation detector, 'consists of a scintillation crystal (sodium iodide activated with a little thallium) affixed to the window of a photomultiplier tube just outside the photocathode (cesium-antimony intermetallic). Each incident x-ray photon striking the phosphor is converted to a burst of visible light photons, which fall on the photocathode. The photocathode emits photoelectrons, which in turn, initiate a secondary electron multiplication process in the photomultiplier tube. The current pulse occurring at the anode of the tube is amplified by a charge sensitive preamplifier and sent to the x-ray system processing electronics. The scintillation counter supplies pulses whose height is proportional to the energy of the incident quanta.'

Results of the two tests are found in Figure 5-1 peaks and peak intensities that differ are marked with arrows. The crystal structure of both materials is similar to $ZrMn_2$.

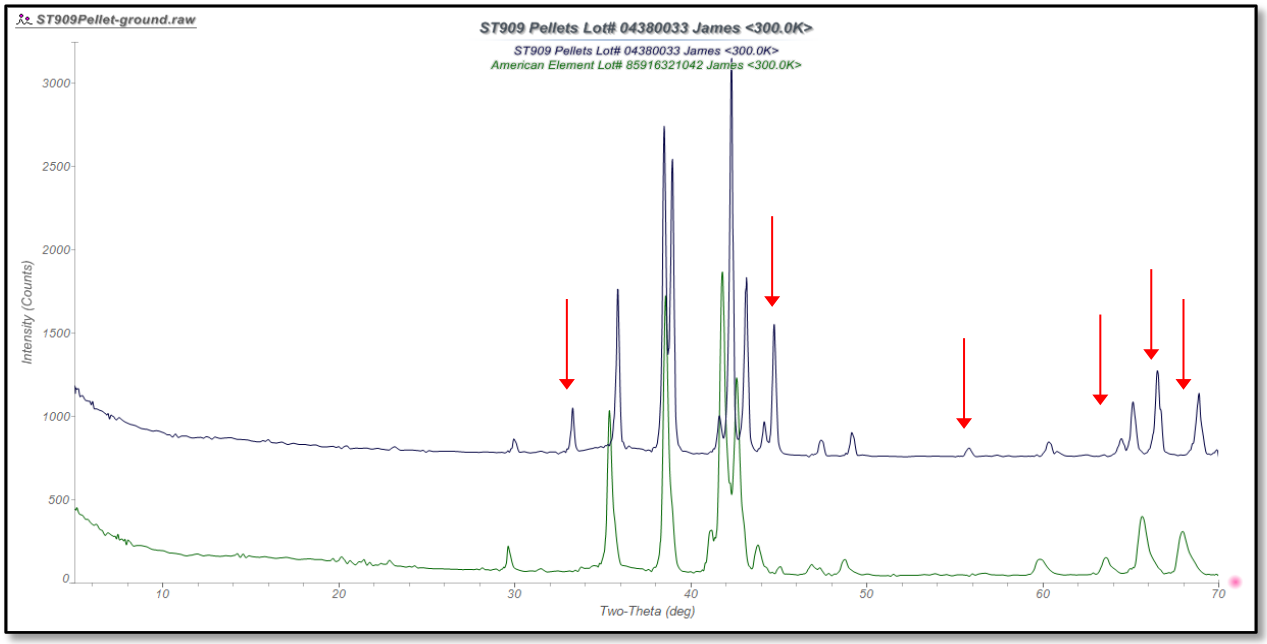

Figure 5-1: ST909 and AME ZrMnFeAl equivalent XRD results

5.4 Analytical X-Ray Fluorescence

X-Ray fluorescence (XRF) was performed on the ST909 and 'equivalent' American Elements sample by Analytical Development. This is accomplished using the Amptek system. According to procedure L16.1-ADA-1129 [37]:

> 'The Amptek system is a computer-controlled x-ray fluorescence spectrometer used for non-destructive elemental analyses of elements. A sample is irradiated with x-rays which cause the loss of inner shell electrons from the constituent atoms. These inner orbital vacancies can be filled by electrons in a higher energy shell. To maintain conservation of energy, an x-ray photon, whose energy is the difference between the two levels, is produced. The energy of each emitted x-ray is well-defined and characteristic of the element from which it originated. The rate at which x-ray photons are emitted by a particular element is related to the concentration of the element.
>
> The Amptek system features an energy-dispersive lithium-drifted silicon detector and a transmission target miniature x-ray tube. The sample is fluoresced by the characteristic and bremsstrahlung x-rays emitted from the tube.
>
> A sample, mounted onto a 2" x 2" square plate, is inserted into the sample chamber and positioned underneath the x-ray tube and spectrometer by a spring loaded backing plate. A shield door, which covers the sample access area, must be slid into place and engage a micro-switch before the tube can be energized.'

The EDXRF K-ratios from the ST909 and "equivalent" American Elements sample are nearly identical as is shown in Table 5-3. Smoothed curves of the data are found in Appendix B.

Table 5-3: X-ray fluorescence results of ST 909 and AME ZrMnFeAl samples

	Inten_0	ST909	K Ratio	AmElem	K Ratio
Zr Ka	10249.1	5127.9	0.500	5103.7	0.498
Zr Kb	1453.2	783.8	0.539	782.4	0.538
Zr La	890.8	371.7	0.417	422.0	0.474
Fe Ka	25936.1	5739.4	0.194	6190.1	0.211
Fe Kb	3364.6	549.2	0.163	606.6	0.180
Mn Ka	26255.5	5140.6	0.196	5206.4	0.198
Mn Kb	3566.8				

There are differences in the minor elements determined by XRF:

- The ST909 sample has V, Cr, Ni, Cu and Sn (all at < 0.5%) missing from American Elements.
- The American Element sample has Hf (at < 0.5%) missing from ST909.

5.5 Metallurgy

5.5.1 SAES ST909

There are four commonly employed methods for the manufacturing of alloys: the fusion method, the electro-deposition method, the reduction method, and powdered metallurgy. SAES ST909 is produced by a combination of the fusion and powdered metallurgy methods for production.

> According to SAES patents, the ST909 alloys can be produced "by melting lumps or chunks of the desired components in the desired weight ratio. Generally the use of lumps or chunks is preferred as this decreases the amount of surface contamination from atmospheric gases; however, small amounts of powders can be used to achieve the desired weights. Homogeneity can be improved by re-melting the alloy between about two and about five times in which the ingot from the previous melt is crushed and the resulting powders are mixed before the subsequent melt" [7].

5.5.2 American Elements ZrMnFeAl

American Elements produces their alloy by the fusion method in that the samples produced were manufactured by melting chunks of the desired components in the desired weight ratio. However, American Elements does not follow up with the powdered metallurgy method of preparing the final product. American elements indicated that alloy samples are prepared using vacuum melting to ensure high density materials. They anticipate an initial oxygen content of less than 800 ppm. Activation of the material will cause the exterior oxide layer to be absorbed by the getter material in a similar manner to that incurred with ST909.

The main difference that would likely be seen from the two sample preparation methods is a change in surface area. However the surface area of the two materials was not measured.

It is unclear how much the preparation techniques employed by SAES will affect gettering results. Although the composition may be similar, if other trade secrets used in preparation have an effect then changing vendors will not necessarily produce comparable results even if the material composition is similar.

6.0 Experimental Procedure

The description of the apparatus was provided previously; however, major components are described in this document as well [1].

6.1 Apparatus Description

The samples were tested using the flow through experimental system shown in Figure 6-1 and Figure 6-2. The system is equipped with vacuum pumps, pressure transducers (0–10,000 torr), mass flow controllers (0–2000 sccm), heaters, temperature controllers, thermocouples, two residual gas analyzers (RGAs) and Inficon GC micro gas chromatographs. Data logging was accomplished using a data acquisition program developed through LabVIEW.

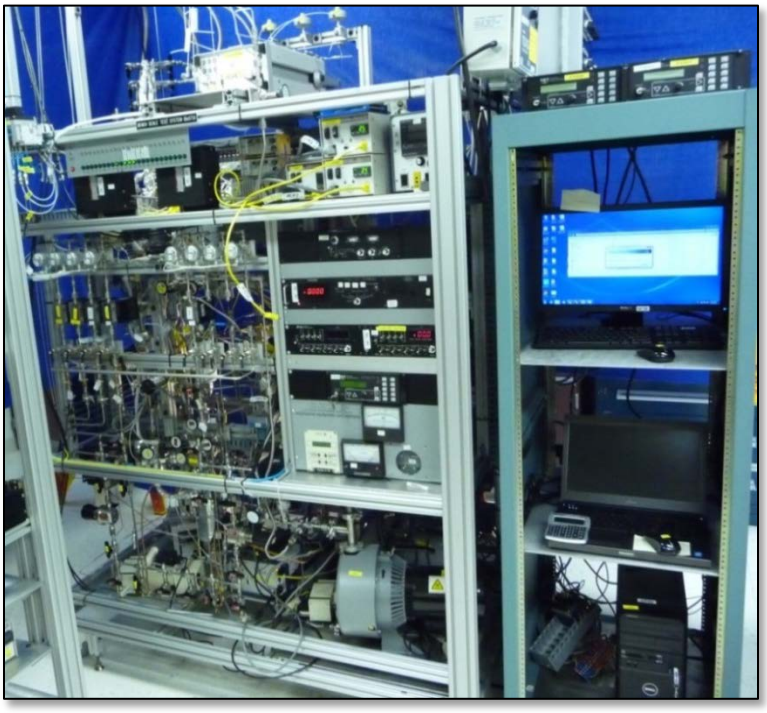

Figure 6-1: Experimental getter evaluation test manifold (front side)

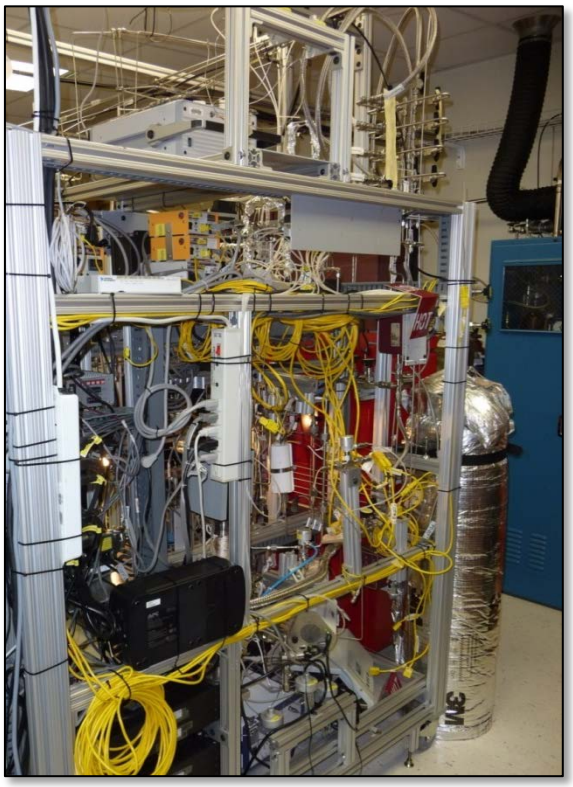

Figure 6-2: Experimental getter evaluation test manifold (back side)

The system was configured for the flow of nitrogen, argon, hydrogen, methane, and gas mixtures containing ammonia, methane, carbon monoxide and/or others. The basic configuration of the system is shown in Figure 6-3, which is a slightly modified schematic of the current system. The schematic does show the two halves of the Bench Scale Test System and some of the general placement of components.

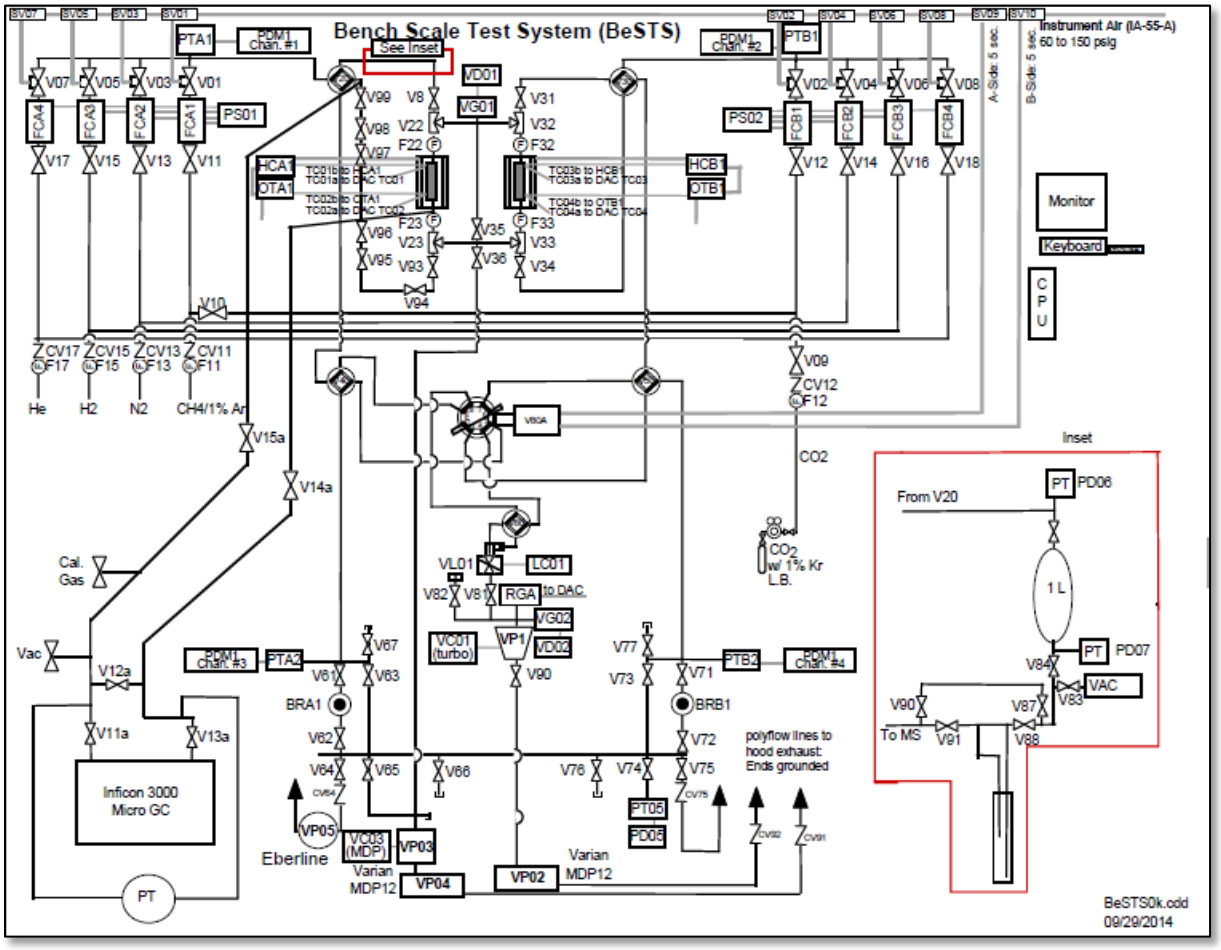

Figure 6-3: Schematic of experimental manifold for evaluation of getter materials

6.2 Test Cell Description

Getter sample materials were loaded into the test cells, an example of which is shown in Figure 6-4. The test cell is constructed of 9.525 mm (3/8 inch O.D.) 0.889 mm (0.035 in wall) 316L stainless steel tubing [38]. The total test cell length is just over 22.86 cm (9 inch) and has two VCR® fittings (VCR-8) welded to the ends with a fritted disk welded in place approximately 1/3 the way up the test cell. The test cell is placed in a vertical configuration during operation. Both ends of the test cell have 0.5 micron stainless steel fritted gaskets to protect the system from the potential migration of particulates.

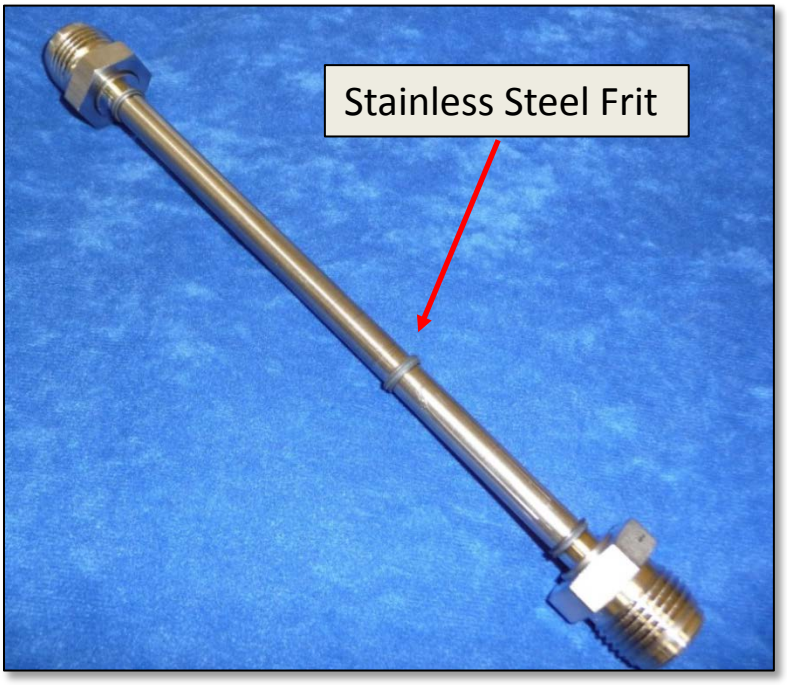

Figure 6-4: Test cell for evaluation of getter materials

The test cells were reused for multiple tests. In an effort to prevent obtaining erroneous results, although a test cell is reused during testing it is only reused for the same getter/alloy material. This ensures that residual pieces of a different sample material does not bias later test results.

Between each test, the cell was cleaned with acetone and cotton swabs and allowed to dry before reloading with the test material and reattaching to the system. This cleaning removes residual carbon that may have deposited on the walls of the test cell during testing. After reinstalling the test cell with new VCR 0.5 μm stainless steel filter gaskets, the system is then evacuated prior to activation of the sample.

Four dual-channel-type-K-1/16" thermocouples are attached to each test cell with wire for temperature control and monitoring. Each test cell is heated using two Watlow clam-shell-style heaters shown in Figure 6-5. Insulation is placed between the test cell wall and the heater at the end of the Watlow clam-shell heaters on either end of the test cell.

Figure 6-5: Vertical test cell configuration used for evaluation of getter materials.

For combination testing two test cells are placed in series. Both test cells have independent temperature control and thermocouples interfaced with the data acquisition system and their respective over temperature controllers.

6.3 Material Quantities

Pellets are stacked in the vertical configuration for testing. An illustration of the stacked configuration is found in Figure 6-6. When pieces are used, the materials are packed into the test cell and the gas flowed through channels that were available.

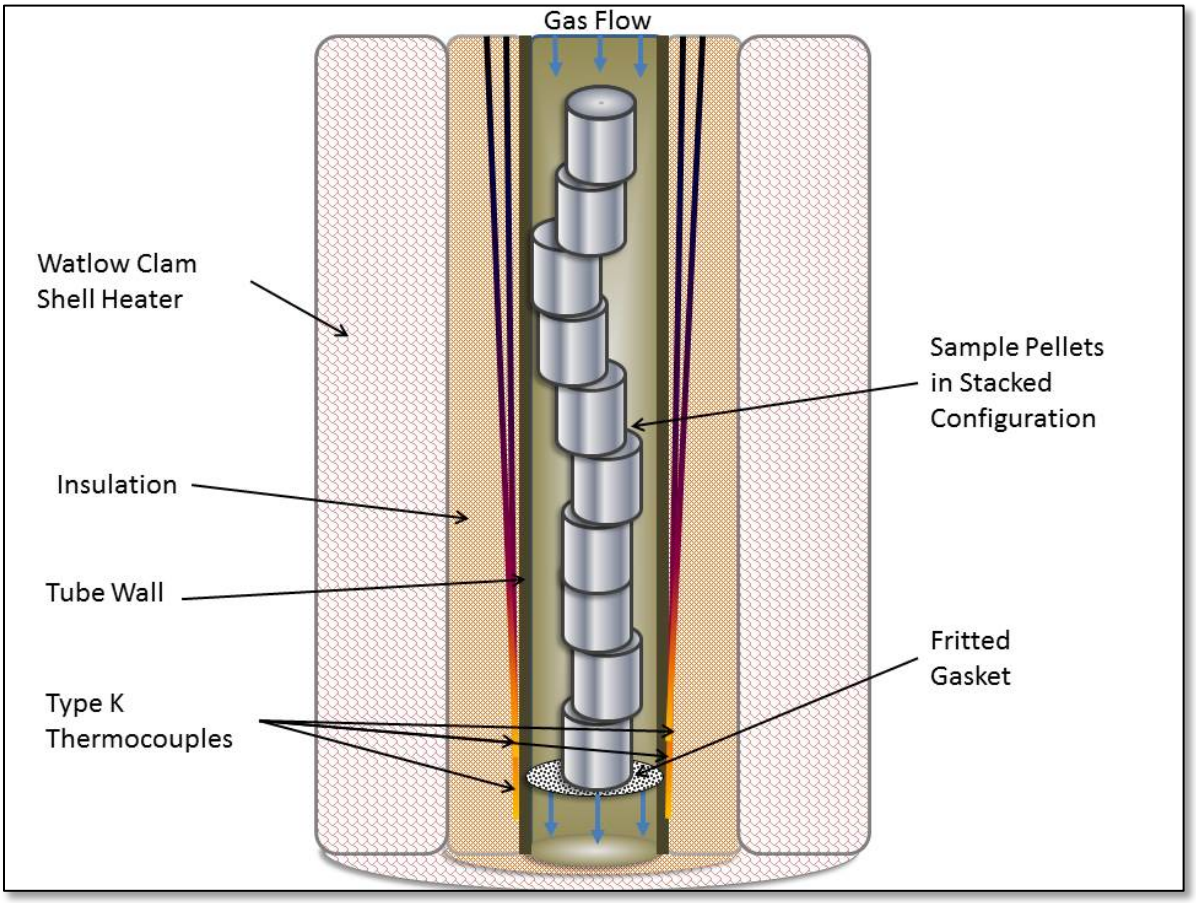

Figure 6-6: Illustration of the stacked configuration of test materials.

During tests, approximately six grams of materials are loaded into the cell. For the pelleted materials this equates to ~10 pellets for several of the getters/materials. Because of the low density of the Ni/k the test cell, 15 Ni/k pellets are loaded for testing. Each Ni/k material pellet weighs ~0.241 grams; whereas, the ST909 pellets each weigh ~0.629 grams. The AME TiMoZr pellets also have a slightly lower density. Eleven pellets are used per test and each pellet weighs approximately ~0.563 grams.

6.4 General Activation Procedure

To activate the getter/alloy materials, argon is used to displace residual air from the ambient temperature bed using a flow rate of 30 sccm and a pressure of ~2100 torr, followed by a nominal temperature ramp to 700°C. The bed temperature is maintained at 700°C for a period of at least twelve hours before the start of the test.

Preliminary testing showed that residual argon remained in the system for some time. To remove the residual argon in the system, at the conclusion of the activation process, the test cell and system are evacuated for a period of one to three hours before the material is exposed to the gas mixtures. Once activation is complete, the test cell temperature is lowered to the operating condition of 670°C, unless otherwise noted.

Although many of the elements that make up the composition of the alloys, such as zirconium or titanium, can form hydrides at room temperature, these materials can also quickly oxidize at room temperature. The test temperature of 670°C was chosen based on previous reports and findings for ST909 [17, 23, 38-41]. This temperature is preferable because the ST909 performance may be less sensitive to impurities at higher temperatures.

6.5 Gas Mixture Apparatus

It was determined, during preliminary testing in FY15 using the ST909 material, that the flow controllers could not adequately be used to make the low concentration gas mixtures required for testing. For this reason, a gas mixture manifold was utilized for preparing gas samples for testing.

The gas mixture manifold is a series of valves interconnected for the purpose of mixing volumes of gases at known concentrations. These volumes are useful when flow controllers cannot provide accuracy or precision for the combinations of low levels of gas constituents, particularly when gases are run at below 1% of the total gas stream of 30 sccm.

Figure 6-7 is an illustration of the major components of the mixing manifold.

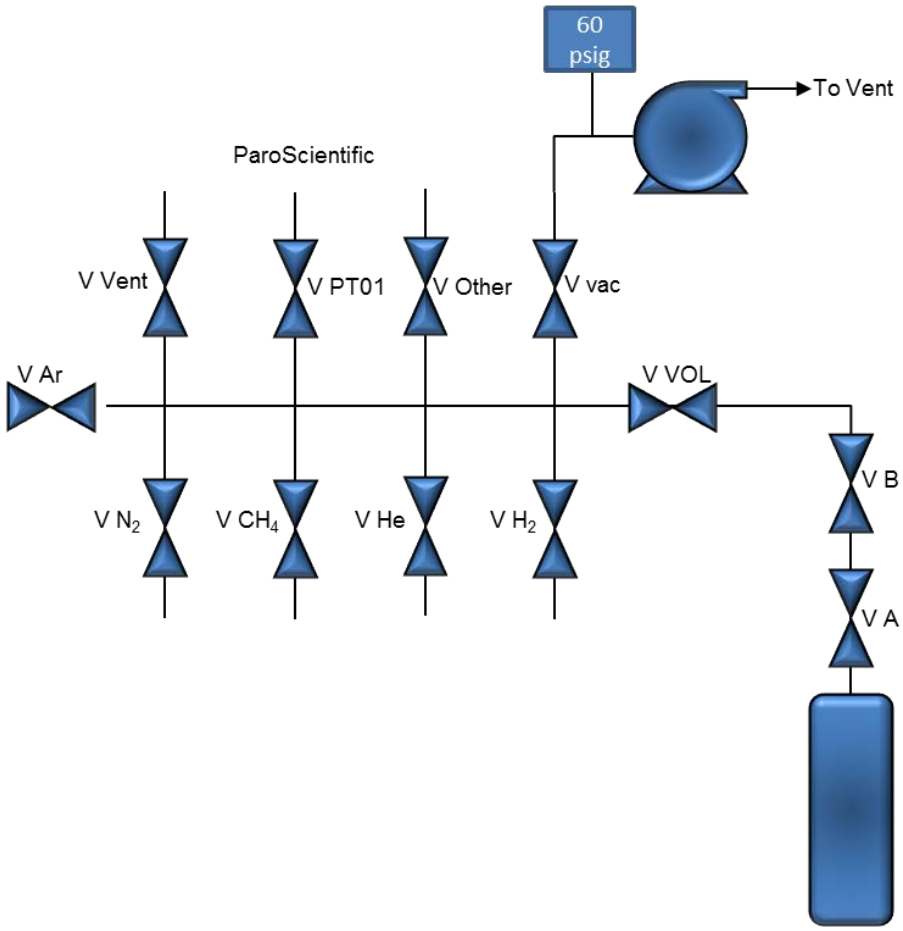

Figure 6-7: Schematic of gas mixture manifold used to prepare gases for evaluations

The gas mixing manifold has inputs from up to 6 different gas sources (hydrogen, helium, nitrogen, argon, methane, and various impurities). The gas mixing manifold also contains a vacuum pump as well as a Paroscientific, Digiquartz Intelligent model No 6000-200A pressure transducer.

To determine the total mixed gas percentages, the following equation was used.

$$Percent_i = \frac{Pressure_i}{Total\ Pressure} 100\%$$

The pressure reading of the pressure transducer connected to the gas mixing manifold was stabilized between additions of other gases. Between gas additions, the mixing manifold was isolated from the tank-at valve A-and evacuated.

6.6 GC Configuration

During ST909 testing, non-ammonia gas mixtures are primarily analyzed with an Inficon 3000 μ-GC. Measuring a chemical species using a micro gas chromatograph (μ-GC) is dependent on the column used, flow of carrier gas, type of carrier gas, type of detector, and method of injection (purge and trap versus direct injection).

The Inficon 3000 μ-GC is equipped with dual molecular sieve columns (14 m x 320 μm x 30 μm) and a thermal conductivity detector. The sample inlet, sample injector, and column are controlled at 60°C. The sample injection time is 20 milliseconds and 40 milliseconds for Channels A and B, respectively. The column pressure is 25 psi for the carrier gases: helium and argon. The μ-GC is automatically configured to sample the gas after the getter test bed at periodic intervals via user input through a developed LabVIEW program in conjunction with air-actuated valves.

The thermal conductivities of the gases play a role in carrier gas choice. The larger the difference in thermal conductivity values between the carrier gas and the target compound, the more sensitive the analysis is for the target compound. Argon is generally the carrier gas of choice for hydrogen analysis; however, the use of argon significantly reduces the sensitivity for other permanent gases. Analyzing these compounds at low concentrations requires the use of a helium carrier gas. The μ-GC was not used for the analysis of ammonia compounds because of the potential for instrument damage.

7.0 Results and Discussion

Based on a literature review conducted in FY15 no known single material that can replace ST909 and perform all the same functions has been identified. The goal of FY16 activities was to identify a combination of materials (or a material) that can crack methane and ammonia under the high nitrogen conditions found in the TPS. Baseline testing was performed to evaluate gettering capabilities of selected materials under the various processing conditions of the TPS with feed sources from N_2 flush gas, Z-bed Recovery, and TEF flush gas. Materials were tested individually and in combination.

The following materials were tested during FY16: SAES ST909, Ni/k, SAES ST707, AME TiMoZr, AME AlNiFe, AME ZrNi, and AME ZrMnFeAl. Each of the tests was operated with

gas streams representative of the impurities found in the TPS feed sources. The concentrations of impurities differed from process gas for detection purposes but testing still provides the behavioral trends the materials would have if placed in full scale operation.

A discussion on how cracking efficiency was determined is provided in Section 7.1. The gases and materials tested are presented in Section 7.2. Results from methane cracking tests are found in 7.2.1. Results from ammonia decomposition testing are found in Section 7.2.2. Results from combination testing in which two materials were used (or in which both methane and ammonia gases were exposed to a material) are found in Section 7.2.4. Observed changes between the as received samples from the manufacturers to post testing are presented in Section 7.3.

7.1 Cracking/Decomposition Efficiencies

Baseline testing consisted of comparing various gas mixture interactions with materials and reviewing the cracking efficiencies of the materials based on the reduction of RGA signal from feed to post testing.

Cracking efficiencies were determined by:

$$Cracking\ Efficiency = 1 - \frac{\left(RGA\ Signal_{gas,} \Big/ RGA\ Signal_{inert,} \right)_{test}}{\left(RGA\ Signal_{gas} \Big/ RGA\ Signal_{inert,} \right)_{feed}}$$

where the subscripts ‘feed’ and ‘test’ indicate the feed gas ratio and the reactor effluent ratio respectively [38]. When inerts were not used the ratio was accordingly adjusted to be simply:

$$Cracking\ Efficiency = 1 - \frac{RGA\ Signal_{gas,test}}{RGA\ Signal_{gas,feed}}$$

7.2 Test Matrix Overview

Different feed gas stream compositions were used to determine methane and ammonia cracking efficiencies of the various materials. A test matrix of conditions explored during FY16 is found in Table 7-1. The test matrix described in Table 7-1 only shows the gas mixtures explored and does not necessarily show all tests that were performed.

Table 7-1: Generalized gas mixtures explored

Material	Gas Impurity Constituents (percent by volume)
ST909	99.5% N_2, 0.5% CH_4
ST909	99.5% N_2, 0.5% NH_3
ST909	93% N_2, 1.5% Ar, 0.5% He, 5% CH_4
ST909	32% N_2, 67% Ar, 0.5% He, 0.5% CH_4
ST909	32% N_2, 66% Ar, 1% He, 0.5% NH_3, 0.5% CH_4
AME ZrMnFeAl	99.5% N_2, 0.5% NH_3
AME ZrMnFeAl	93% N_2, 1.5% Ar, 0.5% He, 5% CH_4
AME ZrMnFeAl	32% N_2, 67% Ar, 1% He, 0.5% CH_4
AME ZrMnFeAl	32% N_2, 66% Ar, 1% He, 0.5% NH_3, 0.5% CH_4
ST707	99% N_2, 0.5% He, 0.5% NH_3
ST707	32% N_2, 67% Ar, 0.5% He, 0.5% CH_4
Ni/k	93% N_2, 1.5% Ar, 0.5% He, 5% CH_4
Ni/k	99% N_2, 0.5% He, 0.5% NH_3
AME TiMoZr	93% N_2, 1.5% Ar, 0.5% He, 5% CH_4
AME TiMoZr	99% N_2, 0.5% He, 0.5% NH_3
AME TiMoZr	32% N_2, 67% Ar, 0.5% He, 0.5% CH_4
AME ZrNi	32% N_2, 66% Ar, 1% He, 0.5% NH_3, 0.5% CH_4

Activation under an argon blanket occurred at 700°C. As indicated in Section 6.4, after activation the test cell temperature was lowered to 670°C and evacuated. System pressure was maintained at ~2100 torr and the total flow rate of gases was maintained at 30 sccm.

Testing showed that the ST909 absorbed from 8 to 9 wt % its initial mass when exposed to solely nitrogen. This result correlates well to the lower performance of ST909 in a nitrogen rich atmosphere.

7.2.1 Methane

Methane is the primary impurity constituent cracked by the ST909 getter material. Testing was performed to compare the behavior of the various materials with consideration of CH_4 cracking efficiency. Results and inferences are based on the RGA as well as the μ-GC for each gas mixture explored.

7.2.1.1 Gas Mixture 99.5% N_2, 0.5% CH_4

7.2.1.1.1 RGA Methane Cracking Efficiencies

As several tests were performed it was necessary to determine if the methods used in data collection could be repeated. Reproducibility of results is demonstrated in Figure 7-1 wherein methane cracking tests of ST909 in a 99.5% N_2, and 0.5% CH_4 gas was performed.

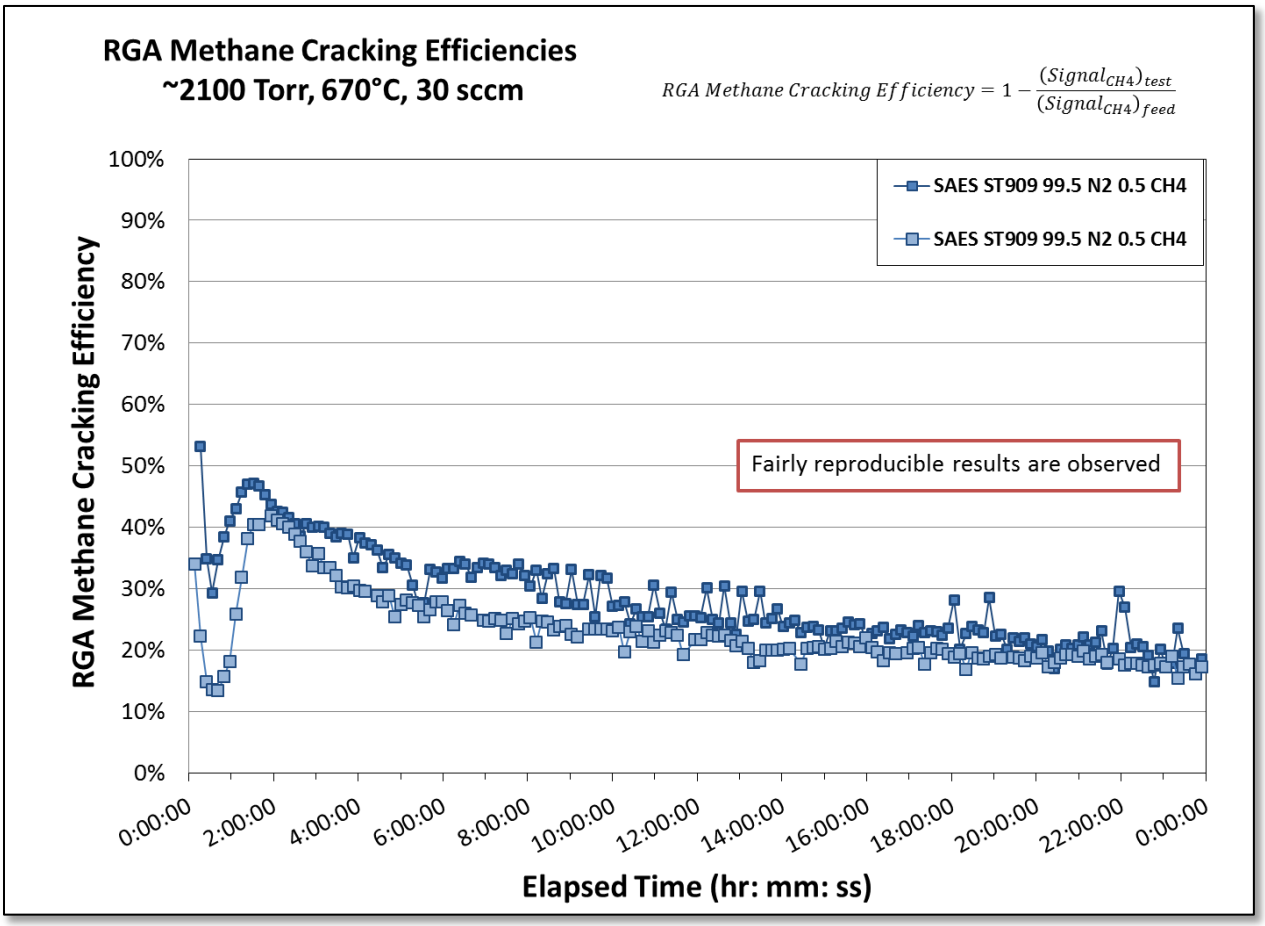

Figure 7-1: Methane cracking efficiencies of ST909 showing reproducibility of results for a 99.5% N_2 and 0.5% CH_4 gas mixture based on RGA analytical methods

Figure 7-1 shows similar trends and general reproducible behavior for the conditions present. For the 0.5% methane with the balance nitrogen gas the methane cracking efficiency was 20% after a

period of 24 hours. The lowered methane cracking efficiency is due to interactions of the ST909 with the nitrogen carrier gas stream.

7.2.1.1.2 μ-GC Results

The Inficon 3000 μ-GC hydrogen signal related to ST909 for a 99.5% N_2 and 0.5% CH_4 gas mixture versus elapsed time is shown in Figure 7-2.

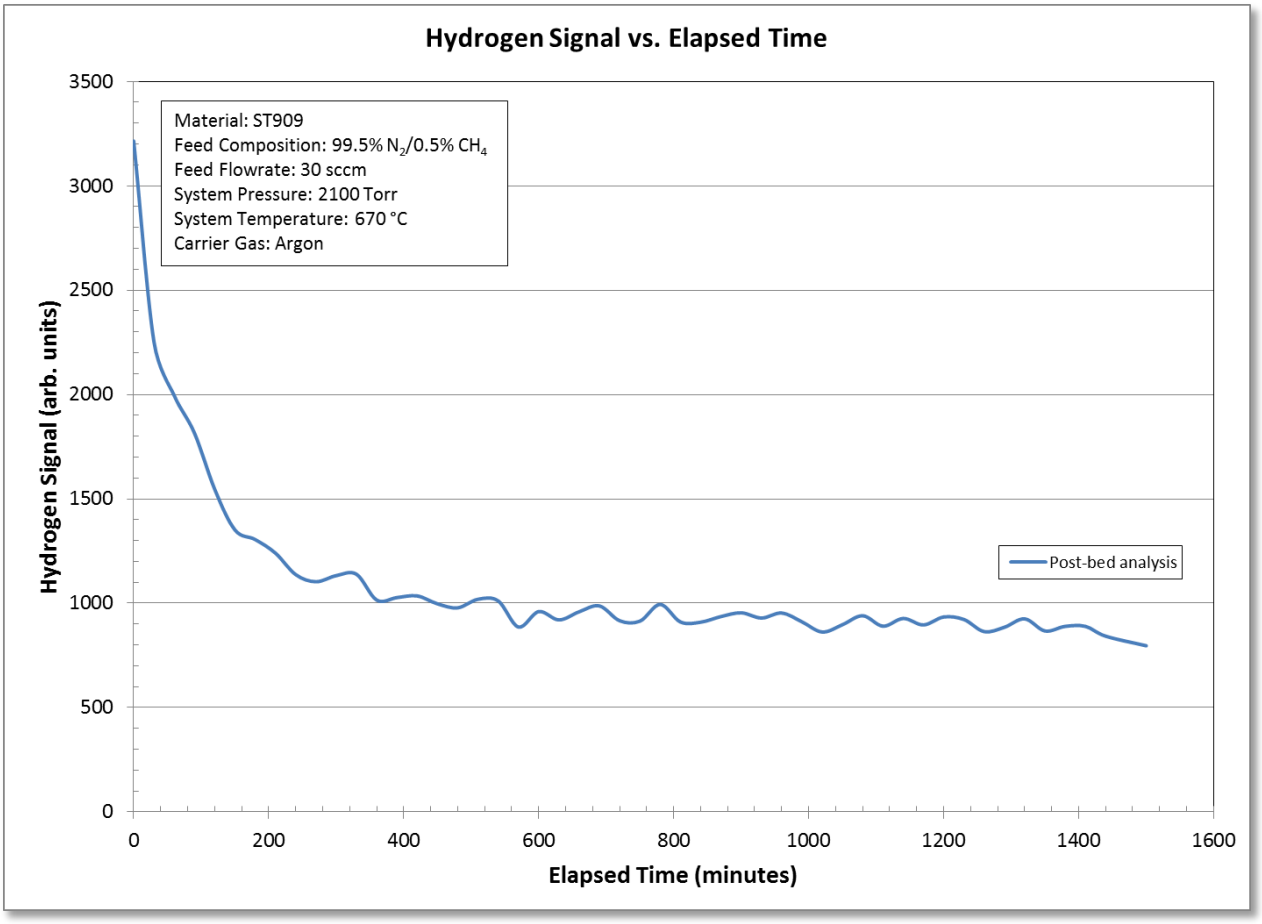

Figure 7-2: Inficon 3000 μ-GC hydrogen signal of ST909 for a 99.5% N_2 and 0.5% CH_4 gas mixture versus elapsed time

The hydrogen signal (peak area) plotted in Figure 7-2 significantly decreases over the time interval of 0 to 300 minutes. This indicates that as time progresses there exists a gradual decrease in the amount of hydrogen that is being released from the cracking of the CH_4 on the ST909. This correlates reasonably well with the methane cracking efficiency shown in Figure 7-1.

7.2.1.2 Gas Mixture 93% N_2, 1.5% Ar, 0.5% He, 5% CH_4

7.2.1.2.1 RGA Methane Cracking Efficiencies

The nitrogen-rich gas causes reduced methane cracking efficiency for many of the materials selected for study. However, in Figure 7-3 it can be seen that even in a nitrogen rich gas stream (93% N_2, 1.5% Ar, 0.5% He, 5 % CH_4), Ni/k has excellent cracking efficiency. It is likely that the gettering efficiency is lowered for many of the zirconium based materials due to the more favorable bond dissociation energies of the nitriding reactions in comparison to methane based reactions. The differences in bond dissociation energy were previously discussed in the text related to Figure 2-4 found in section 2.3.

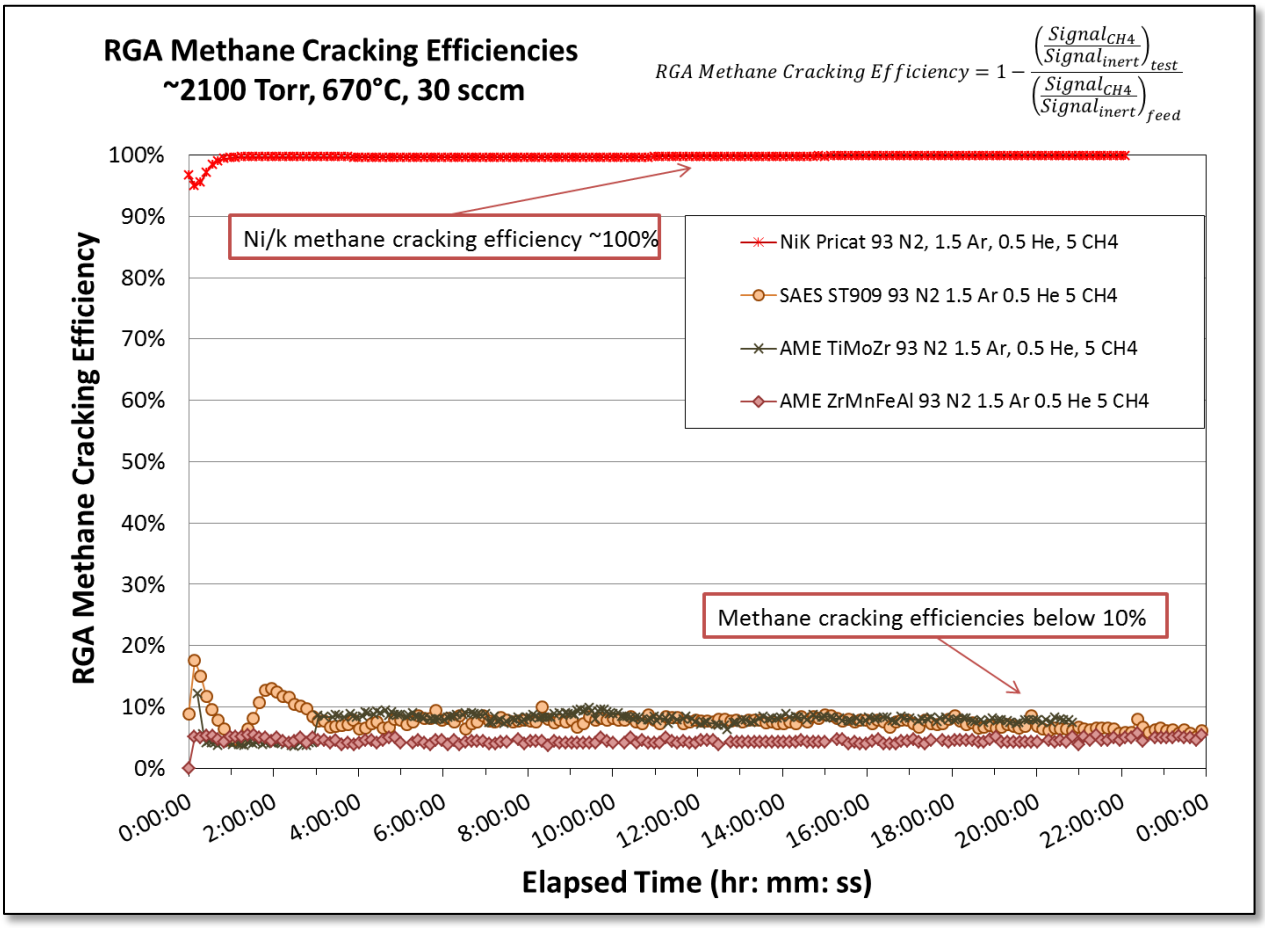

Figure 7-3: Methane cracking efficiencies of various materials with a 93% N_2, 1.5% Ar, 0.5% He, and 5% CH_4 gas mixture based on RGA analytical method

The cracking efficiencies for all materials were below 8%, other than the Ni/k; for the 5% methane gas concentration with 93% N_2, 1.5% Ar, and 0.5% He. Coking on the surface of particles implies that sufficient time is needed for most of the materials to allow getter elements to move inward within the material so that a clean surface for reaction is available. Coking on the particles further indicates that given the right conditions of high hydrogen concentration within

the gas stream the dissociation reactions reversed which would cause a cyclical observance of methane cracking and reforming. It is recommended that the methane concentration be maintained at a minimum. If excessive coking has occurred it may be necessary to replace a getter bed to remove the gettered atoms from the process.

7.2.1.2.2 μ-GC Results

The Inficon 3000 μ-GC hydrogen and methane signals for ST909 and the hydrogen signal related to Ni/k for a 93% N_2, 1.5% Ar, 0.5% He, 5% CH_4 gas mixture versus elapsed time are shown in Figure 7-4 and Figure 7-5, respectively.

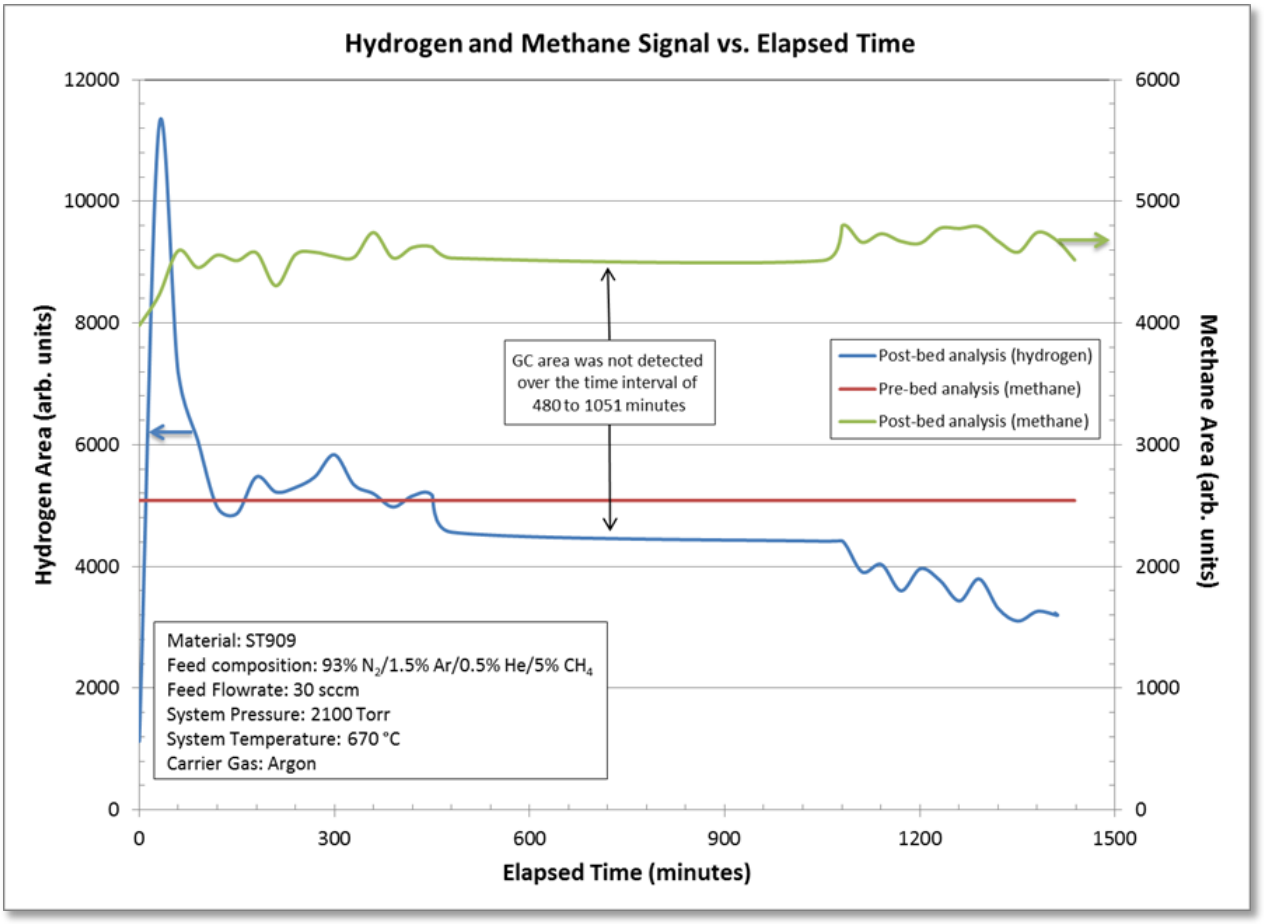

Figure 7-4: Inficon 3000 μ-GC hydrogen and methane signal of ST909 for a 93% N_2, 1.5% Ar, 0.5% He, 5% CH_4 gas mixture versus elapsed time

In Figure 7-4 the hydrogen signal decreases. This is likely due to the loss of active sites for methane cracking as the surface of the ST909 develops a carbon residue. As the carbon residue increases the cracking of methane is less efficient, which results in decreased H_2 release. The methane cracking efficiency on the Ni/k is near 100% for the duration of the test. As the H_2 is liberated from the methane, there is a gradual increase in the H_2 signal as observed in Figure 7-5.

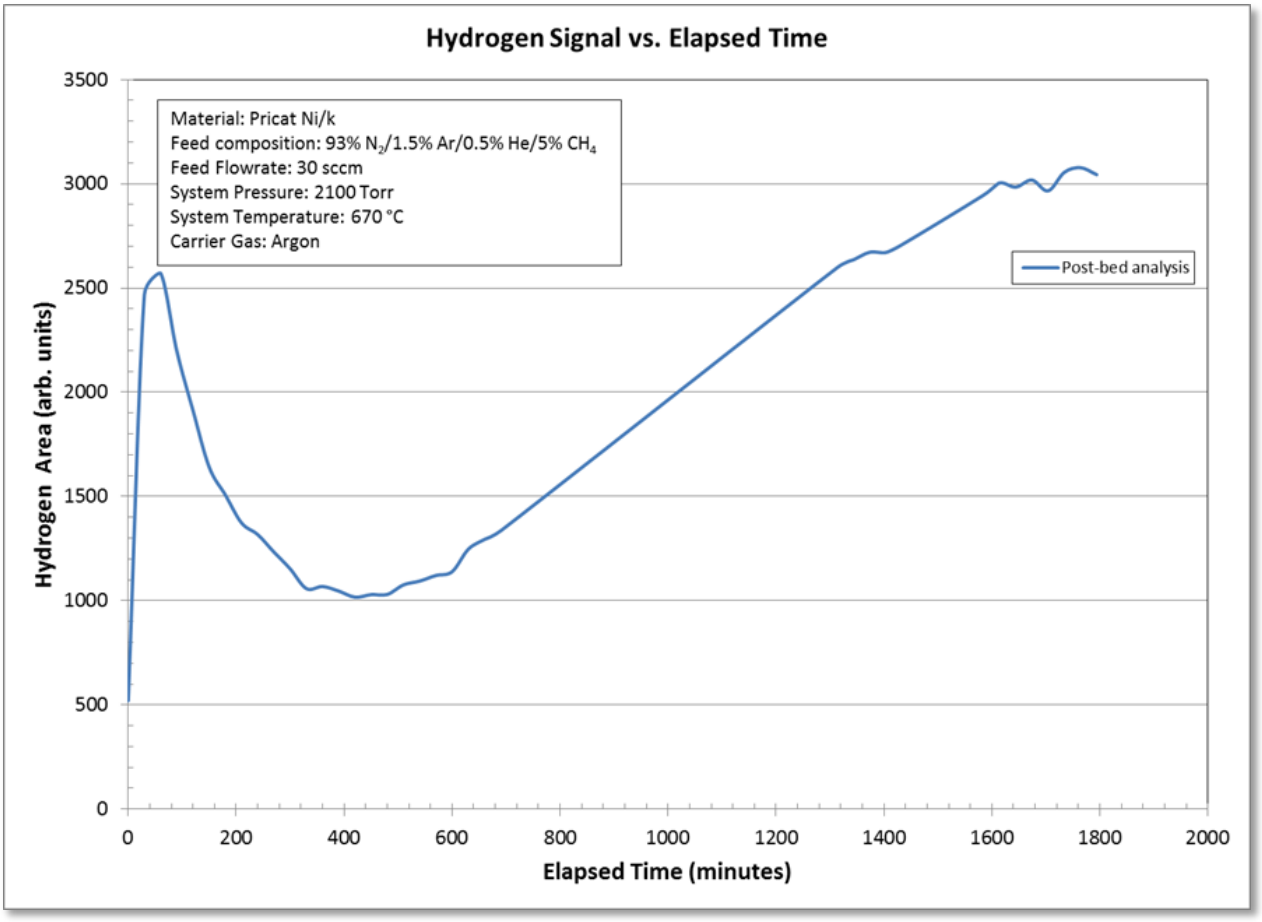

Figure 7-5: Inficon 3000 μ-GC hydrogen signal of Ni/k for a 93% N_2/ 1.5% Ar/0.5% He/ 5% CH_4 gas mixture versus elapsed time

7.2.1.3 Gas Mixture 32% N_2, 67%, Ar, 0.5% He, 0.5% CH_4

7.2.1.3.1 RGA Methane Cracking Efficiencies

Lower N_2 gas concentration does improve initial cracking efficiency. This is shown in Figure 7-6 wherein ST909 has a greater length of time before cracking efficiency diminished. However, although the initial loading may take a greater length of time, the ST909 material still approached 20% cracking efficiency. The comparable AME ZrMnFeAl material's cracking efficiency was fairly consistent over the duration of the test; yet, had a cracking efficiency of only approximately 10%. The AME TiMoZr cracking efficiency was also fairly consistent but only reached a cracking efficiency of ~15% for the given gas mixture of 32% N_2, 67% Ar, 0.5% He, and 0.5% CH_4.

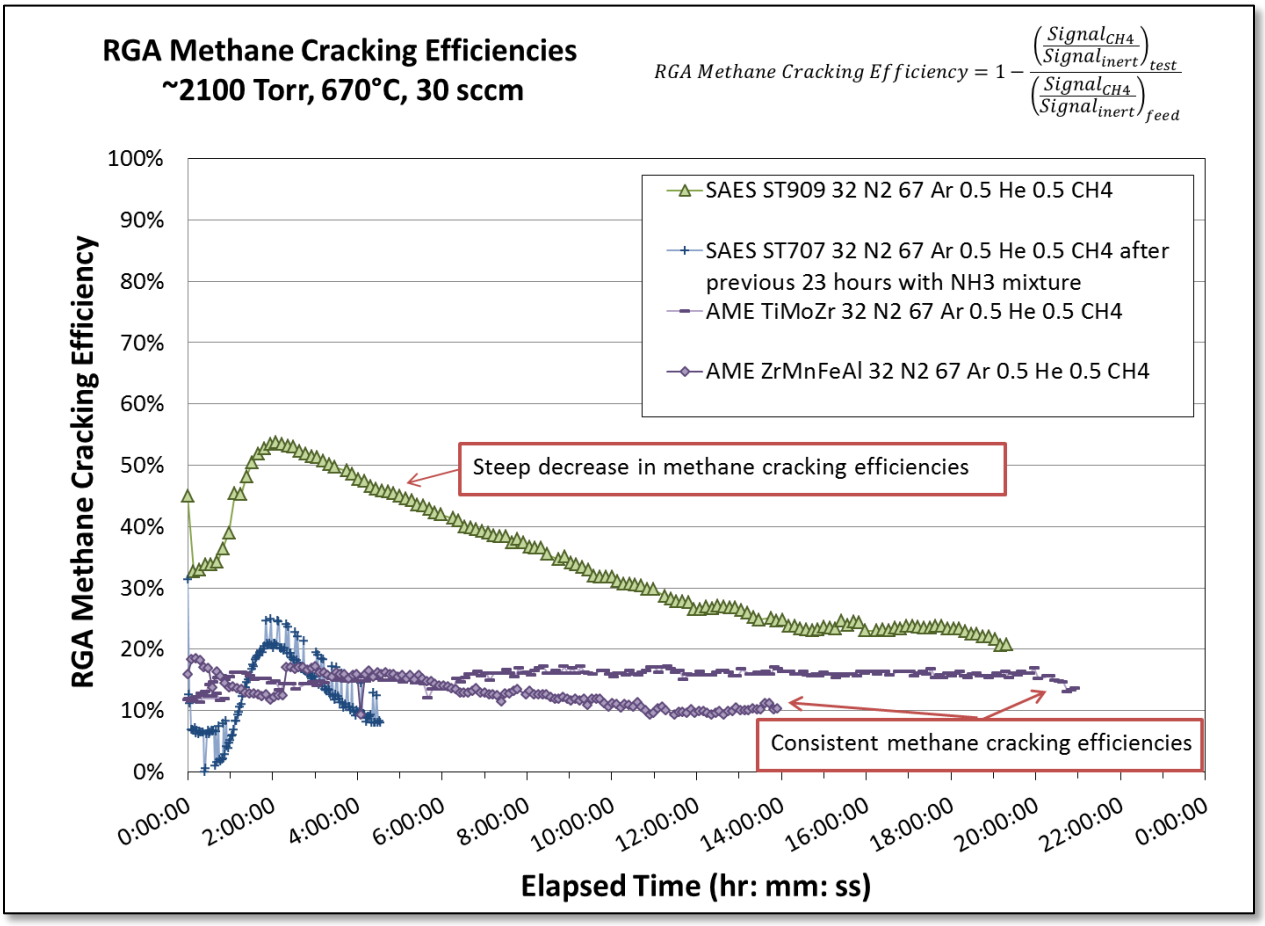

Figure 7-6: Methane cracking efficiencies of various materials with a 32% N_2, 67% Ar, 0.5% He, and 0.5% CH_4 gas mixture based on RGA analytical methods

The SAES ST707 material shows only a short duration as this gas mixture was used in part of a series of tests which looked at the history of the sample. The details of that test are described later in Section 7.2.3. The ST707 material was initially exposed to an ammonia gas sample for 23 hours before being exposed to the 32% N_2, 67% Ar, 0.5% He, and 0.5% CH_4 gas mixture.

Figure 7-7 shows changes of the RGA signal for hydrogen over the course of tests for the 32% N_2, 67% Ar, 0.5% He, and 0.5% CH_4 gas mixture. The data shows that the AME TiMoZr and AME ZrMnFeAl signals have low intensity and minimal fluctuation. The shapes of the curves indicate an initial loading period of two hours. At that point in time, the rates of reactions of methane cracking decrease as is observed by the change in slope of the H_2 signal.

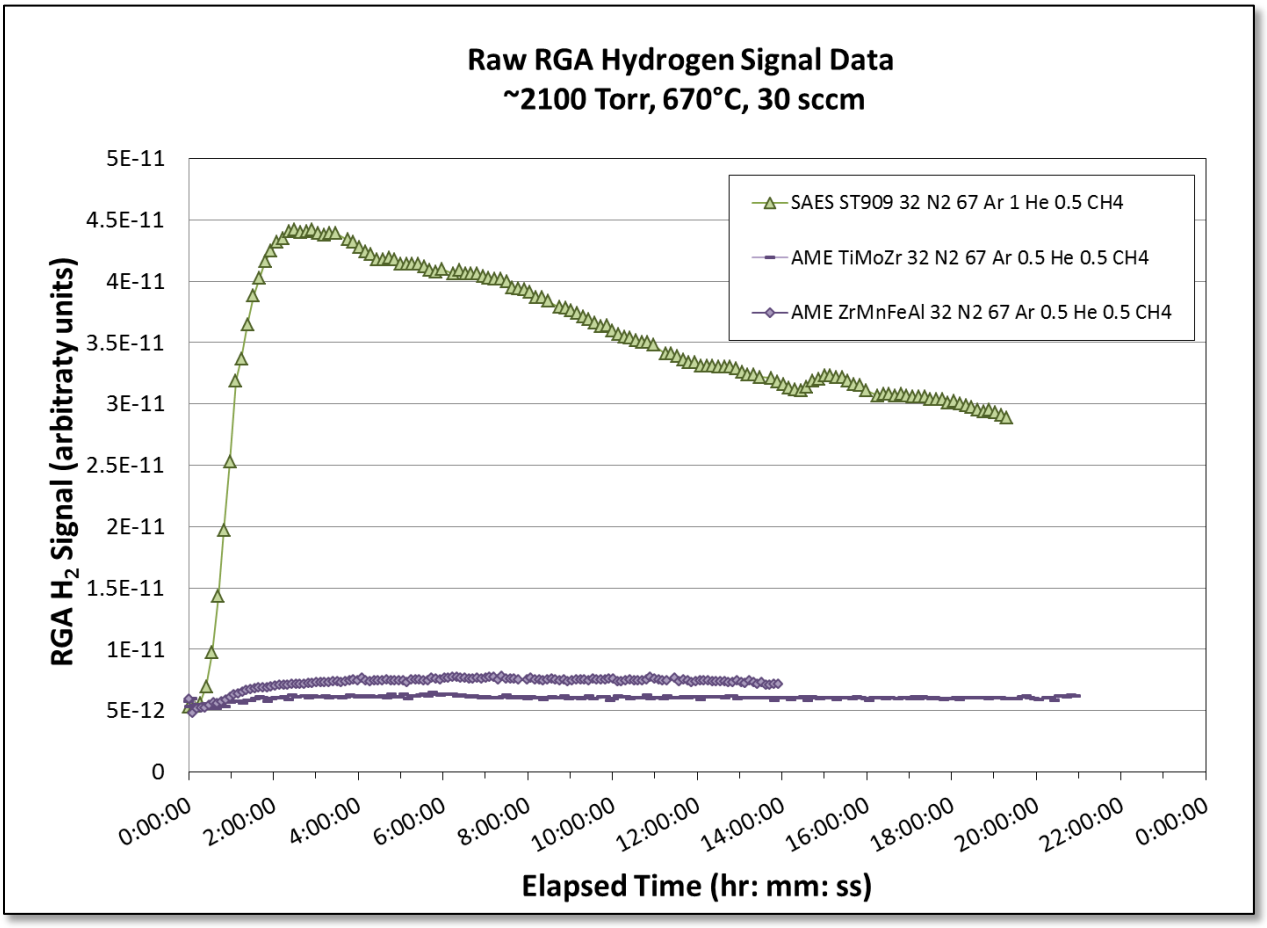

Figure 7-7: RGA Spectrum of H_2 signal of various materials exposed to a 32% N_2, 67% Ar, 0.5% He, and 0.5% CH_4 gas mixture

In Figure 7-7 it is shown that both the AME ZrMnFeAl and the ST909 H_2 signals decreased over time. However, though the signal is much lower than either the ST909 or the AME ZrMnFeAl, the AME TiMoZr shows a slight increase over time. This increase could be related to the hydriding nature of Ti and Zr materials of the alloy. It may take longer for the partial pressure of H_2 over AME TiMoZr to be reached and thus the curve may represent changes that occur to the sample while the H_2 is loading. The decrease in the H_2 signals for the ST909 and AME ZrMnFeAl is likely related to the active sites being blocked for more methane cracking by the nitrogen reactions and the methane on the surface.

7.2.1.3.2 μ-GC Results

The Inficon 3000 μ-GC hydrogen and methane signal of ST909 and the hydrogen signal of AME ZrMnFeAl for a 32% N_2, 67% Ar, 0.5% He, 0.5% gas mixture versus elapsed time is shown in Figure 7-8 and Figure 7-9 respectively.

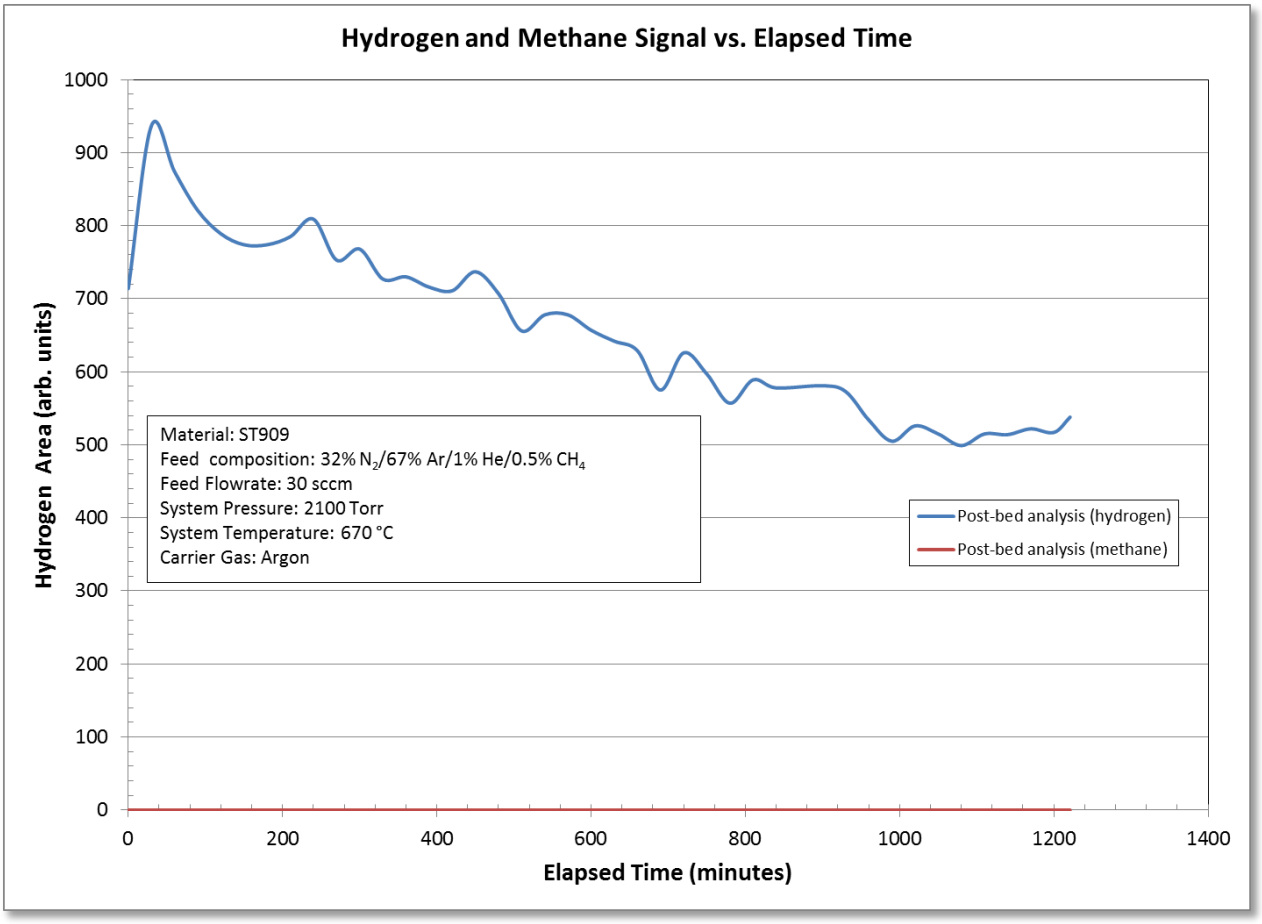

Figure 7-8: Inficon 3000 μ-GC hydrogen and methane signal of ST909 for a 32% N_2, 67% Ar, 0.5% He, 0.5% CH_4 versus elapsed time

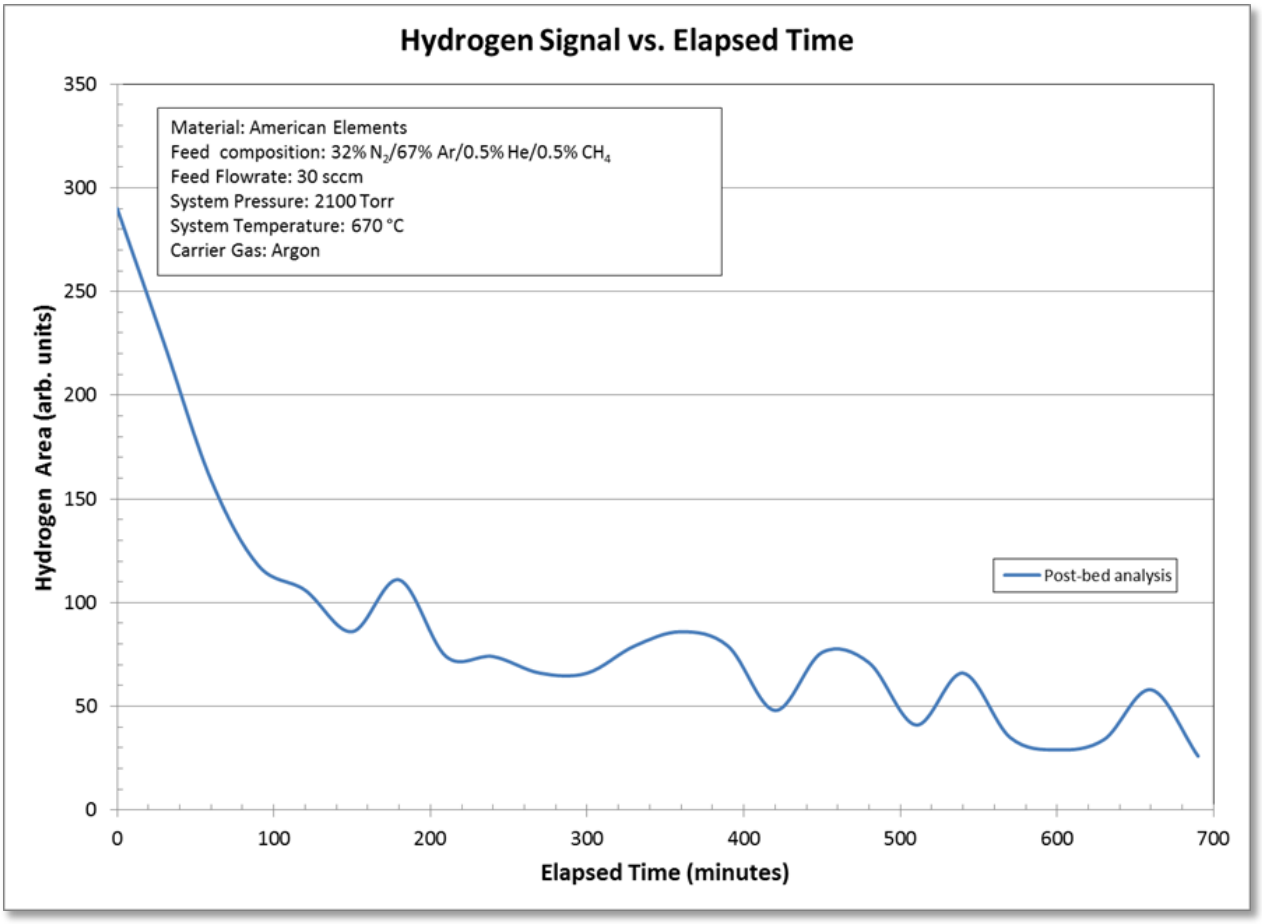

Figure 7-9: Inficon 3000 μ-GC hydrogen signal of AME ZrMnFeAl for a 32% N_2, 67% Ar, 0.5% He, 0.5% CH_4 versus elapsed time

In Figure 7-8 there is no indication of methane in the gas stream after the test cell analyzed with the μ-GC for the ST909 sample. This is likely an artifact of the detection limit of the μ-GC. The RGA indicates that the methane cracking efficiency was initially only 50% followed by a gradual decrease. The decrease in hydrogen signal shown in both Figure 7-8 and Figure 7-9 correlates with a decrease in the methane cracking efficiency.

7.2.2 Ammonia

Ammonia is another impurity that can be removed by the ST909 getter material. Testing was performed to compare the behavior of the various materials in terms of NH_3 decomposition efficiency. No μ-GC spectra were taken during testing with gas mixtures containing ammonia to prevent possible instrument damage.

7.2.2.1 Gas Mixture 99.5% N_2, 0.5% NH_3

A 99.5% N_2, 0.5% NH_3 gas mixture was used to initially compare ST909 with AME ZrMnFeAl. At the operating temperature of 670°C both materials had ammonia decomposition efficiencies greater than 97% as shown in Figure 7-10.

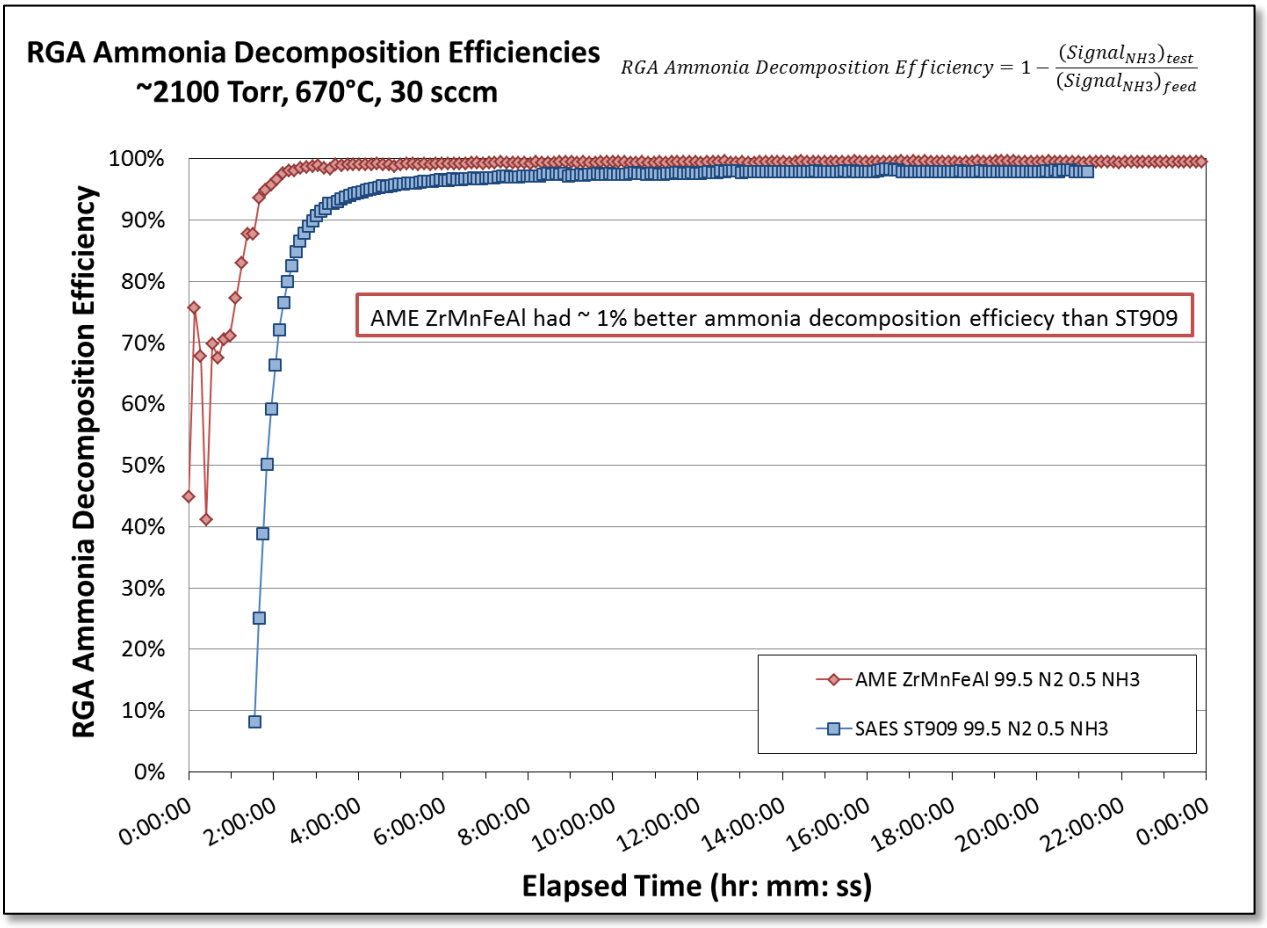

Figure 7-10: Ammonia decomposition efficiencies of ST909 and AME ZrMnFeAl with a 99.5% N_2 and 0.5% NH_3 gas mixture based on RGA analytical methods

As shown in Figure 7-10 the ammonia decomposition efficiency of the American Elements material was only slightly higher (1 to 2%). Both materials performed similarly to one another for the 99.5% N_2 with 0.5% NH_3 gas mixture.

7.2.2.2 Gas Mixture 99% N_2, 0.5% He, 0.5% NH_3

Other materials also had similarly high ammonia decomposition efficiency. A gas mixture of 99% N_2, 0.5% He, and 0.5% NH_3.was used to determine the ammonia decomposition efficiency for the materials shown in Figure 7-11.

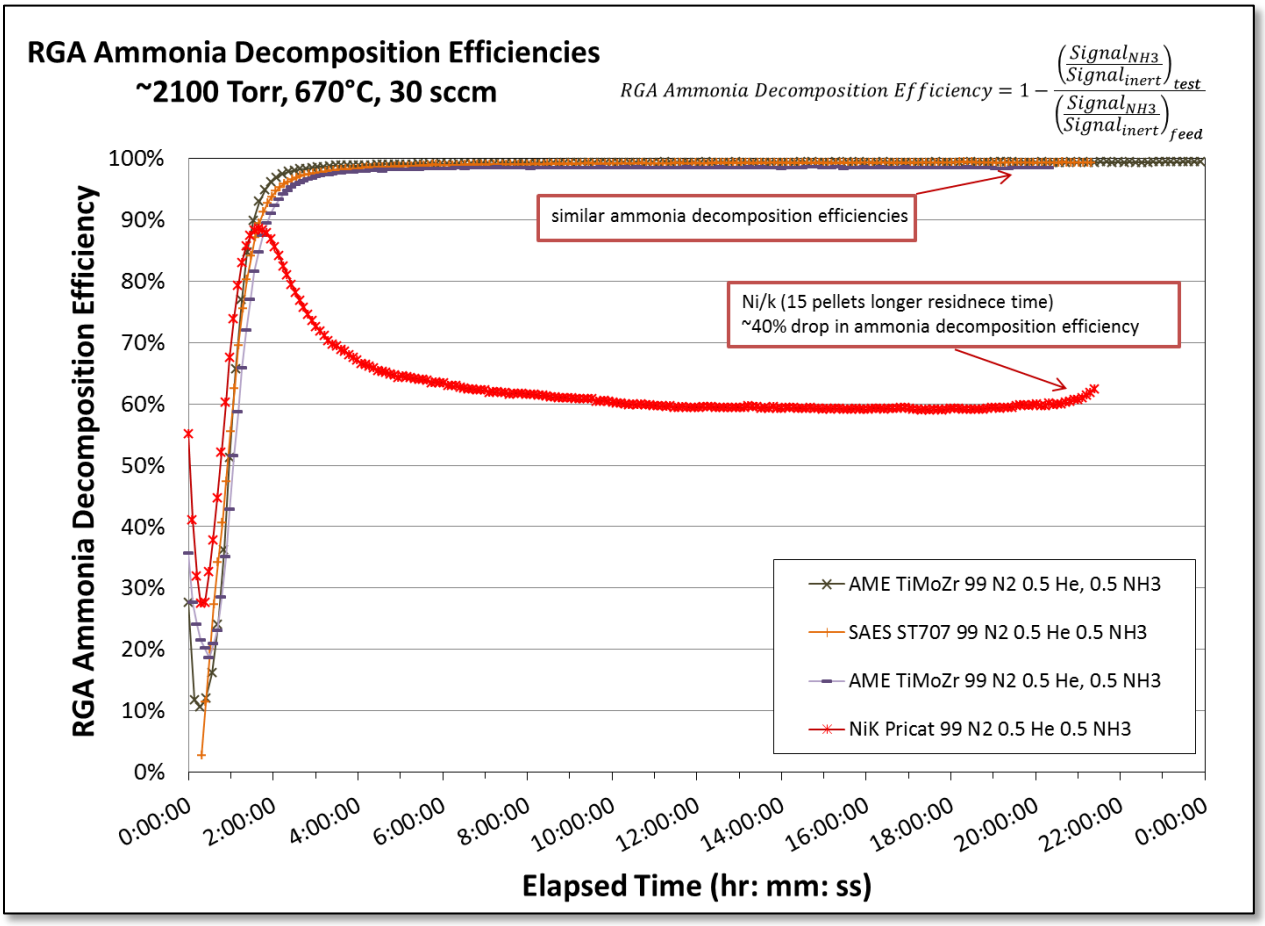

Figure 7-11: Ammonia decomposition efficiencies of various materials with a 99% N_2, 0.5% He, and 0.5% NH_3 gas mixture based on RGA analytical methods

In Figure 7-11 the fact that temperature is not the only consideration in ammonia decomposition becomes more apparent when reviewing ammonia decomposition efficiencies of the Ni/k material. The efficiency of ammonia cracking on Ni/k was reduced by roughly 40% over the course of testing compared to the other materials.

Ni/k has a lower density than any of the other materials tested. Each pellet had roughly a third of the mass of the ST909 material as was discussed in Section 6.3. Therefore 15 pellets, as opposed to 10 pellets of similar dimension, were used in each test. This resulted in a longer residence time for the Ni/k compared to other materials. It is unclear if the kinetics of reaction favored the reverse reaction or if insufficient material was present for ammonia decomposition to occur. It is clear that material interactions change the kinetics and decomposition efficiency of ammonia and that simply heating the gas is not sufficient for decomposing ammonia with great efficiency.

7.2.3 History of a Sample Considered.

7.2.3.1 RGA Methane Cracking Efficiencies

The process conditions relating to ST909 within the TPS may or may not be constant. Understanding the consequence of shifting gas mixtures is of importance. A test was performed to evaluate changes that could occur to a sample during adverse conditions. Within this test, ST909 materials were exposed to three gas mixtures over several days. The first was a 93% N_2, 1.5% Ar, 0.5% He, 5% CH_4 gas mixture (see section 7.2.1.2). Second, an extremely high methane content gas mixture (70.7% N_2, 1.1% Ar, 0.4% He, 27.8% CH_4) was added in an effort to induce a carbon layer on the surface of the ST909. This layer would be representative of what would happen if the materials were only cracking the methane rather than gettering the carbon from the methane. Last, a gas mixture of 91% N_2, 1.8% Ar, 4.7% He, 0.5% CH_4 and 2.2% H_2 was used. The high hydrogen content of this last gas mixture was used to demonstrate the effects mentioned in the discussion surrounding Figure 2-6. If the surface is coated with carbon and a high-hydrogen content gas mixture is flowed over the material more methane could be seen in the gas analysis than the gas mixture originally contained. Results of this test are shown in Figure 7-12.

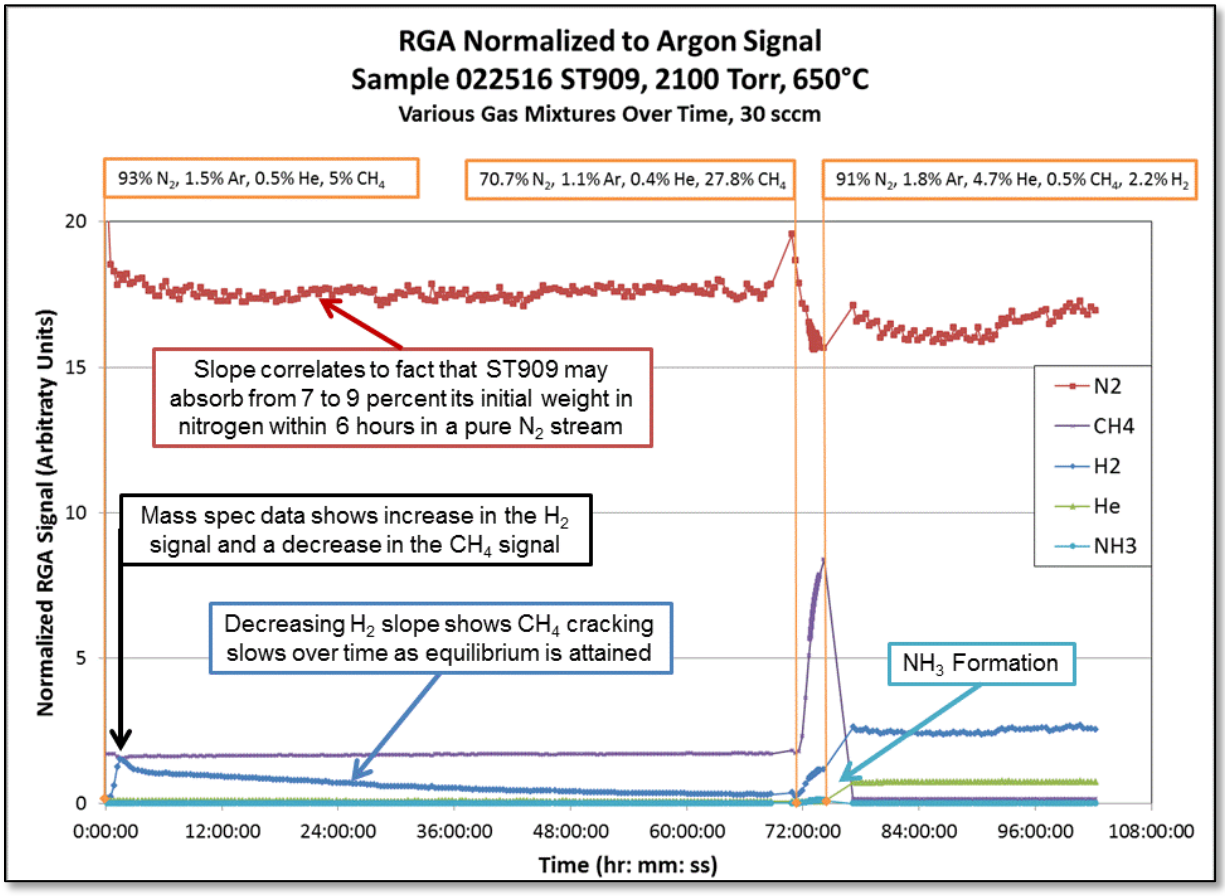

Figure 7-12: History of ST909 considered

Results of the tests comparing changes in the gas stream to cracking efficiency indicate a potential for the formation of ammonia when the concentration of H_2 in the gas stream increases due to the rapid cracking of methane when the sample was subjected to a high concentration of the impurity. Because of the rapid nature of the methane cracking on the surface, the increased RGA signal for methane in the exhaust gas stream could be related to the high hydrogen content of the gas. If the carbon from the methane were truly gettered and Z-C bonds were formed then the hydrogen content would have had minimal effect. Because the carbon rapidly built up on the surface it is likely that methane reformation occurred.

7.2.4 Combination Testing and 32% N_2, 66% Ar, 1% He, 0.5% NH_3 and 0.5% CH_4 Gas Mixtures

Two combination tests were performed which varied the mass of the sample material within the test cell. The two materials were loaded into two test cells that were then placed in series. Although Ni/k showed great promise for cracking methane, during original combination testing the sample material repeatedly clogged the 0.5 micron filters directly downstream of the sample test cell. The combination testing which contained Ni/k was therefore abandoned and a different Ni containing material was chosen. For the new combination test series, the first test cell contained AME ZrMnFeAl and the second test cell contained AME NiFe. The gas mixture used during the course of this testing contained 32% N_2, 66% Ar, 1% He, 0.5% NH_3 and 0.5% CH_4.

For the first successful combination test, 6 grams of AME ZrMnFeAl and 6 grams of AME NiFe were loaded into the two test cells. It was theorized that the greater mass of getter materials would bias the results and not allow for a true comparative study. For the second combination test, the mass of sample materials were adjusted to have 3 grams of each material loaded into their respective test cell.

Single material tests were also performed with the 32% N_2, 66% Ar, 1% He, 0.5% NH_3 and 0.5% CH_4 gas mixture for AME NiFe and AME ZrNi for comparative analysis of different Ni containing materials. ZrNi is a hydride material and was therefore not chosen for initial combination testing.

One difficulty in RGA signal analysis of the downstream gases is that the molecular weight related to mass 16 can represent both methane and ammonia gas species. However, this is overcome by using mass 15 for methane cracking instead of only mass 16 as is used for the analysis of methane mixtures without ammonia. Graphs in which the lines are relatively parallel indicate similar parent gases. Mass 15 better represents the potential for less hydrogen fragmentation from the RGA for the CH_4 than would be required by the NH_3 to get the same mass. A reduction of mass 15 signal with low efficiency does not imply that the cracking efficiencies of any of the materials tested will be that low. The mass 15 signal is based on radicals formed from the process by the RGA to measure data. Its signal is used to verify the mass 16 and mass 17 signals. Ammonia molecules can have mass 17 fragments in the experiment as the hydrogen isotopologue of this test series is assumed protium. Mass 15 RGA signal is shown in Figure 7-13 and the Mass 16 RGA signal is shown in Figure 7-14.

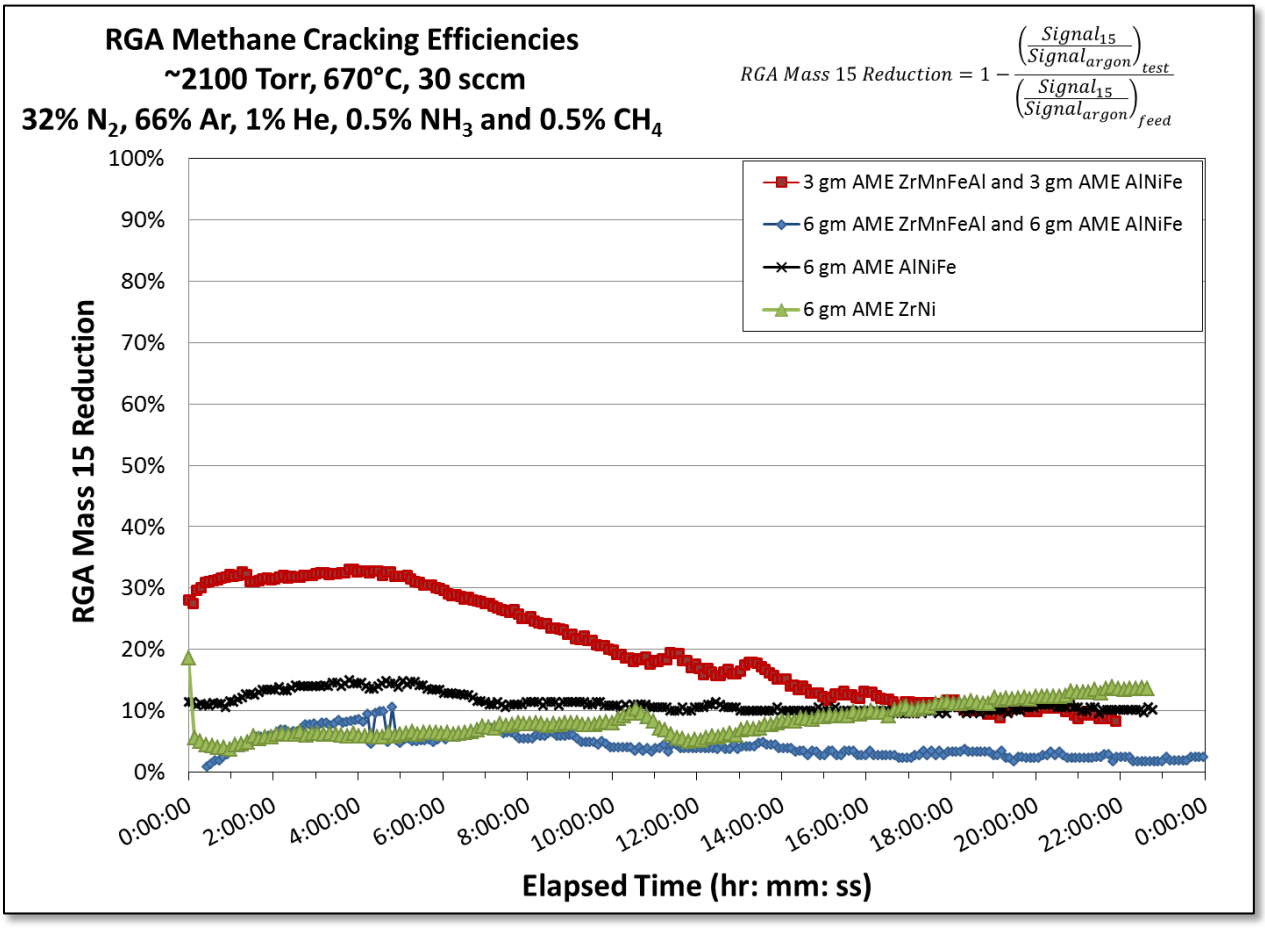

Figure 7-13: Mass 15 signal reduction with a 32% N_2, 66% Ar, 1% He, 0.5% NH_3, and 0.5% CH_4 gas mixture for several test materials

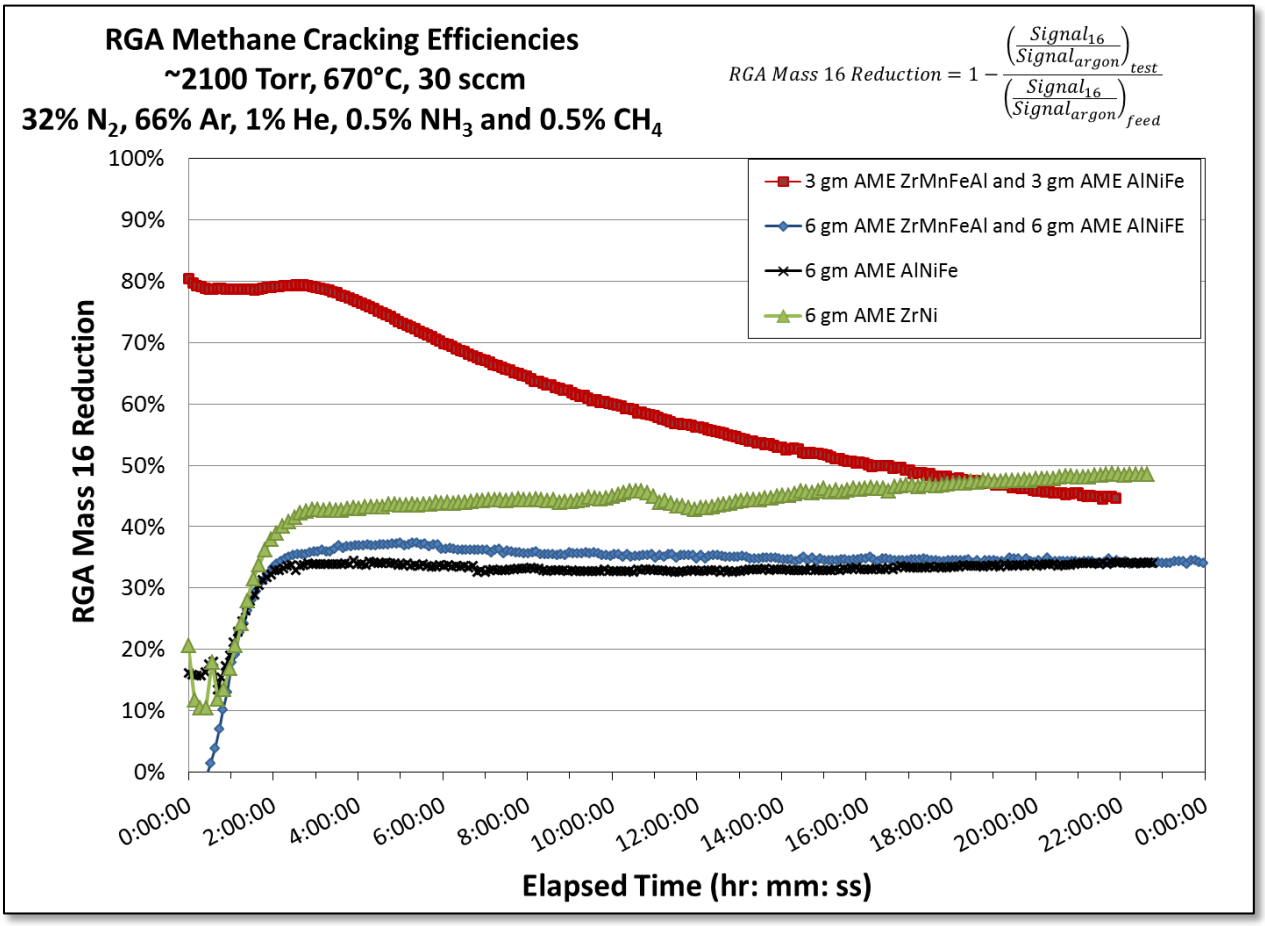

Figure 7-14: Mass 16 signal reduction with a 32% N_2, 66% Ar, 1% He, 0.5% NH_3, and 0.5% CH_4 gas mixture for several test materials

Based on the parallel RGA signals of mass 15 and mass 16 it can be inferred that the methane cracking efficiency of the AME ZrNi material is likely to be better than the ST909 that was also observed for the AME AlNiFe material. The AME AlNiFe material had constant methane cracking throughout the duration of the test.

Mass 17 RGA signal is still used for the ammonia cracking efficiencies shown in Figure 7-15. The results shown in Figure 7-15 indicate that the present set of testing was not optimized. This can be inferred by comparing the results of the 12 gram combination test (total grams of AMEZrMnFeAl and AMEAlNiFe) to the 6 total gram combination test. The 6 gram combination test had greater ammonia decomposition efficiency compared to the 12 gram test. This may be from the recombination of the nitrogen and hydrogen as it goes through the process. If ammonia is cracked in the first stage of testing it may be better to separate the hydrogen or nitrogen released before introduction to a second material. Operating temperature could also be optimized to help minimize ammonia and methane reformation.

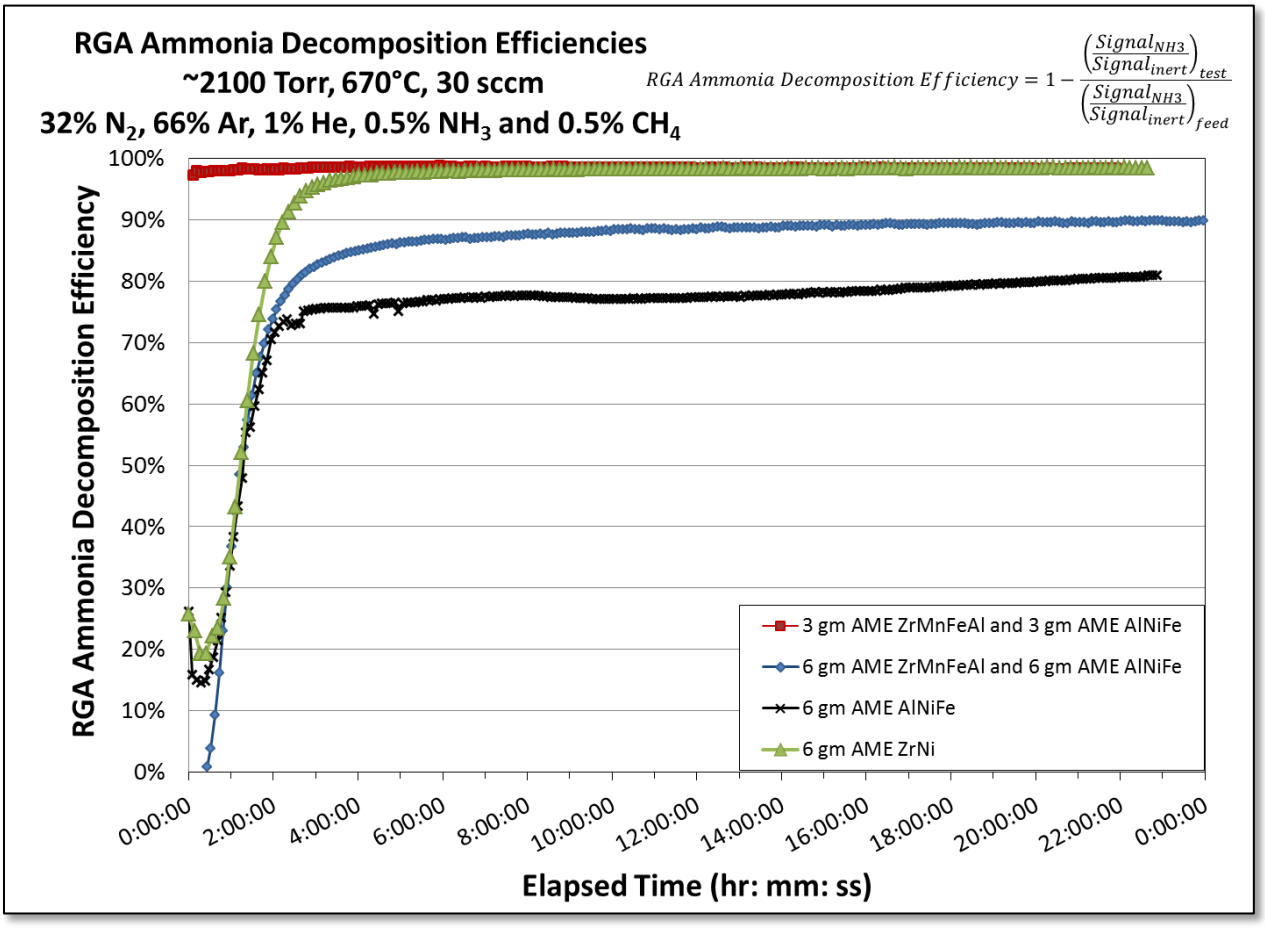

Figure 7-15: Ammonia decomposition efficiencies for several materials with a 32% N_2, 66% Ar, 1% He, 0.5% NH_3, and 5% CH_4 gas mixture

In the discussion relating to Figure 7-11 of section 7.2.2.2, the operating temperature was already mentioned as only one aspect that affects the ammonia decomposition. The residence time of the gases in favorable conditions for ammonia formation should be minimized to keep from forming ammonia within the process. This includes minimizing gas concentrations favorable to formation of ammonia by use of hydrogen inert gas separations technology as well as temperature control.

7.3 Physical Changes to Getters/Alloys Sample Materials

Several changes occurred to the getter/alloy materials upon use in the test system. Observations based on the alloys are discussed in the following subsections. Discussion of physical changes to the materials is briefly mentioned due to the fact that behavior on a small scale may represent behavior in full-scale operation.

7.3.1 ST909

As is shown in Figure 7-16, ST909 pellets are right cylinder pellets approximately 6 mm in diameter by 4 mm tall. Each pellets weighs approximately 0.6 grams [12].

Figure 7-16: SAES ST909 pellets as received from the manufacturer

Post testing using ST909 with a helium gas mixture with methane showed carbon residue on the surface of the particle as is shown in Figure 7-17. Surface carbon residue indicates that not all the carbon from the methane cracked is necessarily gettered. Carbon may be merely chemisorbed on the surface and deposited as a soot residue. In conditions where this occurs, it may be possible to have a cyclical effect of cracking methane in one condition and then reforming it in another as is implied in the discussion related to Figure 2-6 in section 2.3.

Figure 7-17: SAES ST909 pellets post testing with methane and helium

Upon exposure to a 99.5% N_2 and 0.5% NH_3 stream the ST909 pellets showed small golden flex's on the surface of the material. Red discoloration was also observed. An example of this condition is displayed in Figure 7-18.

Figure 7-18: SAES ST909 pellets post testing with 99.5% N_2 and 0.5% NH_3

7.3.2 AME ZrMnFeAl

The virgin ZrMnFeAl material has a dull gray color and is supplied in small (3-6 mm) irregular shaped pieces as is shown in Figure 7-19. These irregular pieces are the product of manufacturing technique in that they were prepared from melted ingots rather than through sintered powdered metallurgy.

Figure 7-19: AME ZrMnFeAl pieces as received from the manufacturer

After exposure to gas streams containing methane (see Figure 7-20) or a combination test of both methane as well as ammonia (see Figure 7-21) the American Elements ZrMnFeAl material changed to have bright gold coloring. The particles that came in contact first with the gas stream

had changed to have a darker gray to black coloration. In the conditions where argon was present the darker coloration was more prevalent as is shown in Figure 7-21.

Figure 7-20: AME ZrMnFeAl pieces post testing with 93% N_2, 1.5% Ar, 0.5% He, and 5% CH_4

Figure 7-21: AME ZrMnFeAl pieces post testing with 32% N_2, 66% Ar, 0.5% He, and 0.5% NH_3 and 0.5% CH_4

7.3.3 ST707

This material has a gray color with a reddish tinge and is supplied small pellets of ~6 mm diameter and 4 mm length as is shown in Figure 7-22. The pellets weighed approximately 0.598 grams each.

Figure 7-22: SAES ST707 pellets as received from the manufacturer.

As is shown in Figure 7-23, post testing showed decrepitation after the ST707 was exposed to gas streams with high nitrogen and ammonia concentration. The decrepitated particles are brownish gold in color. Gas streams with high argon and methane (not shown) also had decrepitation of particles. Hydrogen from the ammonia and methane may adsorb on the material and induce some of this decrepitation; however, this was not proved during testing. Small particles within the process can potentially clog filters or impact other downstream equipment. Another issue to consider is that after exposure to the nitrogen rich gas stream with ammonia, the temperature of the test cell rose sharply and the heaters had to be turned off to let the material cool. This is a confirmation that the nitriding reaction is exothermic.

Figure 7-23: SAES ST707 post testing with 99.5% N_2, 0.5% He, and 0.5% NH_3

7.3.4 Ni/k

The Ni/k material has black shiny coloration and is supplied in small pellets of 6 mm diameter and 4 mm length as is shown Figure 7-24.

Figure 7-24: Pricat Ni/k pellets as received from the manufacturer

The particles are initially brittle. After activation and testing, the Ni/k becomes more inelastic and small particles flake off as hown in Figure 7-25. During post testing, once the material is exposed to air, the reaction with air is exothermic and the particles will heat.

Figure 7-25: Pricat Ni/k pellets post testing with 99% N_2, 0.5% He, 0.5% NH_3

Mass was loss during activation of the Ni/k. Kieselguhr is a form of diatomaceous earth that has varying moisture content based on when and where it is mined. It is possible that the heating of the pellets removed waters of hydration related to the kieselguhr. This was unable to be confirmed at this time due to issues related to thermogravimetric analysis (TGA) equipment. However, during activation the 0.5 micron filters of the test cell clogged on more than one occasion and the filters were covered with what appeared to be the nickel material.

7.3.5 AME TiMoZr

This material has a dull gray color and is supplied in small extruded pellets cut to ~6 mm diameter and 4 mm length as is shown in Figure 7-26. The pellets weighed approximately 0.563 grams each.

Figure 7-26: AME TiMoZr pellets as received from the manufacturer

Post testing showed that the American Elements TiMoZr pellets darkened on the sides of the cylindrical pellets yet became a lighter gray on the top and bottom of the cylindrical pellets in the presence of methane as is shown in Figure 7-27. The ammonia gas mixture caused the exterior of the pellets to take on a reddish tinge with golden highlights as is shown in Figure 7-28.

Figure 7-27: AME ZrMnFeAl pieces post testing with 93% N_2, 1.5% Ar, 0.5% He, and 5% CH_4

Figure 7-28: AME TiMoZr pellets post testing with 99% N_2, 0.5% He, 0.5% NH_3

7.3.6 AME AlNiFe

This AME AlNiFe material has a dull gray color and is supplied in small irregular shaped pieces varying in size from 3-8 mm as is shown in Figure 7-29. There was little visually observable change in the AME AlNiFe sample between pre and post testing.

Figure 7-29: AME AlNiFe pieces as received from the manufacturer

7.3.7 AME ZrNi

The AME ZrNi material has a shiny silver color and is supplied in large irregular shaped pieces varying in size from 3-15 mm as is shown in Figure 7-30. Materials had to be broken up to fit into the test cells.

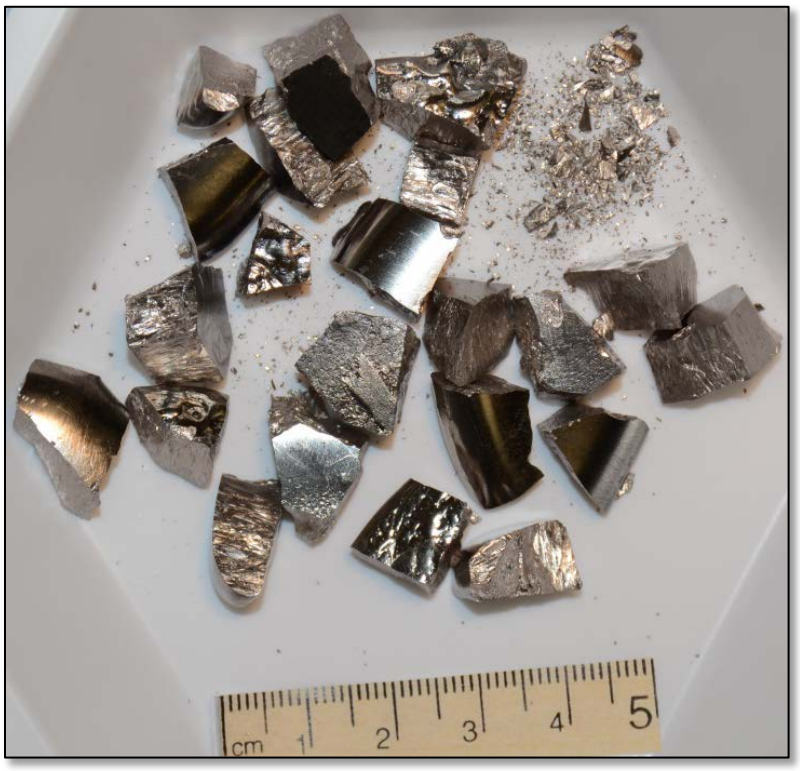

Figure 7-30: AME ZrNi pieces as received from the manufacturer

AME ZrNi material which has undergone testing is shown in Figure 7-31. In Figure 7-31 it can be observed that some particles darkened in coloration and took on a dark gray hue. Other particles took on the golden appearance. The mass of the ZrNi particles increased ~23.3% over a period of nearly 23 hours (see cracking results in Figure 7-13 to Figure 7-15). Post testing visual inspection showed minimal carbon soot formation which may mean that gettering of the carbon occurred rather than simply methane cracking.

Figure 7-31: AME ZrNi pieces post testing post testing with 32% N_2, 66% Ar, 1% He, 0.5% NH_3, and 0.5% CH_4

8.0 Summary of Observations

Several materials were tested during FY16 as alternative to SAES ST909. These materials include: Ni/k, SAES ST707, AME TiMoZr, AME AlNiFe, AME ZrNi, and AME ZrMnFeAl. Each of the tests was operated with gas streams representative of the impurities found in the TPS feed sources of N_2 flush gas, Z-bed recovery, and TEF flush gas. Testing is intended to provide behavioral trends of the materials if placed in full scale operation. The cracking/decomposition efficiencies of methane and ammonia were explored on the various materials.

Analytical analysis of ST909 compared to “chemically equivalent” AME ZrMnFeAl showed that the chemical composition of the two materials is similar. The methane cracking efficiencies observed during testing suggests that the different sample preparation method affects methane cracking in the early stages of testing. However, as time elapses the cracking efficiencies seem to approach similar cracking efficiencies in comparable gas compositions testing.

Results show that the residence time that the ammonia mixtures have with a sample material will likely change the ammonia decomposition capability of the sample. This was seen with both combination testing and with testing of Ni/k. The reduction in Ni/k ammonia decomposition of 40% may be related to the decreased residence time of the material. This assentation will need to be proven by running a Ni/k sample with fewer pellets. The combination testing of the AME ZrMnFeAl and AME AlNiFe sample showed that ammonia decomposition decreased by the increased residence time. This may mean that interstitial hydrogen isotope separation may be

needed in a purification system using getter materials. Any such interstitial method should be able to function over the changing gas compositions that flow through the current ST909 bed.

The cracking of methane on the various materials was confirmed with the μ-GC measurements. There was an increase or decrease in the observed hydrogen signal (area) that correlated to an increase or decrease in the methane cracking efficiency.

Several of the materials showed signs of decrepitation from the exposure and interaction with the test gases. This factor may make them less suitable as an ST909 replacement material.

Material characteristics observed with naked eye indicate that Ni/k not as good for use due to loss of material during operation. In the facility this may not be an issue as the material would be activated at an alternative location rather than in process. Still though, the variable nature of Kieselghur makes its use less appealing under high temperature operating conditions.

The sample preparation method of ST909 has an impact on methane cracking performance. American Elements produced a material of similar composition that had a methane cracking efficiency of ~10% when exposed to an argon rich gas stream. ST909 had a methane cracking efficiency of ~20%.

For an argon rich gas with both ammonia and methane impurities present, combination testing of AME ZrMnFeAl with AME AlNiFe showed methane cracking efficiencies greater than 35%. AME ZrNi had a better methane cracking efficiency at ~48%. AME AlNiFe had 80% an ammonia cracking efficiency and AME ZrNi had a cracking efficiency of ~97% when exposed to the same gas. Combination test of the AME ZrMnFeAl with AME AlNiFe made little difference compared to tests with just the AME AlNiFe.

It is recommended that an evaluation of the various gas streams and the order in which they are processed by the ST909 be completed. The tests reported in this document show that changing gas compositions have the potential for ammonia formation under certain circumstances depending on the history of the sample. It may be appropriate to evacuate TPS before changing the gas composition to minimize impurity formation.

Several holes still exist in the data before an alternate material can be recommended as a replacement for the ST909. The data provided show that a combination of materials may be able to perform the same workload as ST909. However, the optimization of the process at the research and development level is needed. Additional combination testing and the optimization is recommended before any one specific material or set of materials can be recommended.

Based on the results presented in this report there are potentials that have showed to perform better than ST909 under the conditions tested Additional funding is recommended to continue the combination testing of the potential replacement materials for the ST909. In addition, it is necessary to test various combinations of materials under a broader range of operating conditions relevant to the TPS operating conditions. The additional work should be adequate to identify a potential replacement material or combination of materials for the ST909.

9.0 References

1. James, D.W. and G.A. Morgan, *Evaluation of Alternative Impurity Removal Getters (SRNL-STI-2015-00466)*. 2015, Savannah River National Laboratory: Aiken, SC.
2. Nobile, A., et al., *Design Optimization of Metal Getter reactors for Removing Tritium From Flowing Gas Streams.* Fusion Technology, 1995. **28**(Oct): p. 1558 - 1565.
3. Hsu, R.H., *Prototype Getter Bed Testing: I. Actication, Initial Nitrogen Loading and TFM&C Nitrogen Carrier Gas Tests, WSRC-TR-2003-00152*, W.S.R. Company, Editor. 2003, Savanah River Technology Center: Aiken, SC.
4. Klein, J.E., *Effect of Carbon Dioxide on SAES(R) St909 Methane Cracking WSRC-TR-2002-00286-TL*, in *Other Information: PBD: 30 Sep 2002*. 2002. p. Medium: ED; Size: vp.
5. Klein, J.E. *Bench Scale Saes St 909 Tests for Methane and Carbon Dioxide Removal from Helium, Hydrogen, and Nitrogen Gas Streams*. in *AICHE Spring Meeting & 2nd Global Congress on Process Safety* 2006. Orlando, FL: AICHE.
6. Boffito, C. and M. Bolognesi, *Recovery of Tritium and Deuterium from their Oxides and Intermetallic Compounds Useful Therein*. 1991, SAES Getters SpA: USA.
7. Boffito, C. and J.D. Baker, *Getter Materials for Cracking Ammonia* 1999: USA.
8. *ST909 / Pieces (ST909 Pills) SRS-SDS #24546-1*. 2012, SAES Advanced Technologies S.p.A.: Avessano, Italy.
9. Darwent, B.d., *Bond Dissociation Energies in Simple Molecules*. 1970, National Bureau of Standards: Washington, D. C. p. 52.
10. Dean, J.A., *Lange's Handbook of Chemistry 15th Edition*. 1999, McGraw-Hill, Inc.: New York, NY.
11. Simoes, J.A.M. and J.L. Beauchamp, *Tranision Metal-Hydrogen and Metal-Carbon Bond Strengths: The Keys to Catalysis.* American Chemical Society, Chemical Reviews, 1990. **90**(4): p. 629-688.
12. Klein, J.E., *SRNL-L2100-2014_SHINE TPS Process Flow Technical Basis*. 2014: Aiken, SC.
13. Klein, J.E., *SAES St 909 Bench Scale Methane Cracking Tests.* Fusion Science and Technology, 2002. **41**: p. 998-1003.
14. Nigrey, P.J., *An Issue Paper on the Use of Hydrogen Getters in Transportation Packaging SAND2000-0483*. 2000, Sandia National Laboratories: Alburquerque, New Mexico.
15. Fukada, S., Y. Toyoshima, and M. Nishikawa. *Zr[2]Fe and Zr(Mn[0.5]Fe[0.5])[2] Particle Beds for Tritium Purification and Impurity Removal in a Fusion Fuel Cycle*. in *ISFNT-5 International Symposium on Fusion Nuclear Technology No5*. 2000. Rome , ITALIE Elsevier, Amsterdam, PAYS-BAS (1987) (Revue).
16. Cárdenas, R.E., K.D. Stewart, and D.F. Cowgill, *Gettering of hydrogen and methane from a helium gas mixture.* Journal of Vacuum Science & Technology A, 2014. **32**(6): p. 060602.
17. Klein, J.E. and H.T. Sessions, *SAES ST 909 Pilot Scale Methane Cracking Tests*. 2007. Medium: ED.
18. James, D.W. and G.A. Morgan, *ST909 Replacement Material Getter Literature Review (SRNL-L2100-2016-00001)*. 2016, Savannah River National Laboratory: Aiken, SC.

19. Abbas, H.F., Wan Daud, W. M. A.,, *Hydrogen production by methane decomposition: A review.* International Journal of Hydrogen Energy, 2010. **35**(3): p. 1160–1190.

20. Li, J., Chang, H., Ma, L., Hao, J., Yang, R. T., *Low-temperature selective catalytic reduction of NOx with NH3 over metal oxide and zeolite catalysts—A review.* Catalysis Today, 2011: p. 147–156.

21. Klein, J.E., *SAES St909 Material Phases after Methane Cracking*. 2001. Medium: ED; Size: vp.

22. Espe, W., M. Knoll, and M.P. Wilder, *Getter Materials for Electron Tubes.* Electronics, 1950(October): p. 80-86.

23. Klein, J.E. and J.S. Holder, *Screening Tests for Improved Methane Cracking Materials WSRC-STI-2007-0141*. 2007, Savannah River National Laboratory: Aiken, SC. p. Medium: ED.

24. Klein, J.E.a.H., J .S., *Screening Tests for Improved Methane Cracking Materials*. 2007, U.S. Department of Energy: Aiken, SC.

25. Klein, J.E., and Holder, J. S.,, *Screeing Tests for Improved Methane Cracking Materials.* Fusion Science and Technology, 2008. **54**: p. 611 - 614.

26. *Zirconium Manganese Iron Aluminum Pellets, ZRMN-FEAL-01-PE.6MMD (SRS SDS #49106-1)*. 2015, American Elements: Los Angeles, CA.

27. Succi, M. and D.A. Lorimer, *Process for the purification of hydrogen and a purifier therefor*. 1996, Google Patents.

28. Albrecht, H., U. Kuhnes, and W. Asel, *Application of SAES and HWT gas purifiers for the removal of impurities from helium-hydrogen gas mixtures.* Journal of the Less Common Metals, 1991. **172–174, Part 3**: p. 1157-1167.

29. *ST 707 SRS SDS #32361-1*. 1999, SAES Advanced Technologies S.p.A.: Avessano, Italy.

30. *Pricat Ni 60/15 T 6X5MM SRS SDS #48386-1*. 2012, Johnson Matthey Catalysts: Oakbrook Terrace, IL.

31. *Titanium Molydenum Zirconium Pellets (SRS-SDS # 49105-1)*. 2015, American Elements: Los Angeles, CA.

32. *Alumina Nickel Iron Pieces, ALO-NIFE-01-PCS.3T8MM (SRS SDS# 49373-1)*. 2015, Amreican Elements: Los Angeles, CA.

33. Watanabe, K., et al., *Decomposition of methane on Zr–Ni alloys.* Fusion Engineering and Design, 1998. **39–40**(0): p. 1055-1060.

34. *Zirconium Nickel Alloy Pieces (SRS SDS #49375-1)*. 2015, American Elemenets: Los Angeles, CA.

35. *Analytical Operating Procedures Inductively Coupled Plasma - Mass Spectrometer Elemental and Isotopic Analysis for Aqueous Liquid Samples Perkin Elmer Nexion 300D (L16.ADA-1577 rev1)*. 2015, Analytical Development Section, Savannah River National Laboratory: Aiken, SC.

36. *Analytical Operating Procedures Bruker D8 Advance X-Ray Diffraction System Major Revision (L16.1 ADS-1117 rev3)*. 2012, Analytical Development Section, Savannah River National Laboratory: Aiken, SC.

37. *Analytical Operating Procedures Contained Amptek Energy Dispersive X-Ray Flourescence Spectrometer, L16.ADS-1129 rev1*. 2016, Analytical Development Section, Savannah River National Laboratory: Aiken, SC.

38. Klein, J.E., *SAES ST909 Bench Scale Methane Cracking Tests.* Fusion Science and Technology, 2002. **41**(May): p. 998-1003.

39. Klein, J.E., *SAES ST909 Bench Scale Methane Cracking Tests, WSRC-TR-2000-00467*. 2000.

40. Klein, J.E., *SAES(R) ST909 Bench Scale Methane Cracking Tests*. 2001. Medium: ED; Size: vp.

41. Klein, J.E. and J.E. Holder, *SAES St 909 Getter Testing at the Savannah River National Laboratory*. 2005. Medium: ED.

Appendix A. Gibbs Free Energy Minimization

ORIGIN:= 1 mathcad notation to start matrix with 1 rather than 0

kmol := 1000 mol unit conversion

kJ := 1000 J unit conversion

$R_g := 8.31451 \cdot \frac{J}{mol \cdot K}$ Unviersal gas constant

Using the values found in Appendix A.IV on pages 927 and 929 Chemical, Blochemical, and Engineering Thermodynamics by Sandler, find the equilibrium distribution of NH3, N2, and H2 at various temperatures and 760 torr if you mix moles N2 with moles H2

Assume the only reaction is

3H2 + N2 = 2NH3

At these conditions NH3 is a vapor and the ideal gas assumption is okay.

P := 760torr Temp := 573.15K

$\begin{pmatrix} H2 \\ N2 \\ NH3 \end{pmatrix}$ $\nu := \begin{pmatrix} -3 \\ -1 \\ 2 \end{pmatrix}$ Lagrange multiplier based on reaction coefficients

Variable for moles of H2 initially present xxx:= 0.8

Initial moles present in mixture $N_0 := \begin{pmatrix} xxx \\ 1 - xxx \\ 0 \end{pmatrix} \cdot mol$

Moles accounting for multiplier $N_n(i,X) := N_{0_i} + \nu_i \cdot X$ where X represents extent of reaction

Total moles present $N_{tot}(X) := \sum_{i=1}^{3} N_n(i,X)$

Mole Fraction $y(i,X) := \frac{N_n(i,X)}{N_{tot}(X)}$

Gibbs Energy of formation

$$\Delta G_f := \begin{pmatrix} 0 \\ 0 \\ -16.5 \end{pmatrix} \cdot \frac{kJ}{mol} \qquad \Delta G_{re0} := \sum_{i=1}^{3} \left(\nu_i \cdot \Delta G_{f_i} \right) = -3.3 \times 10^4 \cdot \frac{J}{mol}$$

$$\ln K_0 := \frac{-\Delta G_{re0}}{R_g \cdot Temp} \qquad \ln K_0 = 6.925$$

Enthalpy of formation

$$\Delta H_f := \begin{pmatrix} 0 \\ 0 \\ -46.1 \end{pmatrix} \cdot \frac{kJ}{mol}$$

since ΔHr is negative, you should have more N2 as T increases

$$\Delta H_{re0} := \sum_{i=1}^{3} \left(\nu_i \cdot \Delta H_{f_i} \right) = -9.22 \times 10^4 \cdot \frac{J}{mol}$$

Guess value

$$X_g := 0.19 mol$$

$$X := root\left[\ln\left[\prod_{i=1}^{3} \left[\left(y(i, X_g) \cdot \frac{P}{bar} \right)^{\nu_i} \right] \right] - \ln K_0, X_g \right]$$

Find point in which conditions are met

$i := 1 .. 3$

$$y(i, X) = \begin{pmatrix} 0.35382502 \\ 8.78215214 \times 10^{-3} \\ 0.63739283 \end{pmatrix}$$

final mole fraction of the gas

$$N_{tot}(X) = 0.610726995\, mol$$

final total moles (remmeber elements are conserved by moles may or may not be.

$$N_n(i, X) = \begin{pmatrix} 0.21609049 \\ 5.36349738 \times 10^{-3} \\ 0.38927301 \end{pmatrix} mol$$

moles of H2, N2, and NH3 present

Appendix B. X-Ray Fluorescence Raw Data Sets

9.1 SAES ST909

Table 9-1: X-ray fluorescence scan raw data ST909

Peak Energy	Peak Width	Peak Area				
6.388428	0.141328	5739.409		0.011239	26	FeKa_
5.878877	0.133417	5140.6		0.016456	25	MnKa_
15.72359	0.223393	5127.856		0.020407	40	ZrKa_
17.6384	0.212341	783.7784		-0.02976	40	ZrKb_
7.037595	0.144666	549.1762		-0.01685	26	FeKb_
2.038457	0.154207	371.7042		0.025343	78	ZrLa_
2.961232	0.100563	238.0951		0.032368	90	AgLa_
3.145095	0.100531	208.7562		0.023905	92	AgLb13_
1.465561	0.089673	128.8713		0.021106	13	AlKa_
4.128711	0.117832	26.84175		-0.02021	54	
4.659143	0.132804	21.22983	0.003699	-0.01034	57	ESC_
4.926933	0.131756	19.75021		0.022401	23	V Ka_
5.3912	0.131335	19.1192		0.0393	61	CrKa_
8.024286	0.152025	14.64193		0.017047	29	CuKa_
22.12127	0.263382	13.81592	0.002547	-0.0156	47	AgKa_
7.438206	0.149165	11.59625		0.034128	28	NiKa_
3.660945	0.126153	9.545927		0.029722	20	CaKa_
1.792545	0.080609	9.252355		0.013255	38	ZrLl_
21.62633	0.223317	6.463425	0.001259	0.023859	3& 4	SUM_
12.2849	0.168684	6.034482	0.001111	0.040697	88	SUM_
25.19905	0.258905	4.329744		-0.00305	50	SnKa_
2.501626	0.083137	3.631519		-0.00023	84	ZrLg3_
1.206953	0.072131	3.510666	0.014745	0.033047	65	ESC_
12.79757	0.187942	3.236582	0.000564	0.020716	2& 2	SUM_
13.97653	0.208348	3.095726	0.000604	-0.05093	93	ESC_
8.598697	0.148051	2.898883		0.045603	75	ZnKa_
11.79961	0.213452	2.546531		-0.06564	93	
0.942635	0.063541	2.196852		0.035365	60	
9.248289	0.11294	1.772692		-0.00329	31	
11.08361	0.141122	1.388405		0.035687	84	
16.54115	0.131784	1.157703		0.042514	41	

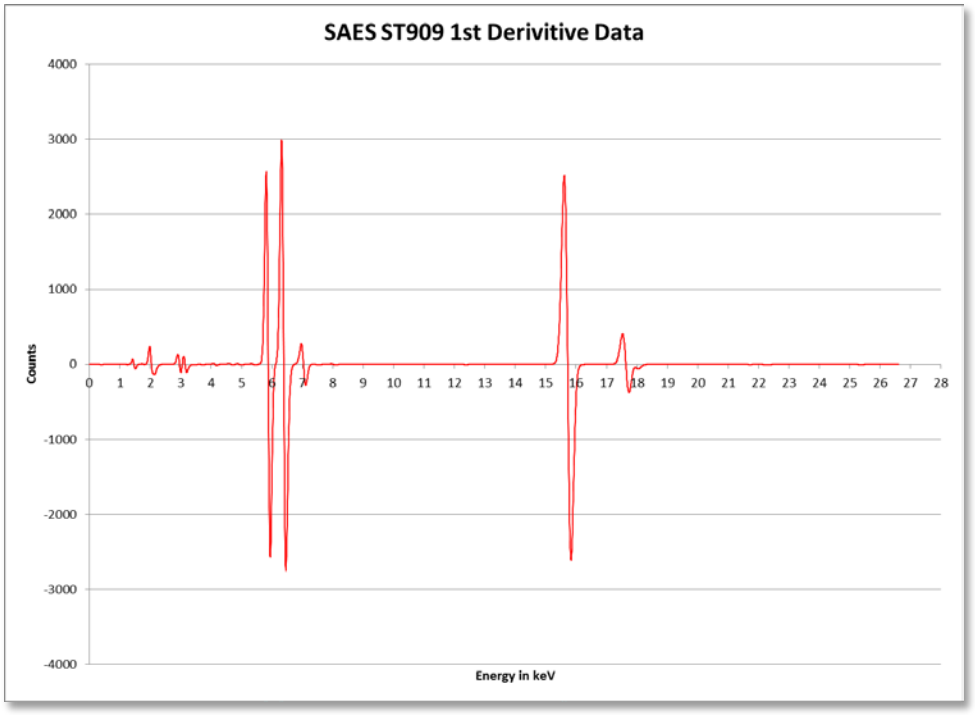

Figure 9-1: X-ray fluorescence scan 1st derivative data for ST909

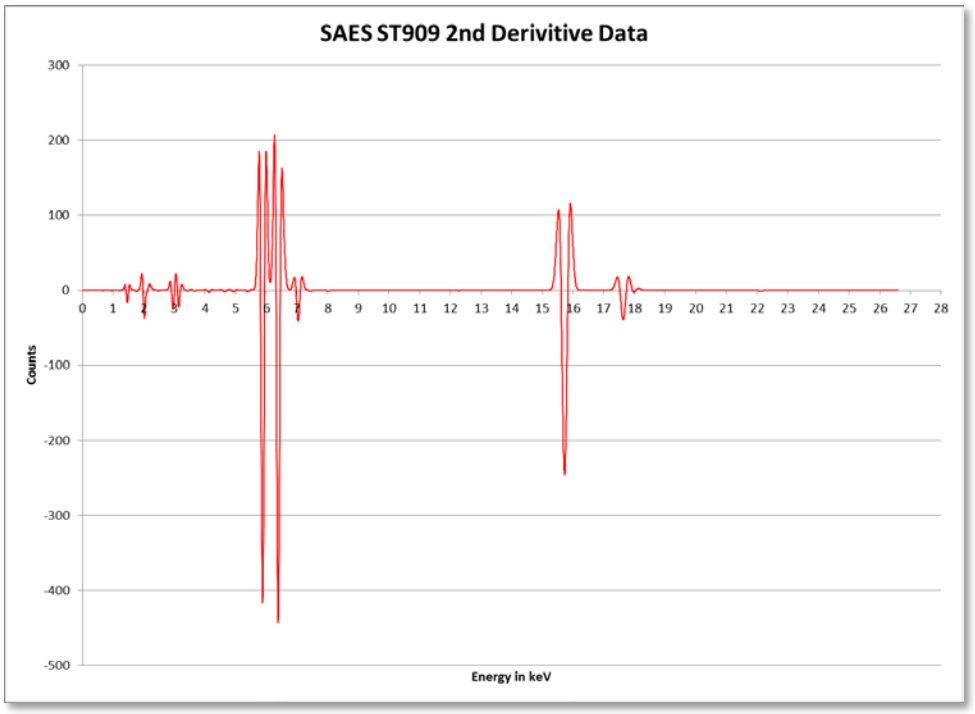

Figure 9-2: X-ray fluorescence scan 2nd derivative data for ST909

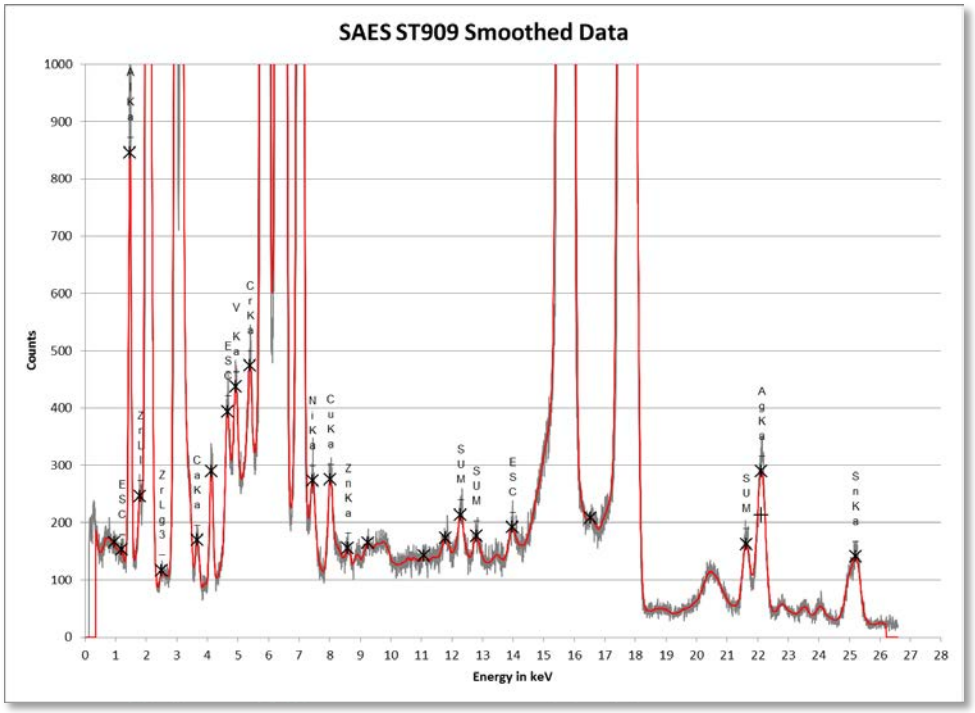

Figure 9-3: X-ray fluorescence scan smoothed data for ST909

9.2 American Elements ZrMnFeAl

Table 9-2: X-Ray Fluorescence Scan American Elements ZrMnFeAl

Peak Width	Peak Area				
0.140947	6190.115		0.011818	26	FeKa_
0.133363	5206.406		0.016505	25	MnKa_
0.223233	5103.739		0.020854	40	ZrKa_
0.2115	782.3659		-0.03058	40	ZrKb_
0.145067	606.5846		-0.01672	26	FeKb_
0.156267	422.0242		0.025509	78	ZrLa_
0.107351	182.1638		0.024457	92	AgLb_
0.098303	124.5465		0.040912	90	AgLa_
0.14945	58.65399		0.004809	72	HfLa_
0.172374	37.31718		0.010389	72	HfLb13_
0.087735	35.84379		0.022569	13	AlKa_
0.114679	24.20184		-0.02427	54	
0.115639	23.38697	0.003778	0.000503	57	ESC_
0.26538	13.64677	0.002428	-0.0156	47	SUM_
0.143101	11.34292		-0.00453	58	
0.139825	9.591696		0.000333	72	HfLb2_
0.162357	7.924782		0.049568	82	HfLg1_

0.08479	6.933326		0.016451	84	ZrLg3_
0.181584	6.794529	0.001197	0.02885	88	SUM_
0.238931	5.91456	0.001147	0.03223	3& 4	SUM_
0.179596	3.995108		0.03415	34	
0.228904	3.761799	0.000737	-0.03605	93	ESC_
0.168034	3.25229		0.025572	74	W La_
0.166003	3.110836	0.000503	0.022307	2& 2	SUM_
0.209841	2.998751	0.000576	-0.06884	86	SUM_
0.165768	2.491638		-0.01738	83	HfLg3_
0.097638	2.302041		0.041781	28	
0.093514	2.163458		0.045589	52	CaKa_
0.087969	2.085109		-0.03979	50	AgLg1_
0.087173	1.79292		0.041643	26	
0.099967	1.706318		0.013387	75	ZnKa_
0.116464	1.511322		0.054529	60	
0.213686	1.337363	0.000608	0.096586	49	

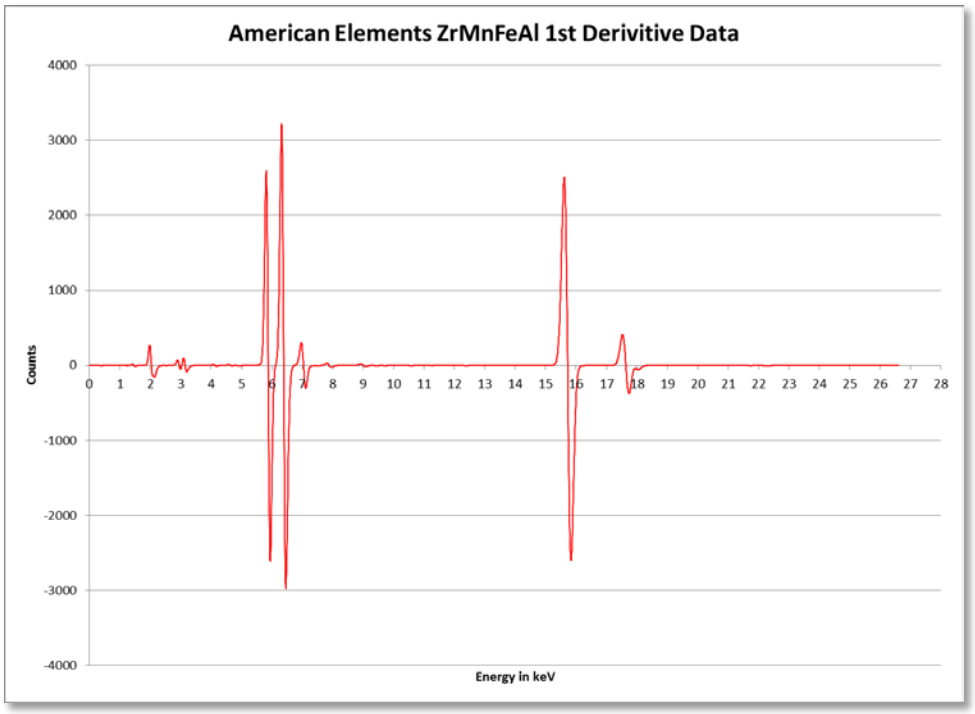

Figure 9-4: X-ray fluorescence 1st derivative data for AME ZrMnFeAl

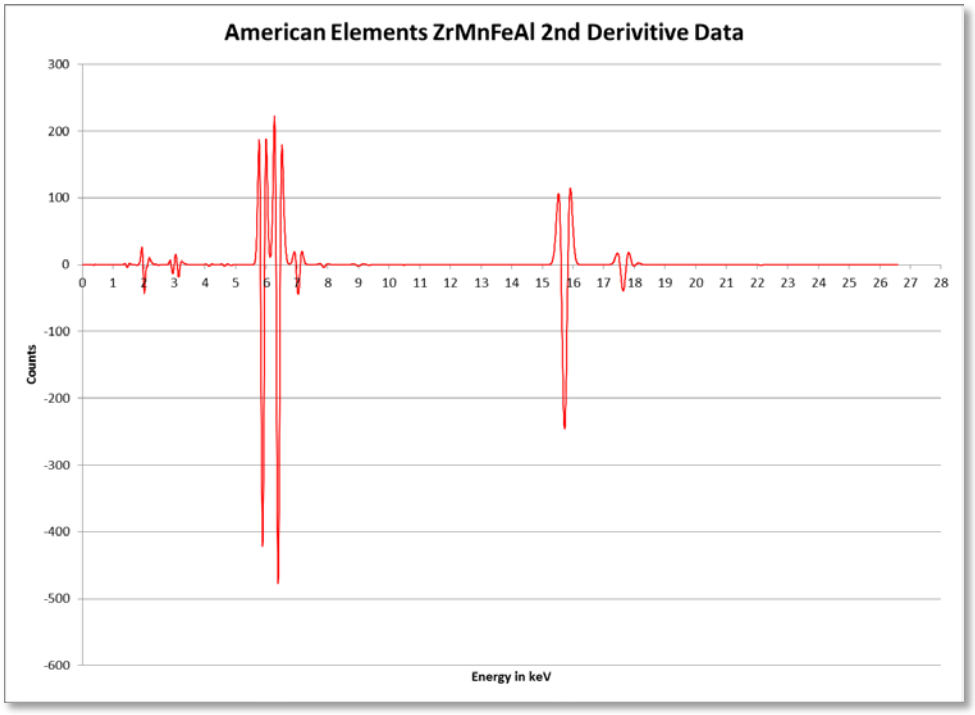

Figure 9-5: X-ray fluorescence scan 2nd derivative data for AME ZrMnFeAl

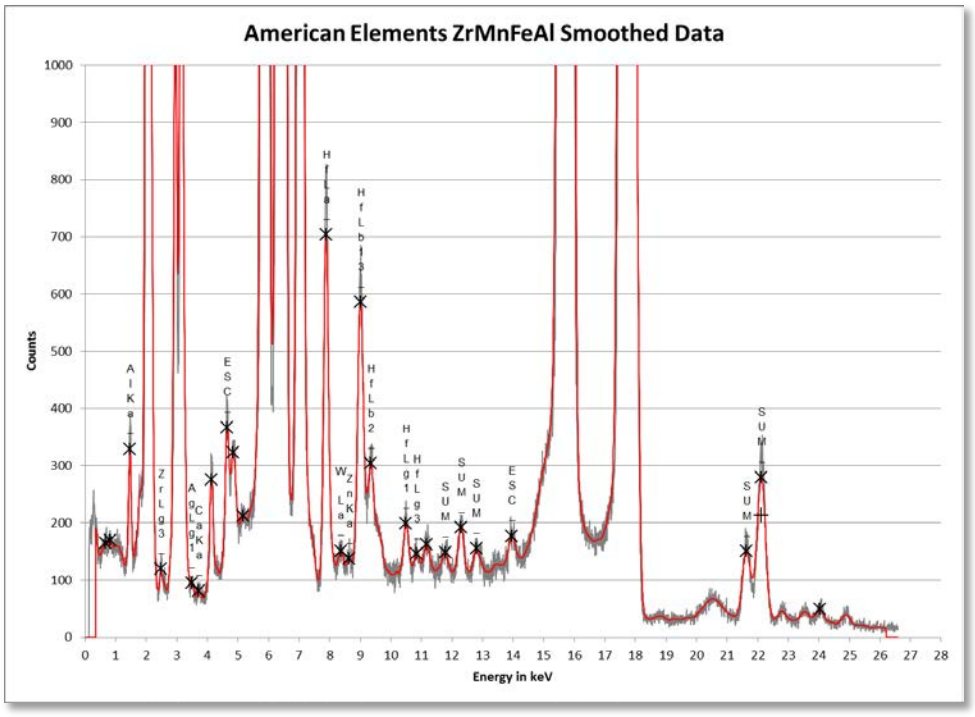

Figure 9-6: X-ray fluorescence scan smoothed data for AME ZrMnFeAl

Appendix C. XRD Raw Data Sets

9.3 SAES ST909

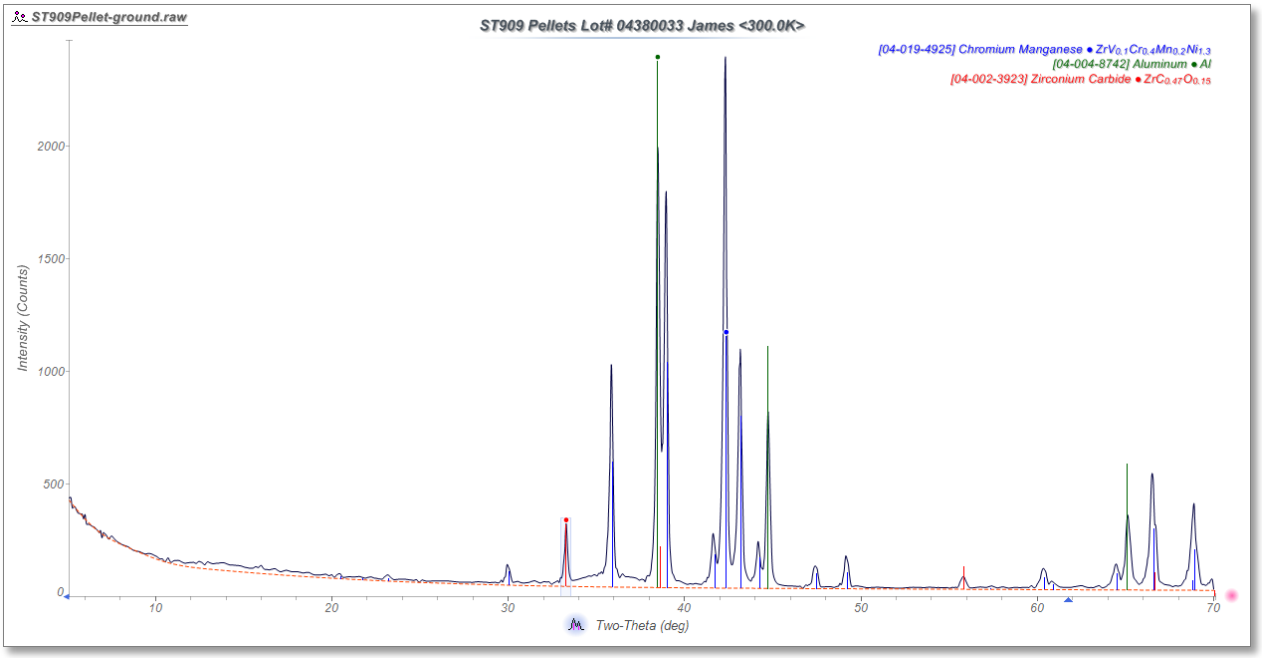

Figure 9-7: XRD Smoothed Data for ST909

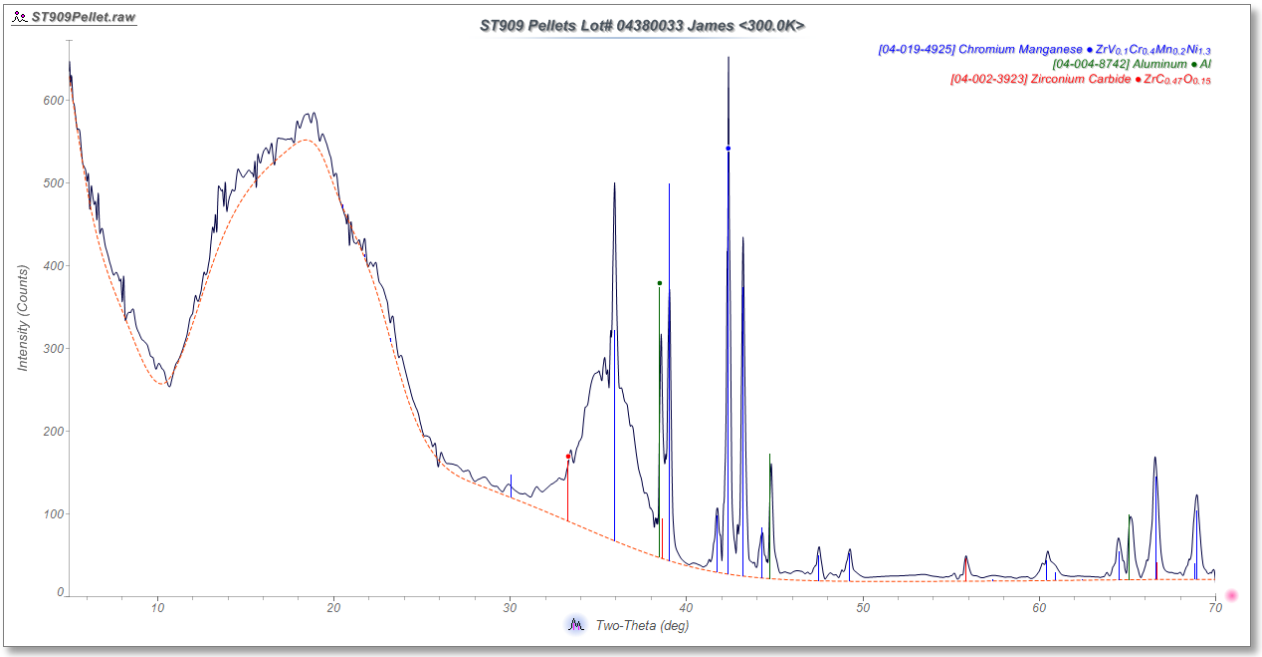

Figure 9-8: XRD Smoothed Data for ST909

9.4 American Elements ZrMnFeAl

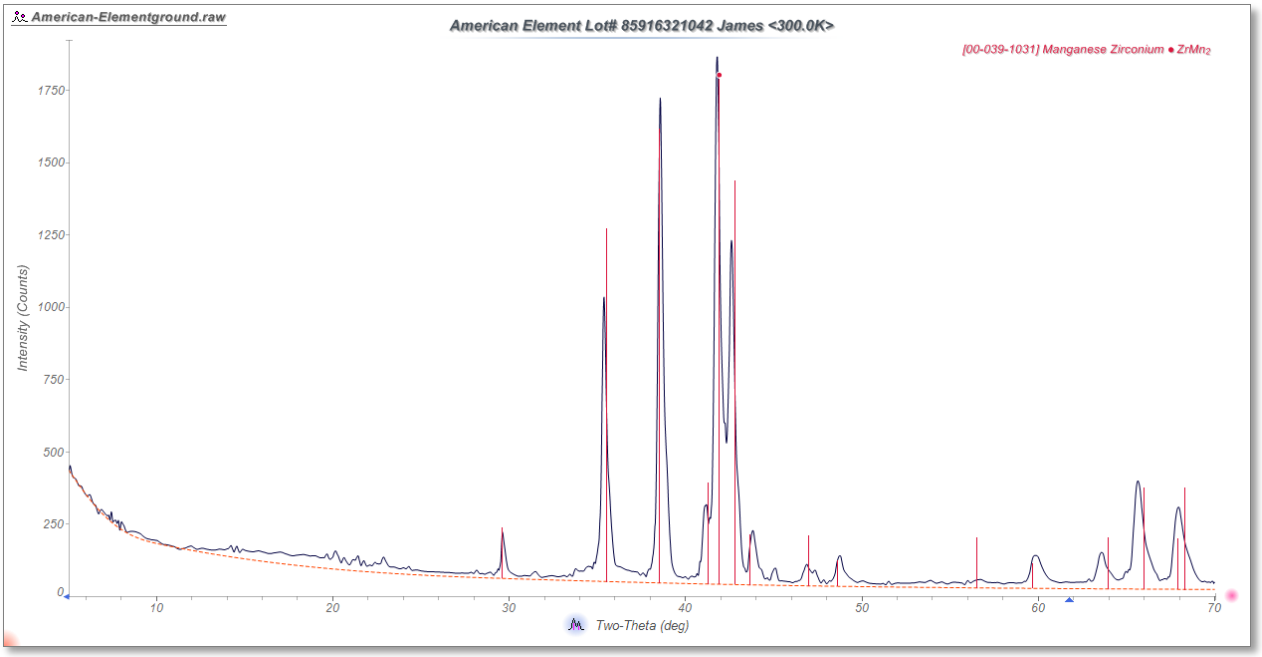

Figure 9-9: XRD Smoothed Data for AME ZrMnFeAl

Appendix D. Identified Getter Materials for Differing Applications

Material	Formula / Composition	Application	Carrier Gases	Operating Temperature	Activation Temperature	Supplier	Known Issues
ST909	$Zr(Mn_{0.5}Fe_{0.5})_2$ (40.5% Zr, 24.5% Mn, 25% Fe, 10% Al)	Q_2O, O_2, CO, CO_2, CQ_4, NO_x, NQ_3	He, Q_2, N_2	700°C		SAES	Does not perform as well in a nitrogen carrier gas. Nitriding reactions do occur
ZRMN-FEAL-01-PE.6MMD	Zr:Mn:Fe:Al (40.5% Zr, 24.5% Mn, 25% Fe, 10% Al)	Assumed same as ST909	Assumed same as ST909	Assumed same as ST909		American Elements	Assumed same as ST909 – Possible new vendor **product needs verification** Special made item
ST707	$Z_{r57}V_{36}Fe_7$ (70% Zr, 24.6% V, 5.4 % Fe alloy)	Q_2O, O_2, CO, CO_2, N_2		20°C to 100°C	450°C	SAES	
ST171	Zr V Fe	Q_2 at lower temperatures			900°C	SAES	
ST172	Zr V Fe	Q_2		110°C, 150°C to 300°C	450°C to 500°C	SAES	

Material	Formula / Composition	Application	Carrier Gases	Operating Temperature	Activation Temperature	Supplier	Known Issues
ST172	Zr V Fe	CQ_4		650°C	650°C	SAES	
	Zr56.5%V43.5%					American Elements	
ST199	Zr_2Ni (75.7 % Zr, 24.3 % Ni)	O_2, H_2, CQ_4,		Above 400°C for methane cracking			
	ZrNi		He				
ST787	ZrCo (80.8 % Zr, 14.2 % Co balance mischmetal alloy)	Q_2 storage		Storage below 400°C		SAES	Nitrogen inhibits hydrogen absorption (would not be a good replacement for ST198)
ST101	$Z_{r6}Al_2$ / $Z_{r61}Al_{29}$ / $Z_{r5}Al_3$ (84 % Zr, 16 % Al)	Q_2O, O_2, CO, CO_2, Q_2		300°C to 450°C	550°C to 900°C	SAES / GTI	
	Deoxo-D	O_2, H_2					Removes Product generates H_2O and CO_2
	$ZrSiO_2$					Mil-Spec industries	

Material	Formula / Composition	Application	Carrier Gases	Operating Temperature	Activation Temperature	Supplier	Known Issues
TI-MOZR-01-PE.6MMD	Ti:Mo:Zr:Fe (Bal:11.5:0.6:4.5 wt%)					American Elements	
	Ni/SiO2 or Ni/k	CQ_4		< 500°C		Sigma Aldrich	Carbon filament formation, Potential for Nickel carbonyl at temperatures below 200°C
	Pd/kieselguhr						Hydride material, expensive
	Pd/alumina						expensive
	Pd / H-ZSM_5			750°C to 900°C			Carbon filament formation, expensive
ST198	Zr_2Fe (76.5% Zr, 23.5% Fe)	Q_2 gettering	He, N_2	350°C		SAES	Nitriding reactions above 425°C

Material	Formula / Composition	Application	Carrier Gases	Operating Temperature	Activation Temperature	Supplier	Known Issues
ZR-FE-01-PE.6MMD	Zr:Fe (76.5:23.5 wt%)	Assumed same as ST198	Assumed same as ST198	Assumed same as ST198		American Elements	Assumed same as ST198 – Possible new vendor **product needs verification** Special made item
	ZrFe2					American Elements	

Distribution:

R. P. Addis, 773-A

D. W. Babineau, 999-2W

E. L. Hamilton, 773-42A

ORG L2110

Records Administration (EDWS)

B. A. Ferguson, 235-H

T. J. Worrell, 246-1H

K. L. Sessions, 246-1H

R. W. Allgood, 246-1H

T. D. Williamson, 246-1H

K. M. Bowen, 246-1H

M. L. Golyski, 246-1H

J. L. Clark R. 246-1H

K. G. Aylward, 248-H

M. A. Collins, 246-2H

B. A. Keefe, 719-H

J. M. Newell, 246-H

R. E. Snyder, 719-H

J. D. Westergreen, 235-H